Summer 8-6-2020

Studies of Lignin-Based Gels as Sorbents

Aditi Nagardeolekar
SUNY College of Environmental Science and Forestry, anagarde@syr.edu

STUDIES OF LIGNIN-BASED GELS AS SORBENTS

By
Aditi Nagardeolekar

A thesis
submitted in partial fulfillment
of the requirements for the
Doctor of Philosophy Degree
State University of New York
College of Environmental Science and Forestry
Syracuse, New York
August 2020

Department of Chemical Engineering

Approved by:
Biljana Bujanović, Major Professor
Cynthia Downs, Chair, Examining Committee
Bandaru Ramarao, Department Chair
S. Scott Shannon, Dean, The Graduate School

Acknowledgements

I am extremely grateful to my advisor, Dr. Biljana Bujanović for her endless guidance, support, encouragement and patience. She has been a great role model not only as a professional, but also as a person. I am also grateful to the rest of my committee, Dr. Anagnost, Dr. Yoo, Dr. Finkelstein, Dr. Leem, and Dr. Downs for their guidance. Dr. Amidon, Dr. Stipanovic, Dr. Kiemle, and Dr. Sally Ralph and Fred Matt (USDA-FPL) have been instrumental in this work. The help of Mr. Appleby, George Westby, Kelly Watson-Collins, Sean Hohm, Mr. Burry, Kevin Guerin and Marlene Braun has been irreplaceable. I sincerely appreciate my lab mates and the undergraduate researchers that I have worked with – Prajakta Dongre, Mat Ovadias, Talon Mahay, Emily Parsons, Chris Wood, Cher Jing, Chen Gong, Derek Corbett, Gina Song, and KuoTing Wang for their valuable help with my experiments, and their friendship.

I am indebted to the Syracuse Pulp and Paper Foundation, Dr. Scott, Debbie DeWitt, and Dr. Ram for their generous support through the Joachim Fellowship, and to Lynn Mickinkle for always being there to help. I am also thankful to Dr. Chatterjee and Dr. Kumar for always having kind words of encouragement for me, all of the faculty and staff at ESF/SU that I have learned so much from, and my fellow GSA members whom I have had the pleasure to serve with.

I would be remiss if I did not mention Krupa Dave and Bhavin Bhayani, and all of my dear friends in Syracuse and back home for their loving friendship and support.

Lastly, I feel blessed to have such a wonderful family that has shaped me into who I am. Words cannot express how especially grateful I am to my parents for their unconditional love and unwavering support. I would be nothing without you.

Table of Contents

List of Figures

CHAPTER 1

CHAPTER 2

CHPATER 3

CHPATER 4

List of Tables

CHAPTER 1

CHAPTER 2

CHAPTER 3

CHPATER 4

List of abbreviations:

AAm	Acrylamide
AgNPs	Silver nanoparticles
AGR	Agricultural residue
AGX	Arabinoglucuronoxylan
AH	Alkali-purified lignin
AOA	Antioxidant activity
APS	Ammonium persulfate
BTX	benzene, toluene, xylene
CA	*p*-Coumarate residue
CG	Commercial reference hydrogel
DCM	Dichloromethane
DMSO	Dimethyl sulfoxide
DP	Degree of polymerization
EC	Acetyl bromide extinction coefficient
EDS	energy dispersive X-ray spectroscopy
EtOAc	Ethyl acetate
EtOH	Ethanol
FA	Ferulate residue
FR	Solvent-insoluble residue of recovered lignin
G unit	Guaiacyl unit
GAX	Glucuronoarabinoxylan
GX	Glucuronoxylan
H unit	*p*-hydroxyphenyl unit
HMW	High molecular weight
HSP	Hildebrand solubility parameter
HWE	Hot-water extraction
IC_{50}	Minimum inhibitory concentration required for 50% radical quenching
KL	Kraft lignin (technical reference lignin)
LCB	Lignocellulosic biomass
LCC	Lignin-carbohydrate complex
LCST	Lower critical solution temperature
LMW	Low molecular weight
MA	Mixed angiosperms recovered lignin
MAAH	Mixed angiosperms alkali-purified lignin
MAFR	Mixed angiosperms solvent-insoluble fraction
Me-α-D-GlcpA	4-O- Methyl-α-D-glucuronic acid
MeOH	Methanol
*M*n	Number-average molecular weight
MS	Miscanthus recovered lignin
MS-SAQ	Miscanthus lignin recovered from soda-anthraquinone pulping liquor
MSAH	Miscanthus alkali-purified lignin
MSFR	Miscanthus solvent-insoluble fraction

*M*w	Weight-average molecular weight
NIPAM	N-isopropyl acrylamide
NMBA	N,N'-Methylene bisacrylamide
OD	Oven dry (moisture free) weight
PAM	Polyacrylamide
PEGDGE	Poly(ethylene glycol) diglycidyl ether
PhOH	Free phenolic hydroxyl group
RecL	Lignin recovered from autohydrolyzate of hot-water extraction
S unit	Syringyl unit
SEM	Scanning electron microscopy
SM	Sugar maple recovered lignin
SMAH	Sugar maple alkali-purified lignin
SMFR	Sugar maple solvent-insoluble fraction
Tg	Glass transition temperature
TGA	Thermogravimetric analysis
TW	Commercial reference hydrogel
UAE (bath)	Ultrasound-assisted extraction in a probe sonicator
UAE (probe)	Ultrasound-assisted extraction in a bath sonicator
W	Willow recovered lignin
WAH	Willow alkali-purified lignin
WFR	Willow solvent-insoluble fraction
WS	Wheat straw recovered lignin
WSAH	Wheat straw alkali-purified lignin
WSFR	Wheat straw solvent-insoluble fraction
α-L-Ara*f*	α-L-Arabinofuranose
β-D-Xyl*p*	β-D-Xylopyranose

Abstract

A. Nagardeolekar. Studies of Lignin-Based Gels as Sorbents.
180 Pages, 76 Figures, 29 Tables, Nature style guide used.

Valorization of lignin is essential for the success of emerging lignocellulosic biorefineries. Additional valorization of non-cellulosic forest resources can also generate secondary revenue streams helpful for their sustainable operation. Toward these goals, lignins recovered from hot-water extracts of angiosperms produced at pilot scale (sugar maple, willow, miscanthus, wheat straw, mixed angiosperms) were characterized and further fractionated to generate fractions with distinct physicochemical properties. The recovered and fractionated lignins were used in synthesis of lignin-acrylamide-kaolin (10.7% w/w total lignin) and lignin-poly(ethylene glycol) diglycidyl ether (PEGDGE) gels (66.7 w/w total lignin). Lignin-acrylamide-kaolin gels were suitable for adsorption-based applications (removal of dye and metallic cations from aqueous solutions), while lignin-PEGDGE gels were suitable for absorption-based applications (absorption and release of fragrances and bioactive solutions). Two types of fractionation were found to influence gel properties differently, demonstrating the importance of lignin-to-carbohydrates ratio in the produced fraction on the hydrogel architecture. The methanolic and aqueous extracts of chaga mushroom (a non-lignocellulosic forest biomass) were found to have viable antioxidant properties. The hot-water extracts of chaga were further used in green synthesis of chaga-silver nanoparticles, expected to have bioactive properties. Lignin-PEGDGE gels were found to be good carriers for the delivery of these nanoparticles.

Keywords: Biorefinery lignin, fractionation, lignin-based gels, chaga mushroom, green synthesis of nanoparticles.

A. Nagardeolekar
Candidate for the degree of Doctor of Philosophy, August 2020
Biljana Bujanović, PhD
Department of Chemical Engineering
State University of New York College of Environmental Science and Forestry,
Syracuse, New York

Chapter I

Introduction

1. Research motivation:

Lignin is one of three major components of lignocellulosic biomass, and the second most abundant natural polymer. Unlike the other two major components of lignocellulosic biomass, (polysaccharides - cellulose and hemicelluloses, commercially exploited for numerous applications), lignin polymer is irregular in nature. It is an amorphous phenylpropanoid polymer, and its structure depends on its origin and extraction method [1], [2]. Because of its variability and inconsistent nature, lignin has long been viewed as an inevitable low-value byproduct of the pulp and paper industry with ~ 50 million tons of lignin produced worldwide annually. It is estimated that the energy stored in generated lignin exceeds the internal energy demand of the pulp and paper industry by about 60% [3]–[5]. More than 95% of this lignin is incinerated as a boiler fuel to produce steam and energy, while the remaining is used in different applications, including the production of adhesives and resins, curing-enhancing additives to cement, and as drilling fluids [4]. The supply of lignin is expected to double in the near future, due to the escalating focus on biorefineries and use of lignocellulosic biomass for the production of fuels, materials, and chemicals [4]. Recent global studies forecast a 2% compound annual growth rate in commercial lignin market through year 2025, with an increase in the total market size from 793 million USD in year 2019 to 985 million USD in year 2025 [6]. Although the studies show an increased interest in lignin, its vast potential still remains underutilized. In order to help the lignocellulosic biorefineries meet their production and revenue goals and make lignocellulosic fuels economically competitive with gasoline, it is imperative to valorize the lignin, which will

inevitably be produced in these biorefineries [4]. Instead of handling lignin as an energy resource, exploiting it as a chemical / material resource is key for lignin valorization. Lignin used in production of chemicals / biomaterials (low volume / high value) is far more profitable than unmodified lignin burned for energy purposes (high volume / low value) [3]. One strategy of converting lignin into high-value products involves hydrodeoxygenation of lignin to produce BTX (benzene, toluene, xylene) chemicals, high grade transportation fuels and specialty chemicals [4], [7]. Another strategy is to take advantage of the naturally occurring polymeric nature of lignin and use it as a renewable alternative to synthetic, petroleum-based polymers. Mainstream approaches to the second strategy involve use of lignin in synthesis of thermoplastics, polyurethane foams, binders, adhesives resins and 3D printing resins [3], [8]. However, use of lignin in synthesis of novel polymeric products with high-value niche applications (such as hydrogels) is still a nascent field [9]–[17].

To address the critical need for finding high-value applications for lignin, the goal of this study was to investigate the suitability of biorefinery lignins recovered from hot-water autohydrolyzates of angiospermic biomass for synthesis of lignin-based hydrogels. Towards this effect, it was desired to characterize the recovered lignins, treat them to further fractionation, and study the changes in their physicochemical properties as the result of this treatment. Hydrogels were synthesized from recovered lignins (‘as is’) and from the fractionated lignins in order to study the possible benefits of these treatments. The intended applications of these hydrogels are in agriculture, food packaging, fragrance delivery, wastewater treatment and potentially pharmaceutical fields. An ancillary goal was to isolate a bioactive extract from non-lignocellulosic biomass (chaga mushroom), and synthesize chaga-silver nanoparticles which are suitable to be delivered through the synthesized hydrogels, as an additional attempt to generate

secondary revenue streams for the biorefineries by utilization of non-lignocellulosic forest resources.

2. Outline:

This document is divided into five chapters (Figure 1). Chapter 1 introduces the problem statement and objectives of this work, and provides a general literature review. Chapter 2 synthesizes the results of experiments directed towards characterization of physicochemical properties of lignins recovered from hot-water extraction of selected angiosperms and the effect of further fractionation on these properties. Chapter 3 describes the experiments on synthesis and evaluation of hydrogels from recovered and fractionated lignins. Chapter 4 describes isolation and evaluation of bioactive extracts from non-lignocellulosic forest biomass (chaga mushroom), synthesis of chaga-silver nanoparticles from the extract, and their absorption and release from lignin-based hydrogels synthesized in earlier experiments. Chapters 2, 3 and 4 each include a specific literature review, materials and methods, results and discussion, and pertinent conclusions. Chapter 5 summarizes overall conclusions of this study and gives recommendations for future work.

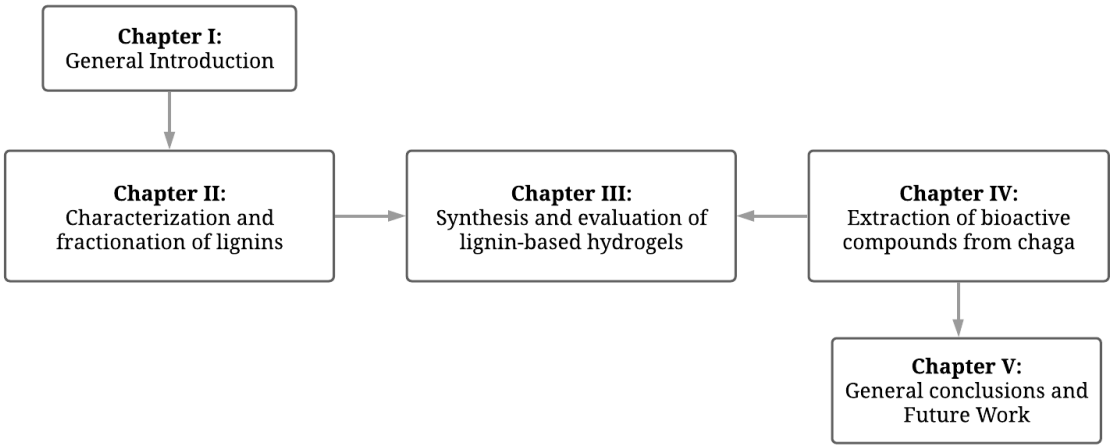

Figure 1: Scheme showing flow and arrangement of this document

3. Biomass used in this study:

The lignocellulosic biomass used in this study were all xylan-rich angiosperms, which are model feedstocks in hot-water extraction-based biorefineries [18].

Sugar maple (*Acer saccharum*, Family: *Sapindaceae*) is a common hardwood found in North-Eastern America. It grows on approximately 12.5 million hectares (9%) of the total land occupied by all hardwoods, and has a net volume of about 130 million m^3 (6%) of the hardwood sawtimber volume in the U.S. New York is one of the major producers of commercial volume. Commercialization of SM has been growing, with increased production of saw logs, pulpwood and more recently, firewood [19]. Apart from the timber, it is also the principle source of maple syrup.

Willow (*Salix spp*., Family: *Salicaceae*) is a hardwood and a short rotation energy crop. Commercial willow biomass has been planted over 500 hectares in the Northeast region alone [20]. Due to its high yields (13.6 ton/hectare/year), fast growth (3-4 years) and high net energy ratio (55), it has been widely researched as an energy crop in a wide variety of locations, including SUNY-ESF, under the 'Willow Project' [21].

Miscanthus (*Miscanthus spp*. Family: *Graminae / Poaceae*) is a C_4 perennial grass and an energy crop. Compared to other model grasses, miscanthus has been shown to yield a higher ratio of biomass to area, with a yield that is consistent regardless of rainfall, nitrogen availability or growing degree days (44 ton/hectare/year) [22], and it is rapidly gaining research interest, especially in the Midwestern US.

Wheat Straw (*Triticum spp*., Family: *Graminae / Poaceae*) is an agricultural residue. Agricultural residues are leftover materials after grain harvest, available in large quantities, and

often low-valued [23]. The U.S. is among the top five wheat producers, producing an estimated total of ~6 megaton wheat straw in the year 2017-2018 [24].

Mixed hardwoods and wheat straw (MA) was a mixture of sugar maple, aspen, red oak, mixed northern and southern hardwoods, and wheat straw.

Chaga mushroom (Chaga; *Inonotus obliquus*, Family: *Hymenochaetaceae*) is a white-rot fungus. It grows parasitically on trees rich in betulinic acid (a pentacyclic triterpenoid), mainly birch (Family: *Betulaceae*), in certain parts the Southern Tier, including those in New York which are abundant in maple/beech/birch [25], [26].

4. Objectives:

1. Lignin characterization:
    1.1. Characterize lignins recovered from hot-water extracts of angiosperms (Sugar maple -SM, willow-W, miscanthus-MS, wheat straw-WS, and mixed angiosperms-MA) for chemical composition (lignin, carbohydrate, and ash content), in addition to physicochemical properties (free phenolic hydroxyl group content, FT-IR characterization, thermal behavior-TGA, acetyl bromide coefficient, and antioxidant activity).
2. Lignin fractionation:
    2.1. Fractionate the recovered lignins using two separate techniques: mild alkali purification (SMAH, WAH, MSAH, WSAH, and MAAH) and sequential organic solvent-fractionation (SMFR, WFR, MSFR, WSFR, and MAFR).
    2.2. Study the changes in the chemical composition and physicochemical properties of lignins after fractionation.
3. Synthesis of lignin-based hydrogels:

3.1. Select appropriate lignin-based hydrogel formulations through literature survey, with a wide applicability and variable ways of incorporation of lignin in the formulation. Synthesize lignin-acrylamide-kaolin hydrogels by partially replacing acrylamide with lignin (23% w/w replacement, 10.7% total lignin) and lignin-poly(ethylene glycol) diglycidyl ether (PEGDGE) hydrogels by combining lignin with PEGDGE (66.7% w/w total lignin). Assess suitability of recovered lignins for use in these formulations.

3.2. Evaluate and compare the sorption characteristics (adsorption kinetics, reusability, and free absorbency capacity) and mechanical properties (compression modulus) of hydrogels synthesized from recovered lignins, technical (Kraft) lignin and commercial hydrogels among each other.

3.3. Assess the application versatility of lignin-based hydrogels (adsorption of dye, and metallic cations; and absorption / release of non-aqueous fragrances, and aqueous bioactive solutions)

3.4. Determine the effects of fractionation on sorption characteristics and mechanical properties of lignin-based hydrogels.

4. Extraction of bioactive compounds from chaga mushroom:

4.1. Study the effect of extraction solvent, extraction method, and extraction intensity on the extraction yield, antioxidant activity and free phenolic hydroxyl group content of the extracts.

4.2. Assess the suitability of selected chaga extract (based on antioxidant activity) to participate in green synthesis of silver nanoparticles.

4.3. Assess the suitability of chaga-silver nanoparticles to be delivered through lignin-PEGDGE hydrogels.

5. Literature Survey:

5.1. Chemical composition of lignocellulosic biomass:

Lignocellulosic biomass (LCB) is mainly composed of three major polymeric components: cellulose, hemicelluloses and lignin. These three components are closely associated with each other and compositely make up the lignocellulosic biomass of higher plants, which are further classified into hardwoods, softwoods and grasses (including agricultural residues, AGRs).

In addition to these major, structural constituents, LCB also contains minor, accessory constituents, which are low-molecular weight organic (extractives) and inorganic compounds (ash) (Table 1) [1]. The amounts and composition of individual components differ depending on the species and environmental conditions during growth.

Table 1: Selected examples of composition of lignocellulosic biomass (LCB) species [19], [21], [20], [17]

LCB type	Species	Cellulose (% w/w)	Hemicellulose major type (total % w/w)	Lignin (% w/w)	Extractives (% w/w)	Ash (% w/w)
Softwood [27]	*Pinus radiata*	37.4	Glucomannan (28.9)	27.2	1.8	0.4
	Juniperus communis	33	Glucomannan (27.2)	32.1	3.2	1.4
	Latrix sabirica	41.4	Glucomannan (20.9)	26.8	1.8	0.4
Hardwood [27]	*Acer saccharum*	40.7	Glucuronoxylan (27.3)	25.4	2.5	0.8
	Fagus sylvatica	39.4	Glucuronoxylan (29.1)	24.8	1.2	1.3
	Eucalyptus globulus	51.3	Glucuronoxylan (21.3)	21.9	1.3	0.3
	Salix spp [28]	36.9	Glucuronoxylan (12.6)	24.9	8.2	1.5
Perennial grass	*Miscanthus spp* [29]	39.8	Arabinoxylan (19.8)	22	6.6	4.2
AGRs	*Triticum spp* [30]	34.6	Arabinoxylan (23.4)	18	15.4	5.6

5.1.1. Cellulose:

Cellulose is the main constituent of lignocellulosic biomass, making up to 40-45% of the dry weight in most wood species. It is located primarily in the secondary cell wall. Cellulose is a homopolysaccharide composed of β-D-glucopyranose units linked together by (1→ 4)-glycosidic bonds (Figure 2; [31]), formed in a reaction catalyzed by cellulose synthase complex [27]. Water is expelled as the glucopyranose units polymerize, organized in higher plants in rosettes containing 36 subunits and producing simultaneously 36 cellulose chains called elementary fibrils. Cellulose chains have a strong tendency to form intra- and intermolecular hydrogen bonds, which result in a stable, linear structure. Bundles of cellulose chains in the form of elementary fibrils are thus aggregated together to form microfibrils, where crystalline regions of cellulose alternates with amorphous cellulose. Microfibrils build up fibrils and finally cellulose fibers (Figure 3; [31]). This fibrous structure and the strong hydrogen bonding impart high tensile strength to cellulose, and render it insoluble in most solvents. The degree of crystallinity of cellulose (0.6-0.73), its molecular weight and its degree of polymerization (500-15000) vary considerably depending on the species [27].

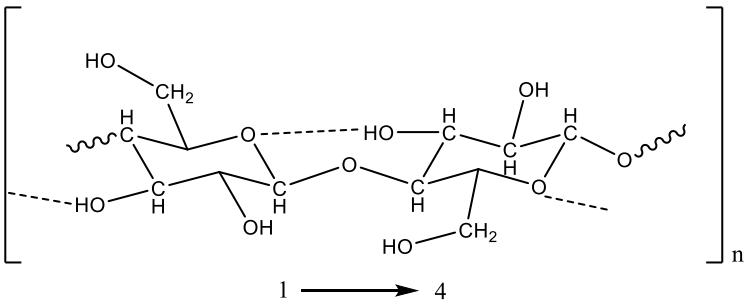

Figure 2: Repeating unit of cellulose, showing directionality of β-D-glucopyranose (1→ 4)-glycosidic linkage, and intrachain hydrogen bonding (dotted lines). Redrawn from [31].

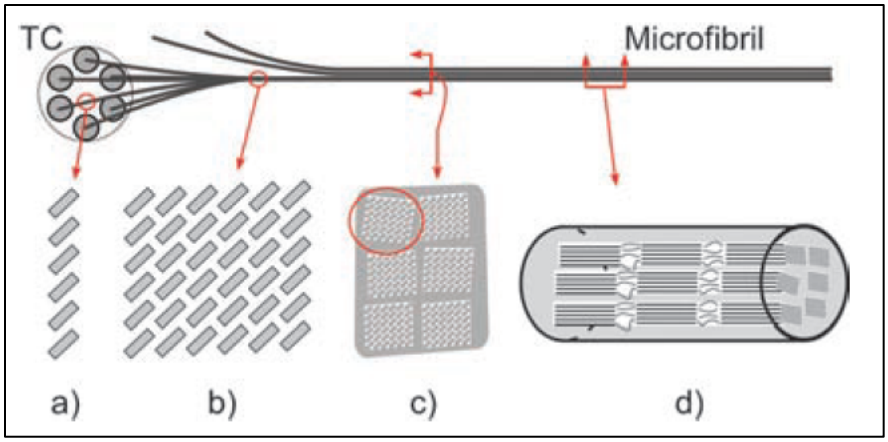

Figure 3: Organization of cellulose in a microfibril

a) minisheet cross-section of a single subunit, held together by van der Waal's forces. Each grey box represents a cellulose chain looking down the chain axis. b) Elementary fibril cross-section. The consolidation of multiple elementary fibrils forms a microfibril. c) microfibril cross-section composed of 6 elementary fibrils. d) microfibril lateral section showing the series configuration of amorphous and crystalline regions of cellulose. Reprinted with permission from [31]

5.1.2. Hemicelluloses:

Incorrectly thought to be precursors of cellulose, the term 'hemicelluloses' was originally proposed to describe polysaccharides extractable in aqueous alkaline solutions [32]. The monomer units in hemicelluloses backbone and branches range from hexoses such as β-D-Glucopyranose (β-D-Glc*p*), β-D-Mannopyranose (β-D-Man*p*), and β-D-galactoyaranose (β-D-Gal*p*) to pentoses (hence sometimes referred to as pentosans) such as β-D-xylopyranose (β-D-Xyl*p*) and α-L-arabinofuranose (α-L-Ara*f*) and to uronic acids such as α-D-glucuronic acid, α-D-galacturonic acid and low-molecular weight aromatic residues such as ferulic acid (Figure 4).

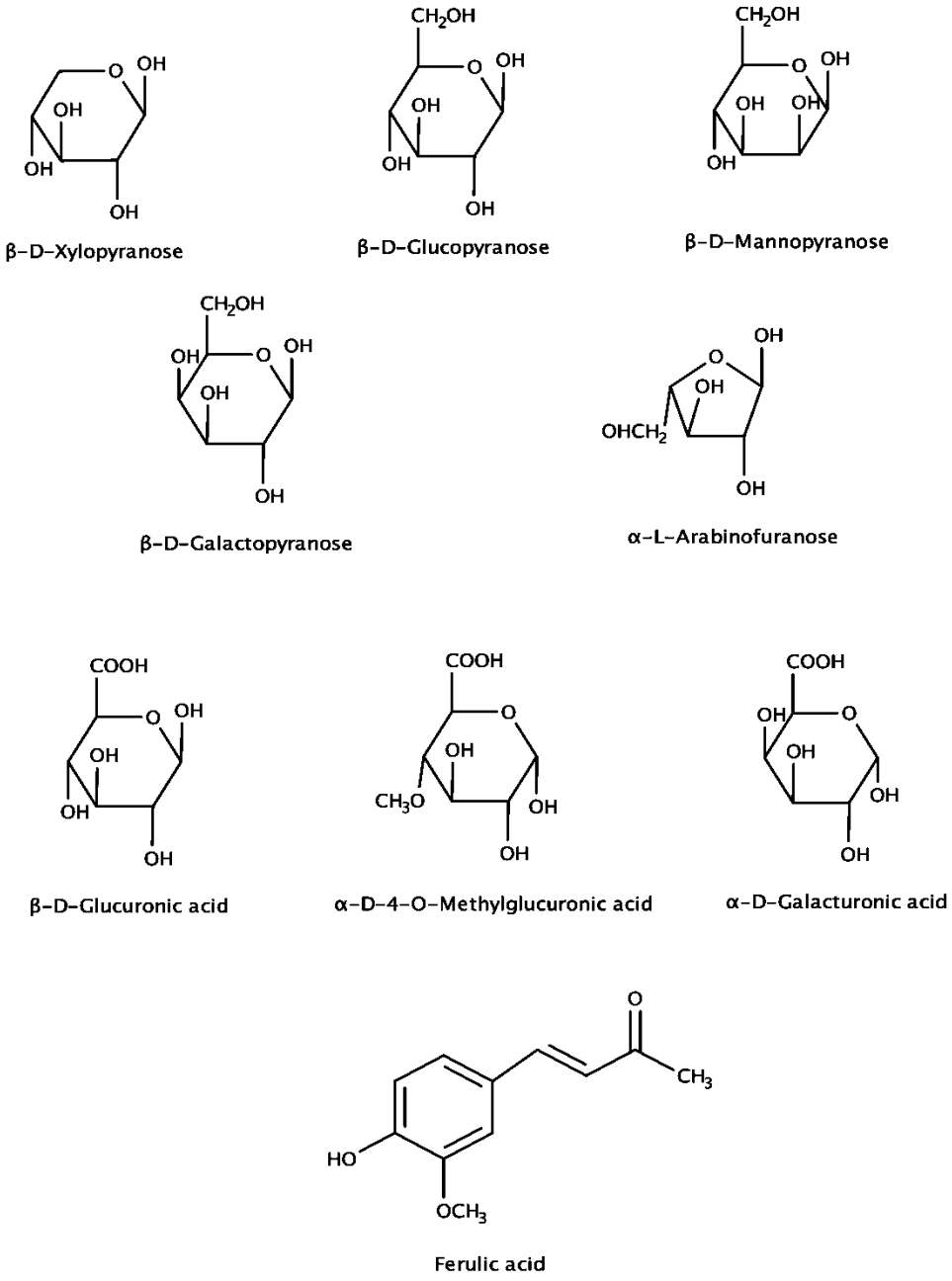

Figure 4: Common carbohydrate monomers present in hemicelluloses and ferulic acid. Redrawn from [32]

Based on the predominant sugar present in the polysaccharide backbone, hemicelluloses are further classified into four classes (Table 2) [32]:

Table 2: Classification of hemicelluloses [32], [33]

Class	Backbone monomer
1. Xylans	β-D-Xyl*p*
2. Glucomannans	β-D-Man*p,* β-D-Glc*p*
3. β- glucans with mixed linkages	β-D-Glc*p*
4. Xyloglucans	β-D-Glc*p*
5. Galactans	β-D-Gal*p*

This document will focus on xylan-type hemicelluloses, as other classes are out of the purview of current discussion.

Structure of xylans:

Xylans are heteropolysaccharides containing a β (1→4) linked D-xylopyranose (Xylp) backbone carrying various types of substituents depending on the species[4]. They are the most abundant hemicelluloses, which constitute up to 25-30% dry mass of hardwoods, 5-10% dry mass of softwoods and 15-30% of dry mass of graminae biomass (grasses and agricultural residues) [34], [35]. Depending on the most abundant sugar present on the backbone, xylans of higher plants are classified into different types (Table 3).

Table 3: Classification of xylans [36]

Abbreviations used: Ac: acetyl groups, α-L-Ara*f*: α-L-arabinofuranose, Me-α-D-Glc*p*A: 4-O-Methyl-α-D-glucuronic acid, β-D-Xyl*p*: β-D-xylopyranose

Xylan Type	**Main substituents on the backbone**	**Type of LCB**	**Example**	**Amount present (% HC dry LCB)**	**Reference**
Glucuronoxylan (GX)	α-D-MeGlc*p*A, Ac	Hardwoods	Sugar maple, Birch Yellow poplar, Aspen (β-D-Xyl*p*:α-D-MeGlc*p*A:Ac = 10:1:6)	15-30	[37] – [40]
Arabinoglucuronoxylan (AGX)	α-L-Ara*f*, more α-D-MeGlc*p*A,	Softwoods	Pine Douglas Fir (β-D-Xyl*p*:α-L-Ara*f*: α-D-MeGlc*p*A = 10:1:2)	5-10	[41] – [43]
Arabinoglucuronoxylan (AGX) / Glucuronoarabinoxylan (GAX)	α-L-Ara*f*, α-D-MeGlc*p*A, FA	Graminae / Non-endospermic tissue of grains	Corn cob (Xyl*p*:α-L-Ara*f*: α-D-MeGlc*p*A:FA = 19:3:2:0.2)	15-30	[44] – [46]

The most predominant hemicelluloses in hardwoods are *O*-acetyl-4-O-methylglucuronoxylans (simply called glucuronoxylans, GX, Figure 5). On average, the backbone is substituted with one Me-α-D-Glc*p*A residue per 8-20 β-D-Xyl*p* residues. The average molar mass has been reported at 5600 – 40000 Da, and the average degree of polymerization is 100-220, depending on the species, mode of isolation and analysis method. Most of the β-D-Xyl*p* residues that carry a Me-

α-D-Glc*p*A side chain at C-2 have been found to additionally contain an O-acetyl group at C-3. On average, 4-7 acetyl groups are present per 10 β-D-Xyl*p* residues [35].

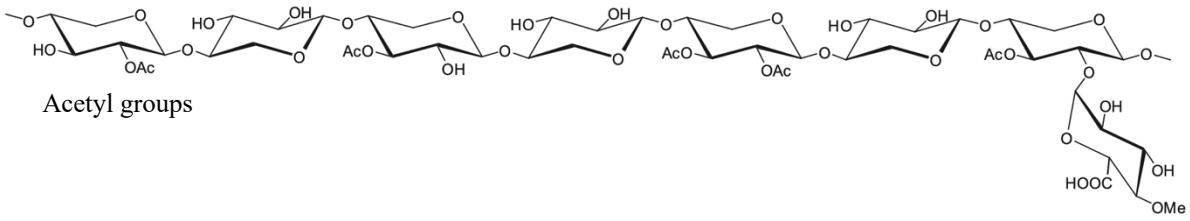

Figure 5: Representative structure of *O*-acetyl-4-O-methyl glucuronoxylan, typical of hardwoods. Redrawn from [35]

Softwoods contain the least amount of xylans, as the main hemicelluloses in those plants are glucomannans [10-20% w/w, two types – fraction with a lower content of α-D-Gal*p* and α-D-Gal*p* rich fraction; 24, 94]. Xylans of softwood are arabinoglucuronoxylans (AGX), which contain α-L-Ara*f* substituents at the C-3 position on the xylan backbone (Figure 6). One α-L-Ara*f* residue occurs per *8-9* β-D-Xyl*p* residues. One Me-α-D-Glc*p*A residue occurs per 5-6 β-D-Xyl*p* residues at C-2, much higher in proportion as compared to hardwood GX [35]. Unlike hardwood GX, no acetyl groups have been found.

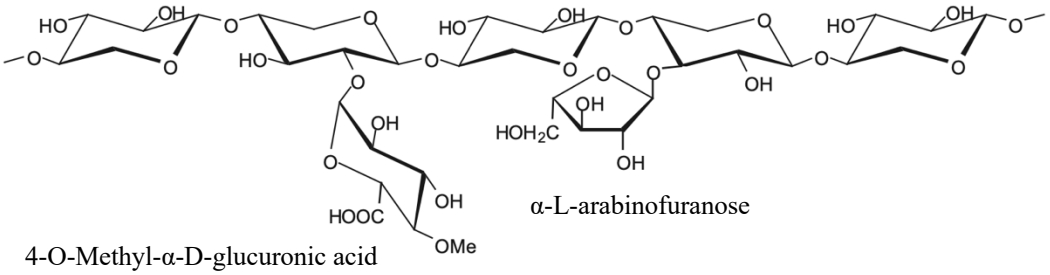

Figure 6: Representative structure of Arabino-4-O-methyl glucuronoxylan, typical of softwoods. Redrawn from [35]

Graminae biomass generally contains the most amount of xylans on the basis of percent dry weight, in comparison to hardwoods and softwoods. Graminae xylans are either AGX, or glucuronoarabinoxylans (GAX; fewer Me-α-D-Glc*p*A residues than AGX). As a characteristic feature, monocot AGX contain *p*-hydroxycinnamic acid residues such as ferulic acid residue (FA) and coumaric acid residue (CA). Feruloylation occurs via an ester linkage at the C-5 position of α-L-Ara*f* side chain through the carboxylic group of FA (Figure 7). This FA residue can further form an ether linkage with lignin though its hydroxyl group (lignin-ferulate-xylan complex [47]), or it can cross-link two AGX chains through dimer formation (Figure 8; [48]). FA can represent up to 3% of the dry weight of graminae cell walls. The FA ester-ether bridges between AGX and lignin have been shown to aid in increasing pathogen resistance, and reducing the cell-wall digestibility and fermentability of graminae biomass [48].

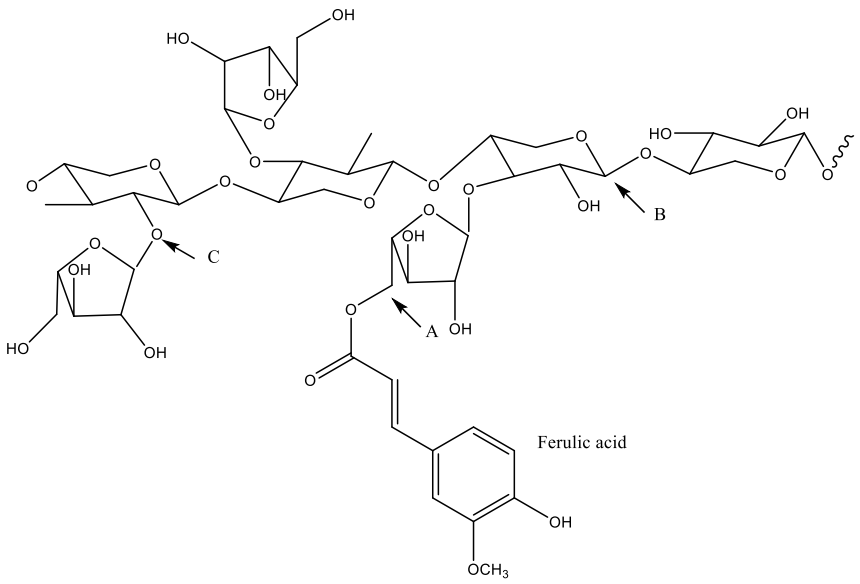

Figure 7: Representative structure of arabinoglucuronoxylan typical of graminae biomass, with (A) Ferulic acid ester linked to O-5 of α-L-Ara*f*; (B) β-(1→4) linked D- Xyl*p* backbone; (C) α-(1→2) linked L-Ara*f*. Redrawn from [48]

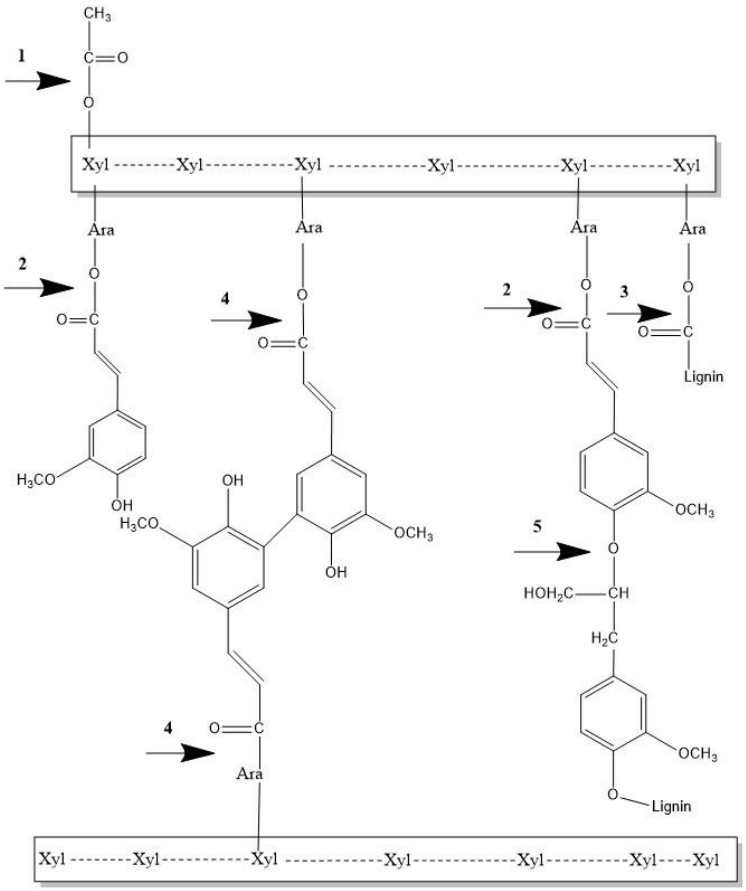

Figure 8: Ferulic acid (FA) bridge between two arabinoglucuronoxylan (AGX) chains in grasses (1) acetyl group (2) ester linked FA to AGX (3) arabinose-lignin (Lignin-carbohydrate complex – LCC) (4) 5-5 ester linked FA dimer cross linking AGX chains (5) FA ether linked to lignin. Reprinted with permission from [48]

5.1.3. Lignin:

Lignin is a polymer of phenylpropanoid units. It is the most abundant aromatic polymer, and accounts for approximately 30% of the total organic carbon in the biosphere [49]. It has been commonly believed that lignin evolved as an adaptation of plants to a terrestrial life, to provide biomechanical support and hydrophobicity, and protection from UV-radiation, and from terrestrial herbivores. The ability to deposit lignin in cell walls arose with tracheophytes, allowing them a significant survival advantage, as compared to their predecessors [50].

Softwoods contain 26-32% lignin by weight, while hardwoods contain 20-30% lignin [27]. Graminae biomass contains the lowest amount of lignin by weight, ~17-20% [30], [51]. Compared to celluloses and hemicelluloses, lignin does not have a precisely defined structure, and in fact is a generic term for a large group of aromatic polymers, derived from hydroxycinnamyl alcohols (monolignols): *p*-coumaryl alcohol, coniferyl alcohol, and sinapyl alcohol, which produce corresponding *p*-hydroxyphenyl (H), guaiacyl (G), and syringyl (S) units [26] (Figure 9, Figure 10).

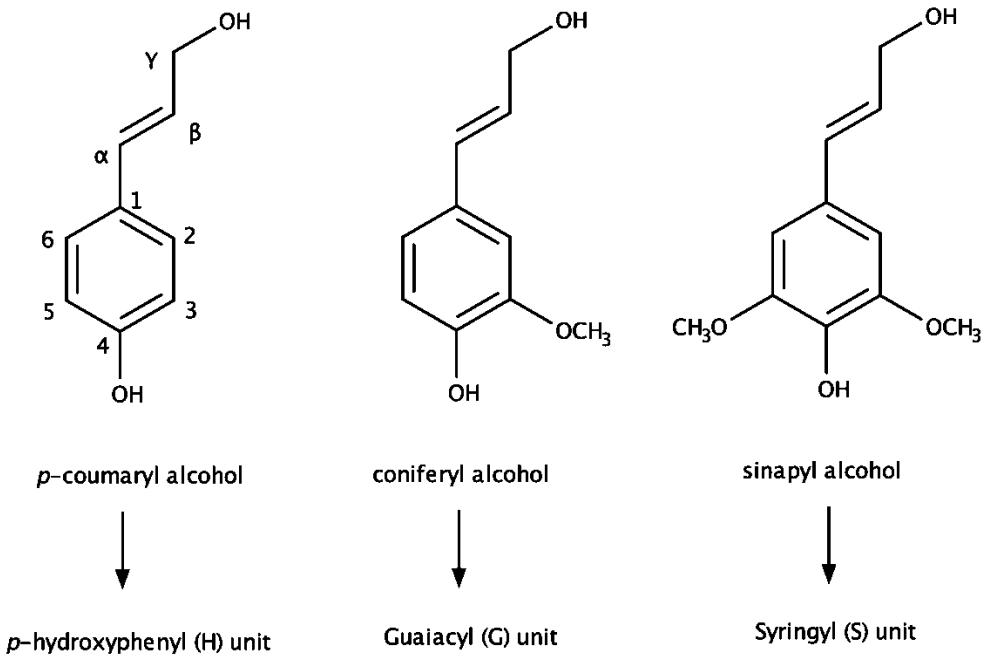

Figure 9: Monolignols and lignin units. Redrawn from [52]

Softwood lignins are composed of G- (dominant) and H-units (minor amounts), while hardwood lignins are composed of S- and G-units (variable proportions). Graminae biomass contains H-units, in addition to S- and G-units [53]. Additionally, some uncommon units and linkages might be also be present depending on the species, as described in later sections. The different lignin units are linked through multiple potential C-O-C (ether) and C-C structures (Table 4). Although

the frequency of occurrence of these linkages is dependent on the species, ether linkages dominate, making up to two thirds or more of total linkages [27].

Table 4: Proportions of different types of linkages connecting the phenylpropane units in lignin [27], [54], [55]

Linkage type	Dimer structure	Percent of total linkages		
		Softwood[c]	Hardwood[c]	Graminae
β-O-4	Arylglycerol-β-aryl ether	50	60	57[a]-75[b]
α-O-4	Noncyclic benzyl aryl ether	2-8	7	7[a] -11[b]
β-5/α-O-4	Phenylcoumaran	9-12	6	-
5-5	Biphenyl	10-11	5	-
4-O-5	Diaryl ether	4	7	-
β-1	1,2-Diaryl propane	7	7	-
β-β	Linked through side chains	2	3	4[a] -8[b]
5-5/β-O-4/α-O-4	Dibenzodioxocin	4-5 [102]	Trace [102]	3[b]

[a] Wheat straw milled wood lignin (MWL)[54]
[b] Miscanthus organosolv lignin [55]

Functional groups on lignin:

Functional groups greatly affect the reactivity of lignin. Similar to its precursors, the lignin polymer contains a variety of functional groups. One of the most important determinants of lignin reactivity are the characteristic phenyl hydroxyl (PhOH) groups of lignin. Only a relatively few phenolic hydroxyls are free, since most of them are occupied through linkages to neighboring units. The syringyl groups in hardwood lignin are especially etherified. In addition to these, aliphatic hydroxyl, benzyl alcoholic, methoxyl and some terminal aldehyde groups are also found (Table 5) [27].

Table 5: Functional groups of lignin (per 100 C6C3 units) [27]

Group	Softwood lignin	Hardwood lignin
Methoxyl	92-97	139-158
Phenolic hydroxyl	15-30	10-15
Benzyl alcohol	30-40	40-50
Carbonyl	10-15	-

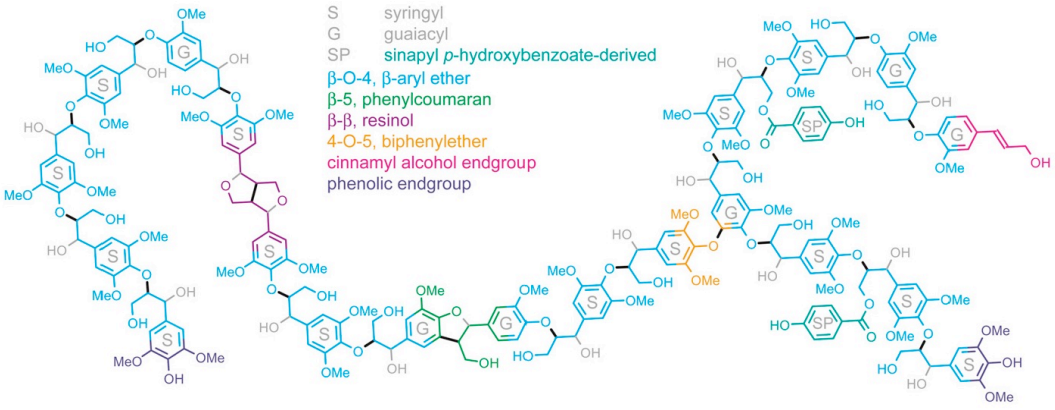

Figure 10: NMR-analysis predicted structure of poplar lignin, showing major lignin units, linkages and functional groups. Reprinted with permission from [52]

Uncommon structures in lignin:

Apart from the above-mentioned common lignin units and linkages, lignin has been reported to carry various uncommon units. For example, esters of *p*-hydroxybenzoic acid are typical in willow (4.4% - 6.5%, Figure 11) and aspen lignins (hardwoods) [27], [56].

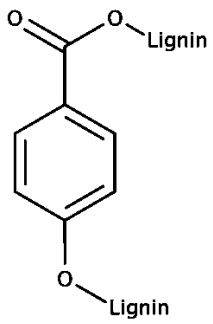

Figure 11: Possible lignin linkages to p-hydroxybenzoate. Redrawn from [56]

A characteristic feature of graminae lignin is the presence of *p*-hydroxycinnamic acid residues, FA and CA [48], [48]. Apart from being ether linked to lignin, evidence suggests that FA acts as a lignin monomer, which is esterified with lignin at the Cγ position during lignin synthesis, providing a branching point and covalently coupling two lignin polymers (Figure 12) [106, 107, 108]. The *p*-coumarate moieties preferentially remain as a decoration on the lignin backbone, and do not produce lignin branching or interconnections [57]. It might be worthy to recall that FA and CA are also associated with the AGX of graminae biomass through the α-L-Ara*f* side chain as described earlier (Figure 8), and are thus able to link lignin with the hemicelluloses, contributing to lignin-carbohydrate complexes.

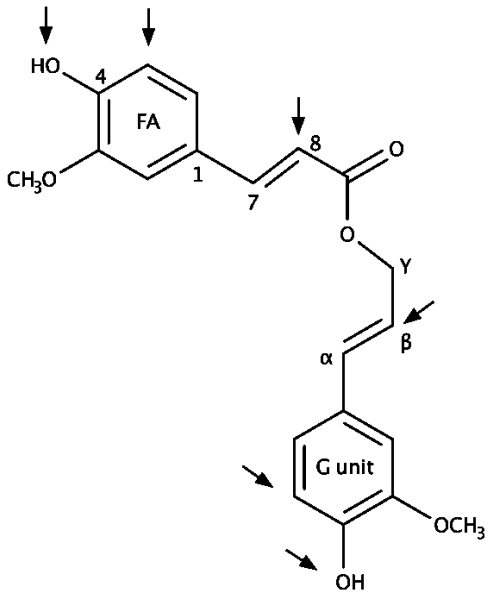

Figure 12: Cγ ester conjugate between ferulic acid (FA) and G unit of lignin. Arrows indicate possible branching points. Redrawn from [58]

Lignin-carbohydrate complexes (LCCs)

The complex chemical moieties formed through the covalent linkages between lignin and hemicelluloses in native wood are termed 'lignin-carbohydrate complex (LCC)' [59]. These linkages are mainly of three types (Figure 13). First are ester linkages between acidic side chains (e.g. MeGlc*p*A, and FA) on hemicelluloses backbone and hydroxyl group on lignin [60]. The second type are benzyl ether linkages: C-1 linkages between the α-position of lignin and OH groups on the side chain sugars on O-2 or O-3 of xylose backbone and C-2 linkages between the α-position of lignin and secondary OH groups of carbohydrates, mainly of lignin-xylan type [61]. Ester linkages are alkali-labile, while benzyl ether linkages are more common and stable in alkaline conditions [62]. The third and the least common are phenyl-glycosidic linkages between the C-1 of hemicelluloses backbone and lignin [47].

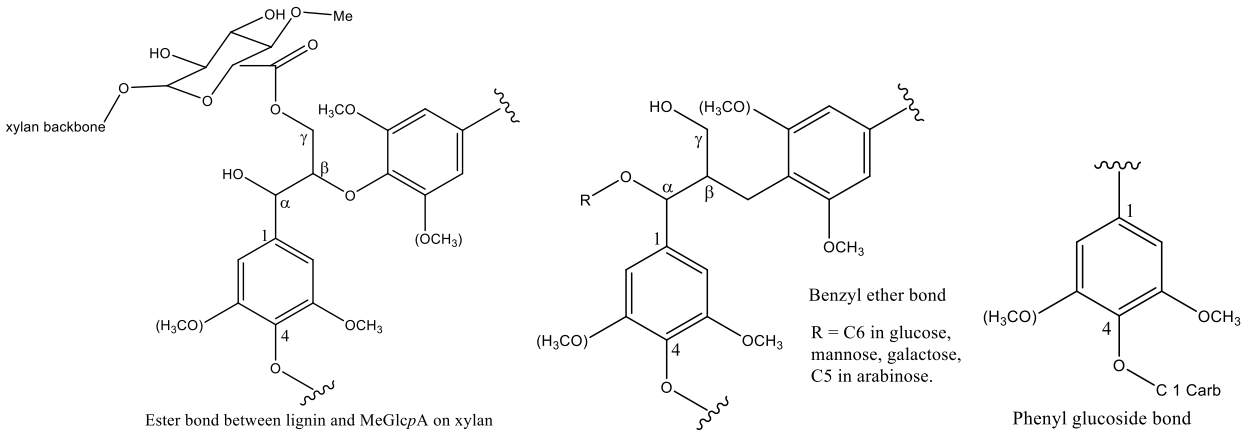

Figure 13: Types of LCC linkages. Redrawn from [61].

Due to the hydrophobic nature of lignin and the partial hydrophobic-hydrophilic nature of xylans, a core-corona structure has been proposed for LCCs in solutions, with hydrophobic lignin core surrounded by xylans that have their hydrophilic side chains oriented toward the surface [42]. LCCs have a significant effect on delignification and have also been reported to possess biological activity [63]–[66]. Additional effects such as contribution to the recalcitrance of graminae biomass toward digestion have been mentioned earlier.

Lignin as polymer:

The weight-average molecular weight (M*w*) of softwood lignins has been reported to be of the order of 20,000 g/mol, whereas lower values have been reported for hardwood lignins. The polydispersity has been reported around 2.5-3 for softwood milled wood lignin [27]. The average length of a linear lignin chain in poplar lignin has been estimated to be between 13 and 20 units [52].

Table 6: Average molecular weights and polydispersity indices (PDI) of selected milled wood lignins [51]

Biomass	M*n* (g/mol)	M*w* (g/mol)	PD
Eucalyptus[b]	2600	6700	2.6
Norway spruce[a]	6400	23500	3.7
Southern Pine[b]	4700	14900	3.2
Bamboo	5410	12090	2.23
Miscanthus	8300	13700	1.65

[a] Vibratory milled
[b] Ball milled for 28 days

6. Biomass recalcitrance and the need for pretreatment in a biorefinery:

The composite structure of LCB, made of intertwined and cross-linked polymers renders it recalcitrant to processes necessary for harvesting materials, chemicals and energy from it. Therefore, a pretreatment is required to make LCB more susceptible to subsequent processes. Specific factors which are suggested to contribute to biomass recalcitrance are:

(1) Crystallinity, high degree of polymerization, and low solubility of cellulose in most solvents;

(2) Highly organized supermolecular structure of cellulose as microfibrils;

(3) Presence of hemicelluloses and lignin surrounding the cellulose matrix, thus sheathing cellulose and decreasing the accessible surface area;

(4) Cross-linking within and between the matrices (e.g. lignin-carbohydrate complexes);

The goals of a pretreatment are to make cellulose more accessible to chemicals or enzymes, usually by partial removal of hemicelluloses / lignin from the biomass and/or disrupting the

crystalline structure of cellulose [67] (Figure 14). An ideal pretreatment fulfills following specific criteria [68], [69], where it:

(1) Minimizes energy demands and costs;

(2) Is suitable for multiple species;

(3) Produces highly accessible pretreated solid;

(4) Limits formation of degradation products that inhibit growth of fermentative microorganisms;

(5) Allows generation of a higher-value lignin co-product;

(6) Limits use of environmentally harmful chemicals, and generation of toxic waste.

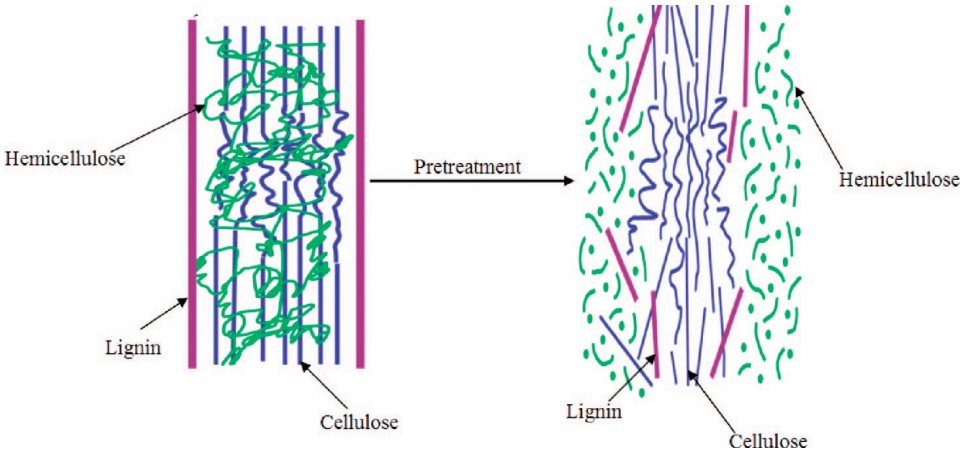

Figure 14: Goals of a pretreatment on lignocellulosic material. Reprinted with permission from [67]

Numerous pretreatments have been proposed, including physical, chemical, and biological processes [68]. A summary of selected cost-effective pretreatments and their effects on LCB is presented in Table 7.

Table 7: Effect of pretreatment methods on lignocellulosic biomass [68], [70]

Pretreatment	Increase Surface area	Decrease Cellulose crystallinity	Removal Hemicelluloses	Removal Lignin	Change lignin structure	Generation Fermentation inhibitors	Advantages	Challenges
Liquid hot water	■	□	■		□	□	No chemicals, high sugar yield	Large water req.
Steam explosion	■	□	■		□	■ (at higher temp)	Short time, Low energy	Lignin condensation on biomass
Ammonium fiber explosion (AFEX)	■	■	□	■	■	□	Dry process, high cellulose retention	Corrosive materials, special reactor req.
Mild alkali	■	ND	□	■	■		Limited sugar degradation as compared to dilute acid	Lignin degradation
Dilute acid	■		■		■	■	High reaction rates	Degradation of extracted sugars; Corrosive materials, special reactor req.

■: Major effect
□: Minor effect
ND: Not determined

6.1. Liquid hot-water pretreatments – Hot-water extraction (HWE):

Liquid hot-water pretreatments use pressure to maintain the water in a liquid state at elevated temperatures (160-240^{o}C) [69]. The objective of these pretreatments is mainly to solubilize the hemicellulose to make cellulose more accessible. The cellulose-enriched biomass can be utilized in a wide range of cellulose fiber based applications, while the removed xylan-based carbohydrates can be recovered from the hydrolyzate and further utilized to produce an array of

products, including fuels, chemicals, and polymers, such as ethanol, furfural, lactic acid, and polyhydroxyalkanoates [18], [71], [72].

These pretreatments are environmentally preferred, since there is no need to add external chemicals - the catalysts required for the hydrolysis and dissolution of lignocellulosic constituents are derived from the LCB itself (hence often referred to as autohydrolysis). Hot-water extraction (HWE) is an example of liquid hot water pretreatment. This treatment is more effective on xylan-rich LCB, and has been suggested as a suitable pretreatment for angiosperms (hardwoods and graminae) [18]. It uses water at subcritical conditions (160-170ºC, 2 hours), and also follows the mechanism of in situ-acid catalyzed hydrolysis (autohydrolysis) [18], [73]. Under these conditions, hydronium ions are initially generated by auto-ionization of water. In the later stages, acetyl groups of xylans are hydrolyzed producing acetic acid (up to 90% of the initial acetyl groups may be removed). Deacetylation lowers the pH of the extraction liquor, and leads to acid-catalyzed cleavage of the glycosidic bonds of xylan [74]. Hydronium ions catalyze the cleavage of glycosidic bonds at random intervals on the xylan chain, causing depolymerization to form xylan oligomers of a lower degree of polymerization (DP). The oligomers are dissolved and extracted into the liquid phase when DP falls below 25. Due to the higher susceptibility of the glycosidic linkages to acid-catalyzed cleavage, xylan that is not chemically bound to lignin is removed first. Xylan covalently bound to lignin (LCC; Figure 11) is then removed at a relatively slower rate [75]. The solubility of xylans is influenced by molecular weight and the presence of side chain substituents. Acetyl groups, arabinose and α-Me-α-D-Glc*p*A on xylan chain usually increase the xylan solubility, while association with lignin lowers its solubility [75]. The severity of the HWE treatment is indicated by the P-factor

(standing for prehydrolysis; Eqn. 1), which takes into account the temperature and the duration of the treatment, and correlates well with the degree of xylan removal [76], [77].

$$\text{P-factor} = \int_0^t e^{\left(40.48 - \frac{15106}{T}\right)} dt \qquad (1)$$

where, T is the extraction temperature in Kelvin, and t is the extraction time in hours.

The acidic conditions present during HWE may further degrade the hemicelluloses removed from LCB to C6 and C5 monosaccharides. The C6 (hexoses) and C5 (pentoses) monosaccharides may further be converted to 5-hydroxymethylfurfural and furfural, respectively by acid-catalyzed degradation [18]. These degradation products have been recognized as fermentation inhibitors, and are undesirable in fermentation-based applications [18].

While hemicelluloses (xylans) are affected the most during HWE, lignin is also partially removed during this process in variable amounts (10-40%) depending on the species (Table 8). In general, benzyl ether linkages are more susceptible, leading to an increase in phenolic hydroxyl groups on lignin [78]. Acidic conditions during the autohydrolysis lead to formation of a carbonium ion by proton-induced elimination of water from the benzylic position. In the β-O-4 structure, the carbonium ion may further react with cleavage of β-ether linkage. However, in the presence of other electron-rich carbons, such as C-2/C-6 of S and G units of lignin, condensation reactions may occur, leading to simultaneous repolymerization of lignin (Figure 15) [78].

Table 8: Delignification in selected species after hot-water extraction at 160 ºC, 2 hours

Species	Reactor volume	Water: Biomass	Delignification % lignin removed
Willow (*Salix spp.*) [28]	65 ft^3	4.5	16.7
Sugar maple [73] (*Acer saccharum*)	300 cm^3	50	30.4
	4 L	4	9.4
	65 ft^3	4	17.2
Paulownia tomentosa [73]	300 cm^3	50	26.1
	4 L	8	15.7
Paulownia elongata [73]	300 cm^3	50	20.9
Miscanthus spp.[29]	300 cm^3	40	42.8
	4 L	10	32.5
	65 ft^3	8	32.1
Wheat straw (*Triticum spp.*)	65 ft^3	8	26
Apricot pit shell [79] (*Prunus armeniaca*)	300 cm^3	20	24

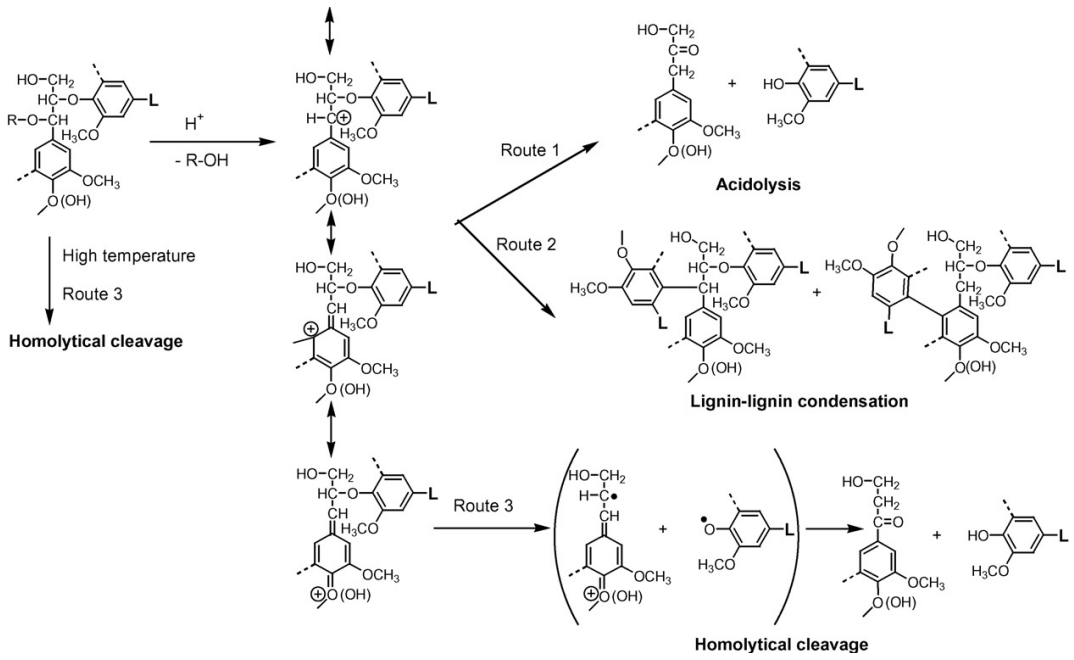

Figure 15: Degradation routes for β-O-4 linkages between lignin units. Route 1 and 3: Lignin depolymerization; Route 2: Lignin repolymerization. Reprinted with permission from [78]

Lignin is a desirable by-product of HWE, which can be recovered from hot-water autohydrolyzates by acid-induced precipitation, and can be utilized as a renewable source of chemicals / materials by the biorefineries, as suggested at the beginning of this chapter.

7. Lignin valorization

In spite of the considerable efforts made in lignin exploration, utilization of lignins for the production of value-added products faces multiple challenges: Lignin has evolved to be a robust polymer with a highly heterogenous structure, which makes it resistant to chemical or enzymatic degradation [80]. Additionally, its relatively high molecular weight and amorphous nature result in limited solubility, and further limit its utilization potential [80]. However, the challenges presented by lignin also present opportunities. The intrinsically polymeric form and aromatic nature of lignin and its high energy-density make lignin an ideal starting material for production of fuels, value-added chemicals, and functional materials. The most common current application

of lignin is its direct use in power production, which is priced at $50 per ton. In contrast, the more profitable applications of lignin involve its conversion to BTX chemicals and phenol [80]. The average prices of BTX and phenol are around $1200 and $1500 per ton. Apart from fine chemicals, lignin also has a tremendous potential to be used in polymeric materials (e.g. resins, thermoplastics, etc. as described in later sections), due to its wide availability, aromatic structure, and a variety of potential modifications offered by its chemical nature [81]. On average, the use of lignin as a bioproduct can increase it price many times than when its used as a fuel. Despite of the lucrative market size, only 2% of the lignin produced from the pulp industry is used for value-added products [82].

7.1. Technical sources of lignin:

Technical lignins originate from different LCB sources and separation processes. Hence, they differ from each other to a significant extent. Current industry practices mainly focus on optimization of fermentable sugar yields, and hence can cause significant structural modifications on native lignin [80]. Selected technical lignins are described below. A summary of properties of technical lignins is compared to an example of lignin recovered from hot-water autohydrolyzate is shown in Table 9.

Kraft lignin: Kraft lignin is the product of sulfate (kraft) pulping process. Kraft pulping uses an aqueous solution of sodium hydroxide and sodium sulfide to solubilize lignin and hemicelluloses to produce the so-called black liquor [81], [82]. During this process, lignin undergoes degradation and condensation reactions, resulting in significant structural modification [Crestini]. The annual worldwide production of Kraft pulp equals 130 million tons, giving rise to approximately 55-90 million tons of Kraft lignin, that is mainly used for energy purposes [83].

Soda lignin: Soda lignin is a co-product derived from soda or soda-anthraquinone process. This process uses alkaline solutions to dissolve lignin at conditions similar to Kraft, but differs from the Kraft process mainly with the sulfur-free medium of cooking liquor. As a result, soda lignin is sulfur-free, as opposed to Kraft lignin and lignosulfonates [82]. The absence of sulfur makes this lignin more suitable for polymeric applications [81].

Lignosulfonates / (bi)sulfite lignin: These are water-soluble anionic polyelectrolytes, containing charged groups. This lignin originates from the sulfite cooking, involving HSO_3^- and SO_3^{2-} [82]. High amounts of sulfur are incorporated into the lignin structure during cooking, bound to the benzylic carbon. This type of lignin is used as a dispersant, and additive in coal-water slurry [81].

Organosolv lignin: Organosolv lignin is obtained through the organosolv pulping. This process uses a mixture of organic solvents (e.g. acetic acid, formic acid, ethanol) and water as the cooking medium. This lignin a lower molecular weight, lower polydispersity, and higher chemical purity than the other types of technical lignins, and is more similar to native lignin than others described above, due to the limited condensation reactions [81], [82]. It is, however, hydrophobic and has low water solubility, and it is hard to commercialize due to the high capital investments required because of high recovery costs.

Table 9: Physicochemical properties of technical lignins [81], [82], compared with lignin recovered after hot-water extraction [29]

Lignin	Ash content (% w/w)	Sulfur content (% w/w)	Lignin content (% w/w)	Carbohydrate content (% w/w)	Molecular weight (Mw)	Polydispersity	Annual production (kt/yr)[e]
Kraft	27.1 [a]	1.0 – 3	66.1[a]	3.28	1500-500 Up to 25000	2.5 – 3.5	~90
Soda[d]	0.74 [a]	0	97.7[a]	2.39	1000-3000 Up to 15000	2.5 – 3.5	~5-10
Ligno-sulfonates	9.3 [a, b]	3.5 – 8	56.5 [a, b]	NA	1000-50000 Up to 150,000	4.2 – 7	~1000
Organosolv	1.71 [a, c]	0	94.2 [a, c]	1.16	500-5000	1.5	~3
Miscanthus lignin recovered from hot-water autohydrolyzate [20]							
Recovered lignin	0.4	NA	87	4.9	9805	3.8	NA

[a]: [84]
[b]: Lignosulfonate from unidentified feedstock
[c]: Miscanthus sinensis organosolv lignin
[d]: Soda-anthraquinone lignin from a mix of fiber plants
[e]: Average values [81]

7.2. Applications of lignin as a polymer:

Lignin in biocomposites: Lignin has been used in combination with natural fibers to form composite materials of low density, good biodegradability and biocompatibility. The intended applications of lignin-based biocomposites are in the field of industrial engineering, biomedical engineering, and electronic or automotive industry applications. An example is Arborform®, developed from injectiction molding of lignin matrix (30-60%), natural fibers like hemp or flax (10-60%) and other additives (0-20%) [82]. Lignin-polylactic acid (PLA) composites have also been reported for biomedical applications and for 3D printing [85], [85].

Lignin in thermoplastics: Lignin has been used as a filler, matrix, coupling agent, or compatibilizer in thermoplastic blends or composites [86]–[88]. Incorporation of lignin in thermoplastics has been reported to lower the water absorption and swelling, while improving

the thermal properties [82]. Additionally, lignin has been reported to confer antibacterial and biodegradation properties to the thermoplastic materials, useful in food-packaging applications. However, lignin exhibits low compatibility with these materials, and requires structural modification in order to be blended with these materials.

Lignin in phenol-formaldehyde (PF) resins: Being a phenolic polymer, lignin has been used to replace phenols in resin applications [87]. Replacement of up to 70% phenol by lignosulfonates has been reported in production of lignin-phenol-formaldehyde resins for plywood, without any significant changes to plywood failure. Additionally, lignin-phenol-glyoxal resins have also been reported, which avoid the use of toxic formaldehyde [89].

Lignin for carbon fibers and activated carbon [44, 70, 71, 72]: Carbon fibers are versatile materials useful in various industrial fields. These are lightweight materials, which possess high mechanical strength. The traditional precursor of carbon fibers (polyacrylonitrile) is not cost-efficient. Use of non-petroleum precursor, such as lignin, has hence been recommended for carbon fiber production. Lignin is expected to save up to 49% total production cost. Lignin is also being investigated as a precursor of activated carbon in carbon anodes [90]–[92].

Lignin-base hydrogels: Reviewed in Chapter 3.

References:

[1] E. Sjöström and R. Alen, *Analytical Methods in Wood Chemistry, Pulping, and Papermaking*. Springer Science & Business Media, 2013.

[2] M. Norgren and H. Edlund, "Lignin : Recent advances and emerging applications," *Curr. Opin. Colloid Interface Sci.*, vol. 19, pp. 409–416, 2014.

[3] I. Demuner, J. Colodette, and A. Demuner, "Biorefinery review: Wide-reaching products through kraft lignin," *BioResources*, vol. 14, pp. 7543–7481, 2019.

[4] A. Grossman and W. Vermerris, "Lignin-based polymers and nanomaterials," *Curr. Opin. Biotechnol.*, vol. 56, pp. 112–120, Apr. 2019, doi: 10.1016/j.copbio.2018.10.009.

[5] A. J. Ragauskas *et al.*, "Lignin valorization: improving lignin processing in the biorefinery," *Science*, vol. 344, no. 6185, p. 1246843, May 2014, doi: 10.1126/science.1246843.

[6] "Lignin Market Size Worth $1.12 Billion By 2027 | CAGR: 2.0%." https://www.grandviewresearch.com/press-release/global-lignin-market (accessed Jul. 27, 2020).

[7] R. N. Olcese, J. Francois, M. M. Bettahar, D. Petitjean, and A. Dufour, "Hydrodeoxygenation of Guaiacol, A Surrogate of Lignin Pyrolysis Vapors, Over Iron Based Catalysts: Kinetics and Modeling of the Lignin to Aromatics Integrated Process," *Energy Fuels*, vol. 27, no. 2, pp. 975–984, Feb. 2013, doi: 10.1021/ef301971a.

[8] M. N. Collins *et al.*, "Valorization of lignin in polymer and composite systems for advanced engineering applications - A review," *Int. J. Biol. Macromol.*, vol. 131, pp. 828–849, Jun. 2019, doi: 10.1016/j.ijbiomac.2019.03.069.

[9] W. K. El-Zawawy, "Preparation of hydrogel from green polymer," *Polym. Adv. Technol.*, vol. 16, no. 1, pp. 48–54, 2005, doi: 10.1002/pat.537.

[10] W. K. El-Zawawy and M. M. Ibrahim, "Preparation and characterization of novel polymer hydrogel from industrial waste and copolymerization of poly(vinyl alcohol) and polyacrylamide," *J. Appl. Polym. Sci.*, vol. 124, no. 5, pp. 4362–4370, 2012, doi: 10.1002/app.35481.

[11] Q. Feng, F. Chen, and H. Wu, "Preparation and characterization of a temperature-sensitive lignin-based hydrogel," *BioResources*, vol. 6, no. 4, pp. 4942–4952.

[12] L. I. Grishechko *et al.*, "New tannin–lignin aerogels," *Ind. Crops Prod.*, vol. 41, pp. 347–355, Jan. 2013, doi: 10.1016/j.indcrop.2012.04.052.

[13] Z. Peng and F. Chen, "Synthesis and Properties of Lignin-Based Polyurethane Hydrogels," *Int. J. Polym. Mater. Polym. Biomater.*, vol. 60, no. 9, pp. 674–683, Aug. 2011, doi: 10.1080/00914037.2010.551353.

[14] L. Passauer *et al.*, "Dynamic Moisture Sorption Characteristics of Xerogels from Water-Swellable Oligo(oxyethylene) Lignin Derivatives," *ACS Appl. Mater. Interfaces*, vol. 4, no. 11, pp. 5852–5862, Nov. 2012, doi: 10.1021/am3015179.

[15] D. Ciolacu, A. M. Oprea, N. Anghel, G. Cazacu, and M. Cazacu, "New cellulose–lignin hydrogels and their application in controlled release of polyphenols," *Mater. Sci. Eng. C*, vol. 32, no. 3, pp. 452–463, Apr. 2012, doi: 10.1016/j.msec.2011.11.018.

[16] L. Perez-Cantu, F. Liebner, and I. Smirnova, "Preparation of aerogels from wheat straw lignin by cross-linking with oligo(alkylene glycol)-α,ω-diglycidyl ethers," *MICROPOROUS MESOPOROUS Mater.*, vol. 195, pp. 303–310, 2014.

[17] D. Mahata *et al.*, "Lignin-graft-Polyoxazoline Conjugated Triazole a Novel Anti-Infective Ointment to Control Persistent Inflammation," *Sci. Rep.*, vol. 7, Apr. 2017, doi: 10.1038/srep46412.

[18] T. E. Amidon, C. D. Wood, A. M. Shupe, Y. Wang, M. Graves, and S. Liu, "Biorefinery: Conversion of Woody Biomass to Chemicals, Energy and Materials," Jun. 2008. https://www.ingentaconnect.com/content/asp/jbmb/2008/00000002/00000002/art00002 (accessed May 07, 2020).

[19] "Acer saccharum Marsh." https://www.srs.fs.usda.gov/pubs/misc/ag_654/volume_2/acer/saccharum.htm (accessed Jul. 27, 2020).

[20] M. C. Heller, G. A. Keoleian, M. K. Mann, and T. A. Volk, "Life cycle energy and environmental benefits of generating electricity from willow biomass," *Renew. Energy*, vol. 29, no. 7, pp. 1023–1042, Jun. 2004, doi: 10.1016/j.renene.2003.11.018.

[21] T. A. Volk, J. P. Heavey, and M. H. Eisenbies, “Advances in shrub-willow crops for bioenergy, renewable products, and environmental benefits,” *Food Energy Secur.*, vol. 5, no. 2, pp. 97–106, 2016, doi: 10.1002/fes3.82.
[22] E. A. Heaton, F. G. Dohleman, and S. P. Long, “Meeting US biofuel goals with less land: the potential of Miscanthus,” *Glob. Change Biol.*, vol. 14, no. 9, pp. 2000–2014, 2008, doi: 10.1111/j.1365-2486.2008.01662.x.
[23] M. P. Yadav and K. B. Hicks, “Isolation, characterization and functionalities of bio-fiber gums isolated from grain processing by-products, agricultural residues and energy crops,” *Food Hydrocoll.*, vol. 78, pp. 120–127, May 2018, doi: 10.1016/j.foodhyd.2017.04.009.
[24] Fitria, H. Ruan, S. C. Fransen, A. H. Carter, H. Tao, and B. Yang, “Selecting winter wheat straw for cellulosic ethanol production in the Pacific Northwest, U.S.A,” 2019, Accessed: Jul. 27, 2020. [Online]. Available: https://pubag.nal.usda.gov/catalog/6341062.
[25] H. K. Ju, H. W. Chung, S.-S. Hong, J. H. Park, J. Lee, and S. W. Kwon, “Effect of steam treatment on soluble phenolic content and antioxidant activity of the Chaga mushroom (Inonotus obliquus),” *Food Chem.*, vol. 119, no. 2, pp. 619–625, Mar. 2010, doi: 10.1016/j.foodchem.2009.07.006.
[26] S. Wasser, “Medicinal mushroom science: Current perspectives, advances, evidences, and challenges,” *Biomed. J.*, vol. 37, no. 6, p. 345, 2014, doi: 10.4103/2319-4170.138318.
[27] E. Sjöström, *Wood Chemistry*, 2nd ed. Elsevier, 1993.
[28] A. Nagardeolekar, M. Ovadias, K.-T. Wang, and B. Bujanovic, “Willow Lignin Recovered from Hot-Water Extraction for the Production of Hydrogels and Thermoplastic Blends,” *ChemSusChem*, vol. n/a, no. n/a, Jul. 2020, doi: 10.1002/cssc.202001259.
[29] K.-T. Wang *et al.*, “Toward Complete Utilization of Miscanthus in a Hot-Water Extraction-Based Biorefinery,” *Energies*, vol. 11, no. 1, Art. no. 1, Jan. 2018, doi: 10.3390/en11010039.
[30] J. Littlewood, R. J. Murphy, and L. Wang, “Importance of policy support and feedstock prices on economic feasibility of bioethanol production from wheat straw in the UK,” *Renew. Sustain. Energy Rev.*, vol. 17, no. C, pp. 291–300, 2013.
[31] R. J. Moon, A. Martini, J. Nairn, J. Simonsen, and J. Youngblood, “Cellulose nanomaterials review: structure, properties and nanocomposites,” *Chem. Soc. Rev.*, vol. 40, no. 7, pp. 3941–3994, Jun. 2011, doi: 10.1039/C0CS00108B.
[32] A. Ebringerová, Z. Hromádková, and T. Heinze, “Hemicellulose,” in *Polysaccharides I: Structure, Characterization and Use*, T. Heinze, Ed. Berlin, Heidelberg: Springer, 2005, pp. 1–67.
[33] X.-W. Peng, J.-L. Ren, L.-X. Zhong, F. Peng, and R.-C. Sun, “Xylan-rich Hemicelluloses-graft-Acrylic Acid Ionic Hydrogels with Rapid Responses to pH, Salt, and Organic Solvents,” *J. Agric. Food Chem.*, vol. 59, no. 15, pp. 8208–8215, Aug. 2011, doi: 10.1021/jf201589y.
[34] A. Ebringerová and T. Heinze, “Xylan and xylan derivatives – biopolymers with valuable properties, 1. Naturally occurring xylans structures, isolation procedures and properties,” *Macromol. Rapid Commun.*, vol. 21, no. 9, pp. 542–556, 2000, doi: 10.1002/1521-3927(20000601)21:9<542::AID-MARC542>3.0.CO;2-7.
[35] A. Teleman, *5. Hemicelluloses and Pectins*. De Gruyter, 2009, pp. 101–120.
[36] F. Peng, P. Peng, F. Xu, and R.-C. Sun, “Fractional purification and bioconversion of hemicelluloses,” *Biotechnol. Adv.*, vol. 30, no. 4, pp. 879–903, Jul. 2012, doi: 10.1016/j.biotechadv.2012.01.018.
[37] S. K. Bose, V. A. Barber, E. F. Alves, D. J. Kiemle, A. J. Stipanovic, and R. C. Francis, “An improved method for the hydrolysis of hardwood carbohydrates to monomers.,” *Carbohydr. Polym.*, vol. 78, no. 3, pp. 396–401, 2009.
[38] T. Jm, D. Lc, A.-C. Mt, and G. Fm, “The influence of hexoses addition on the fermentation of d-xylose in Debaryomyces hansenii under continuous cultivation.,” *Enzyme Microb. Technol.*, vol. 26, no. 9–10, pp. 743–747, Jun. 2000, doi: 10.1016/s0141-0229(00)00166-6.
[39] A. Teleman, J. Lundqvist, F. Tjerneld, H. Stålbrand, and O. Dahlman, “Characterization of acetylated 4-O-methylglucuronoxylan isolated from aspen employing 1H and 13C NMR spectroscopy,” *Carbohydr. Res.*, vol. 329, no. 4, pp. 807–815, Dec. 2000, doi: 10.1016/S0008-6215(00)00249-4.
[40] W. G. Glasser, “Isolation options for non-cellulosic heteropolysaccharides (HetPS),” *Cellulose*, vol. 7, no. 3, pp. 299–317, Mar. 2009.
[41] G. O. Aspinall, “Chemistry of cell wall polysaccharides,” *Biochem. Plants Compr. Treatise USA*, 1980, Accessed: Jul. 27, 2020. [Online]. Available: https://agris.fao.org/agris-search/search.do?recordID=US8834617.

[42] F. B. Sedlmeyer, “Xylan as by-product of biorefineries: Characteristics and potential use for food applications,” *Food Hydrocoll.*, vol. 25, no. 8, pp. 1891–1898, Dec. 2011, doi: 10.1016/j.foodhyd.2011.04.005.
[43] C. Alvarez-Vasco and X. Zhang, “Alkaline hydrogen peroxide (AHP) pretreatment of softwood: Enhanced enzymatic hydrolysability at low peroxide loadings,” *Biomass Bioenergy*, vol. 96, pp. 96–102, Jan. 2017, doi: 10.1016/j.biombioe.2016.11.005.
[44] F. E. M. Van Dongen, D. Van Eylen, and M. A. Kabel, “Characterization of substituents in xylans from corn cobs and stover,” *Carbohydr. Polym.*, vol. 86, no. 2, pp. 722–731, Aug. 2011, doi: 10.1016/j.carbpol.2011.05.007.
[45] R. B. Garcia, J. L. M. S. Ganter, and R. R. Carvalho, “Solution properties of D-xylans from corn cobs,” *Eur. Polym. J.*, vol. 36, no. 4, pp. 783–787, Apr. 2000, doi: 10.1016/S0014-3057(99)00133-0.
[46] R. Deutschmann and R. F. H. Dekker, “From plant biomass to bio-based chemicals: latest developments in xylan research,” *Biotechnol. Adv.*, vol. 30, no. 6, pp. 1627–1640, Dec. 2012, doi: 10.1016/j.biotechadv.2012.07.001.
[47] A. Cornu, J. Besle, P. Mosoni, and E. Grenet, “Lignin-carbohydrate complexes in forages: structure and consequences in the ruminal degradation of cell-wall carbohydrates,” *Reprod. Nutr. Dev.*, vol. 34, no. 5, pp. 385–398, 1994.
[48] M. M. de O. Buanafina, “Feruloylation in Grasses: Current and Future Perspectives,” *Mol. Plant*, vol. 2, no. 5, pp. 861–872, Sep. 2009, doi: 10.1093/mp/ssp067.
[49] J. Ralph, G. Brunow, and W. Boerjan, “Lignins,” in *eLS*, American Cancer Society, 2007.
[50] J.-K. Weng and C. Chapple, “The origin and evolution of lignin biosynthesis,” *New Phytol.*, vol. 187, no. 2, pp. 273–285, 2010, doi: 10.1111/j.1469-8137.2010.03327.x.
[51] A. Tolbert, H. Akinosho, R. Khunsupat, A. K. Naskar, and A. J. Ragauskas, “Characterization and analysis of the molecular weight of lignin for biorefining studies,” *Biofuels Bioprod. Biorefining*, vol. 8, no. 6, pp. 836–856, 2014, doi: 10.1002/bbb.1500.
[52] R. Vanholme, B. Demedts, K. Morreel, J. Ralph, and W. Boerjan, “Lignin Biosynthesis and Structure,” *Plant Physiol.*, vol. 153, no. 3, pp. 895–905, Jul. 2010, doi: 10.1104/pp.110.155119.
[53] M. Baucher, B. Monties, M. V. Montagu, and W. Boerjan, “Biosynthesis and Genetic Engineering of Lignin,” *Crit. Rev. Plant Sci.*, vol. 17, no. 2, pp. 125–197, Mar. 1998, doi: 10.1080/07352689891304203.
[54] J. C. del Río, J. Rencoret, P. Prinsen, Á. T. Martínez, J. Ralph, and A. Gutiérrez, “Structural Characterization of Wheat Straw Lignin as Revealed by Analytical Pyrolysis, 2D-NMR, and Reductive Cleavage Methods,” *J. Agric. Food Chem.*, vol. 60, no. 23, pp. 5922–5935, Jun. 2012, doi: 10.1021/jf301002n.
[55] M. Bergs *et al.*, “Comparing chemical composition and lignin structure of *Miscanthus x giganteus* and *Miscanthus nagara* harvested in autumn and spring and separated into stems and leaves,” *RSC Adv.*, vol. 10, no. 18, pp. 10740–10751, 2020, doi: 10.1039/C9RA10576J.
[56] L. L. Landucci, G. C. Deka, and D. N. Roy, “A13C NMR Study of Milled Wood Lignins from Hybrid Salix Clones,” *Holzforschung*, vol. 46, no. 6, pp. 505–512, Jan. 1992, doi: 10.1515/hfsg.1992.46.6.505.
[57] R. Vanholme, B. De Meester, J. Ralph, and W. Boerjan, “Lignin biosynthesis and its integration into metabolism,” *Curr. Opin. Biotechnol.*, vol. 56, pp. 230–239, Apr. 2019, doi: 10.1016/j.copbio.2019.02.018.
[58] C. G. Wilkerson *et al.*, “Monolignol Ferulate Transferase Introduces Chemically Labile Linkages into the Lignin Backbone,” *Science*, vol. 344, no. 6179, pp. 90–93, Apr. 2014, doi: 10.1126/science.1250161.
[59] N. Westerberg, H. Sunner, M. Helander, G. Henriksson, M. Lawoko, and A. Rasmuson, “Separation of galactoglucomannans, lignin, and lignin-carbohydrate complexes from hot-water-extracted Norway spruce by cross-flow filtration and adsorption chromatography,” *Bioresources*, vol. 7, Aug. 2012, doi: 10.15376/biores.7.4.4501-4516.
[60] F. Nylander, H. Sunner, L. Olsson, P. Christakopoulos, and G. Westman, “Synthesis and enzymatic hydrolysis of a diaryl benzyl ester model of a lignin-carbohydrate complex (LCC),” *Holzforschung*, vol. 70, no. 5, pp. 385–391, May 2016, doi: 10.1515/hf-2014-0347.
[61] J.-L. Wen, S.-L. Sun, B.-L. Xue, and R.-C. Sun, “Recent Advances in Characterization of Lignin Polymer by Solution-State Nuclear Magnetic Resonance (NMR) Methodology,” *Materials*, vol. 6, no. 1, Art. no. 1, Jan. 2013, doi: 10.3390/ma6010359.
[62] A. Toledano, A. García, I. Mondragon, and J. Labidi, “Lignin separation and fractionation by ultrafiltration,” *Sep. Purif. Technol.*, vol. 71, no. 1, pp. 38–43, Jan. 2010, doi: 10.1016/j.seppur.2009.10.024.
[63] H. Sakagami, “Biological Activities and Possible Dental Application of Three Major Groups of Polyphenols,” *J. Pharmacol. Sci.*, vol. 126, no. 2, pp. 92–106, Jan. 2014, doi: 10.1254/jphs.14R04CR.

[64] H. Sakagami, T. Kushida, T. Oizumi, H. Nakashima, and T. Makino, “Distribution of lignin–carbohydrate complex in plant kingdom and its functionality as alternative medicine,” *Pharmacol. Ther.*, vol. 128, no. 1, pp. 91–105, Oct. 2010, doi: 10.1016/j.pharmthera.2010.05.004.
[65] B. Košíková and A. Ebringerová, “Lignin-carbohydrate bonds in a residual soda spruce pulp lignin,” *Wood Sci. Technol.*, vol. 28, no. 4, pp. 291–296, May 1994, doi: 10.1007/BF00204215.
[66] I. Boukari *et al.*, “In Vitro Model Assemblies To Study the Impact of Lignin−Carbohydrate Interactions on the Enzymatic Conversion of Xylan,” *Biomacromolecules*, vol. 10, no. 9, pp. 2489–2498, Sep. 2009, doi: 10.1021/bm9004518.
[67] P. Kumar, D. M. Barrett, M. J. Delwiche, and P. Stroeve, “Methods for Pretreatment of Lignocellulosic Biomass for Efficient Hydrolysis and Biofuel Production,” *Ind. Eng. Chem. Res.*, vol. 48, no. 8, pp. 3713–3729, Apr. 2009, doi: 10.1021/ie801542g.
[68] N. Mosier *et al.*, “Features of promising technologies for pretreatment of lignocellulosic biomass,” *Bioresour. Technol.*, vol. 96, no. 6, pp. 673–686, Apr. 2005, doi: 10.1016/j.biortech.2004.06.025.
[69] P. Alvira, E. Tomás-Pejó, M. Ballesteros, and M. J. Negro, “Pretreatment technologies for an efficient bioethanol production process based on enzymatic hydrolysis: A review,” *Bioresour. Technol.*, vol. 101, no. 13, pp. 4851–4861, Jul. 2010, doi: 10.1016/j.biortech.2009.11.093.
[70] A. W. Bhutto *et al.*, “Insight into progress in pre-treatment of lignocellulosic biomass,” *Energy*, vol. 122, pp. 724–745, Mar. 2017, doi: 10.1016/j.energy.2017.01.005.
[71] J. Xu and S. Liu, “Optimization of ethanol production from hot-water extracts of sugar maple chips,” *Renew. Energy*, vol. 34, no. 11, pp. 2353–2356, Nov. 2009, doi: 10.1016/j.renene.2009.03.025.
[72] W. Pan, J. A. Perrotta, A. J. Stipanovic, C. T. Nomura, and J. P. Nakas, “Production of polyhydroxyalkanoates by Burkholderia cepacia ATCC 17759 using a detoxified sugar maple hemicellulosic hydrolysate,” *J. Ind. Microbiol. Biotechnol.*, vol. 39, no. 3, pp. 459–469, Mar. 2012, doi: 10.1007/s10295-011-1040-6.
[73] C. Gong and B. M. Bujanovic, “Impact of Hot-Water Extraction on Acetone-Water Oxygen Delignification of Paulownia Spp. and Lignin Recovery,” *Energies*, vol. 7, no. 2, Art. no. 2, Feb. 2014, doi: 10.3390/en7020857.
[74] G. Garrote, H. Domínguez, and J. C. Parajó, “Interpretation of deacetylation and hemicellulose hydrolysis during hydrothermal treatments on the basis of the severity factor,” *Process Biochem.*, vol. 37, no. 10, pp. 1067–1073, May 2002, doi: 10.1016/S0032-9592(01)00315-6.
[75] X. Chen, M. Lawoko, and A. van Heiningen, “Kinetics and mechanism of autohydrolysis of hardwoods,” *Bioresour. Technol.*, vol. 101, no. 20, pp. 7812–7819, Oct. 2010, doi: 10.1016/j.biortech.2010.05.006.
[76] G. V. Duarte, B. V. Ramarao, T. E. Amidon, and P. T. Ferreira, “Effect of Hot Water Extraction on Hardwood Kraft Pulp fibers (Acer saccharum, Sugar Maple),” *Ind. Eng. Chem. Res.*, vol. 50, no. 17, pp. 9949–9959, Sep. 2011, doi: 10.1021/ie200639u.
[77] M. Leschinsky, H. Sixta, and R. Patt, “Detailed mass balances of the autohydrolysis of eucalyptus globulus at 170°C,” *BioResources*, vol. 4, no. 2, Art. no. 2, Apr. 2009.
[78] J. Li and G. Gellerstedt, “Improved lignin properties and reactivity by modifications in the autohydrolysis process of aspen wood,” *Ind. Crops Prod.*, vol. 27, no. 2, pp. 175–181, Mar. 2008, doi: 10.1016/j.indcrop.2007.07.022.
[79] D. B. Corbett, N. Kohan, G. Machado, C. Jing, A. Nagardeolekar, and B. M. Bujanovic, “Chemical Composition of Apricot Pit Shells and Effect of Hot-Water Extraction,” *Energies*, vol. 8, no. 9, Art. no. 9, Sep. 2015, doi: 10.3390/en8099640.
[80] H. Wang, Y. Pu, A. Ragauskas, and B. Yang, “From lignin to valuable products–strategies, challenges, and prospects,” *Bioresour. Technol.*, vol. 271, pp. 449–461, Jan. 2019, doi: 10.1016/j.biortech.2018.09.072.
[81] A. Duval and M. Lawoko, “A review on lignin-based polymeric, micro- and nano-structured materials,” *React. Funct. Polym.*, vol. 85, pp. 78–96, Dec. 2014, doi: 10.1016/j.reactfunctpolym.2014.09.017.
[82] A. G. Vishtal and A. Kraslawski, “Challenges in industrial applications of technical lignins," *BioResources*, vol. 6, no. 3, Art. no. 3, Jun. 2011.
[83] A. Tribot *et al.*, “Wood-lignin: Supply, extraction processes and use as bio-based material,” *Eur. Polym. J.*, vol. 112, pp. 228–240, Mar. 2019, doi: 10.1016/j.eurpolymj.2019.01.007.
[84] N.-E. E. Mansouri and J. Salvadó, “Structural characterization of technical lignins for the production of adhesives: Application to lignosulfonate, kraft, soda-anthraquinone, organosolv and ethanol process lignins,” *Ind. Crops Prod.*, vol. 24, no. 1, pp. 8–16, Jul. 2006, doi: 10.1016/j.indcrop.2005.10.002.
[85] M. Tanase-Opedal, E. Espinosa, A. Rodríguez, and G. Chinga-Carrasco, “Lignin: A Biopolymer from Forestry Biomass for Biocomposites and 3D Printing,” *Materials*, vol. 12, no. 18, Art. no. 18, Jan. 2019, doi: 10.3390/ma12183006.

[86] M. Culebras, A. Beaucamp, Y. Wang, M. M. Clauss, E. Frank, and M. N. Collins, “Biobased Structurally Compatible Polymer Blends Based on Lignin and Thermoplastic Elastomer Polyurethane as Carbon Fiber Precursors,” *ACS Sustain. Chem. Eng.*, vol. 6, no. 7, pp. 8816–8825, Jul. 2018, doi: 10.1021/acssuschemeng.8b01170.
[87] Y. Qian *et al.*, “Lignin Reverse Micelles for UV-Absorbing and High Mechanical Performance Thermoplastics,” *Ind. Eng. Chem. Res.*, vol. 54, no. 48, pp. 12025–12030, Dec. 2015, doi: 10.1021/acs.iecr.5b03360.
[88] S. L. Hilburg, A. N. Elder, H. Chung, R. L. Ferebee, M. R. Bockstaller, and N. R. Washburn, “A universal route towards thermoplastic lignin composites with improved mechanical properties,” *Polymer*, vol. 55, no. 4, pp. 995–1003, Feb. 2014, doi: 10.1016/j.polymer.2013.12.070.
[89] N. A. Aziz *et al.*, “Reinforced lignin-phenol-glyoxal (LPG) wood adhesives from coconut husk,” *Int. J. Biol. Macromol.*, vol. 141, pp. 185–196, Dec. 2019, doi: 10.1016/j.ijbiomac.2019.08.255.
[90] R. Wang *et al.*, “Anisotropic thermal conductivities and structure in lignin-based microscale carbon fibers,” *Carbon*, vol. 147, pp. 58–69, Jun. 2019, doi: 10.1016/j.carbon.2019.02.064.
[91] C. Rodríguez Correa, M. Stollovsky, T. Hehr, Y. Rauscher, B. Rolli, and A. Kruse, “Influence of the Carbonization Process on Activated Carbon Properties from Lignin and Lignin-Rich Biomasses,” *ACS Sustain. Chem. Eng.*, vol. 5, no. 9, pp. 8222–8233, Sep. 2017, doi: 10.1021/acssuschemeng.7b01895.
[92] Q. Li *et al.*, “Non-Solvent Fractionation of Lignin Enhances Carbon Fiber Performance,” *ChemSusChem*, vol. 12, no. 14, pp. 3249–3256, Jul. 2019, doi: 10.1002/cssc.201901052.

Chapter II

Fractionation of Lignins Recovered from Hot-Water Extracts of Angiosperms

1. Introduction:

One of the main challenges in valorization of lignin is its highly variable and diverse nature, depending on its lignocellulosic source and isolation conditions [1], [2]. Several strategies of lignin modification have been employed to reduce this heterogeneity, including use of supercritical fluids [3], ionic liquids [4], and catalysts [5]. Fractionation with organic solvents and acids/bases is one such strategy. Its main goal is to alleviate the heterogenous structure of lignin by separating it into relatively homogenous cuts of similar molecular weight distributions, narrower polydispersities, similar functionalities or physicochemical properties [6]. These properties are highly interdependent, and modulation of one can affect others. Fractionation can thus be employed in lignin valorization to control lignin reactivity and its compatibility with other reactants. Since being brought to prominence as a strategy for valorization of heterogenous technical lignins by Argyropoulos et al in 2014 [7], fractionation has received great interest on the path toward development of high-value applications of lignin, such as composites, carbon fiber products, resins [8]–[10], monoaromatic compounds and lignin-oil [11], lignin-based copolymers [12], and PU formulations [13].

1.1. Methods employed in lignin fractionation: Fractionation is an umbrella term that encompasses various approaches utilized for separation of relatively non-uniform lignin into more uniform cuts/fractions. These can be largely divided into two: solvent based and membrane-based (Figure 1).

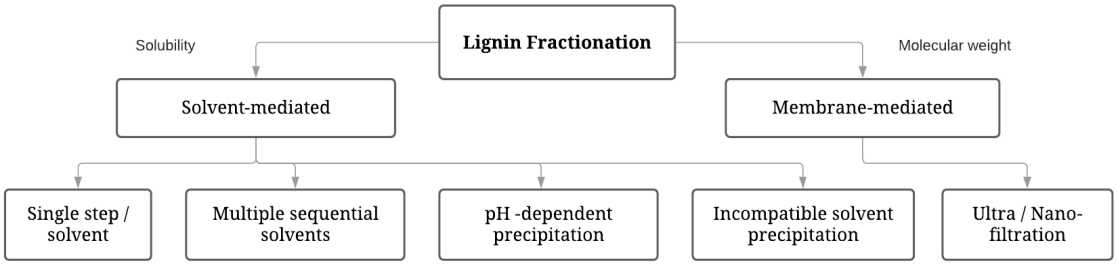

Figure 1: Methods of lignin fractionation

Solvent-based approaches make use of the differential solubilities of lignin fragments depending on the solvent polarity and pH. Solvent-mediated fractionations can be achieved in a single step by employing a single solvent system [7], [14], [15] or via multiple solvent systems employed in a sequential manner [8], [11], [13], [16]. The single step method uses a single solvent to separate soluble and insoluble fractions of lignin. The sequential method consists of serially exposing lignin to increasingly polar organic solvents one after the other. In this method, the lignin residue that has remained insoluble in a less-polar solvent is treated next with a more-polar solvent. The sequence is continued until the last solvent is reached. Anti-solvents have also been used to precipitate lignin fractions from solutions [7], [9], [10]. Alternatively, aqueous acid/base systems can be used instead of organic solvents to modify lignin solubility and cause precipitation of fractions [17].

Membrane-based approaches make use of the differential molecular weights of lignin fragments. Membrane-mediated fractionation can be achieved by use of ultra- and nano- membrane filtration technology [18].

Both, solvent-based and membrane-based approaches have been successfully used largely on technical lignins, with some common trends observed for fractions (Table 1).

Table 1: Summary of lignin fractionation methods

Abbreviations: DCM: Dichloromethane, DMSO: Dimethyl sulfoxide, EtOH: Ethanol, EtOAc: Ethyl acetate, HMW: high-molecular weight (*M*w > 10000 g/mol), LMW: low-molecular weight (*M*w <2000 g/mol), MEK: n-butanone/methylethyl ketone, MeOH: Methanol, OH: hydroxyl group, PGME: propyleneglycol monomethyl ether, PhOH: free phenolic hydroxyl group, T_g: Glass transition temperature, THF: Tetrahydrofuran

Fractionation Method	Lignin	Major trends	Reference
Single step / Single solvent			
Various single solvents: DMSO, THF, MeOH, MEK	Softwood kraft	HMW-fractions: Soluble in higher polarity solvent (MeOH), higher OH content, higher Tg. LMW-fractions: Soluble in low polarity solvent (MEK), lower Tg.	[14]
MeOH	Softwood kraft	HMW-fraction: insoluble in methanol, higher Tg. LMW-fraction: soluble in methanol, lower Tg.	[15]
MeOH	Softwood kraft	HMW-fraction: insoluble in methanol, more condensed, higher Tg, lower PhOH content. LMW-fraction: soluble in methanol, less condensed,	[12]

		lower Tg, higher PhOH content.	
Sequential / Multiple solvents			
DCM, MeOH, mixture of DCM/MeOH (3/7 v/v)	BioLignin™: wheat straw lignin extracted with acetic acid / formic acid / water	HMW-fractions: soluble in DCM/MeOH, higher Tg. LMW-fractions: soluble in DCM and methanol separately, lower Tg.	[13]
Acetone/water, acetone, EtOAc	Soda, organosolv, kraft lignins from hardwood, softwood, grasses	HMW-fractions: more condensed, higher aliphatic OH content. LMW-fractions: soluble in EtOAc and acetone/water, less condensed, lower aliphatic OH content.	[19]
DCM, n-propanol, MeOH, DCM/MeOH	Softwood kraft	HMW-fractions: Insoluble, higher carbohydrate content, lower OH content, higher Tg. More uniform lignin composition. LMW-fractions: soluble in DCM, lower carbohydrate content, higher OH content, lower Tg.	[8]

EtOAc, MeOH, acetone, dioxane/water. Further depolymerized with supercritical EtOH.	Grass soda lignin	LMW-fraction: higher PhOH content, higher lignin-oil yield.	[11]
Hexane, diethylether, DCM, MeOH, and dioxane	Hardwood kraft	HMW-fraction: Insoluble in low polarity solvents, higher Tg, lower S/G.	[16]
Solvent precipitation			
Lignin dissolved in acetone solution precipitated by addition of hexane	Softwood kraft	HMW-fraction: acetone insoluble, higher Tg, higher aliphatic OH. LMW-fraction: hexane precipitated, lower Tg, higher PhOH.	[7]
Lignin dissolved in aqueous acetone (60% v/v) precipitated by addition of acetone	Kraft, soda and organosolv lignins from softwood and grass	Relatively HMW-fractions: precipitated on addition of acetone. Relatively pure, homogenous, low to moderate OH content. Relatively LMW-fractions: soluble in acetone, higher OH content.	[9]
Lignin dissolved in aqueous ethanol (80% v/v), acetone (60% v/v) or PGME (60% v/v) precipitated by	Softwood kraft lignin	HMW-fractions: Insoluble, higher polydispersity. LMW-fractions: soluble,	[10]

addition of water as non-solvent		higher PhOH content, higher carbohydrate content.	
pH precipitation			
1M hydrochloric acid, pH 9 to pH 1, sequential precipitation from liquor	Hardwood kraft lignin	HMW-fractions: precipitated at higher pH, higher ash content, higher Tg. LMW-fractions: precipitated at lower pH, lower ash content, lower Tg	[17]
Membrane filtration			
Solvent-fractionation followed by dialysis (molecular weight cut-off 1000 Da)	Spruce ball-milled lignin	All isolated fractions were HMW lignin-carbohydrate complexes	[18]

1.2. Hildebrand solubility parameter (HSP, δ): It might be worthwhile to briefly discuss here the Hildebrand solubility parameter as it relates to lignin solubility. The HSP for any solvent is defined as the square root of its cohesive energy density (i.e. the square root of the ratio of total cohesive energy, E_{coh}, to the molar volume, V; Eqn. 1), and is based on the principle 'like dissolves like' [20], [21]. The cohesive energy density is a measure of the intermolecular forces of a compound. Thus, if the intermolecular forces between the molecules of a solvent are equal to the intermolecular forces between the molecules of a solute, then that solvent is expected to be a good solvent for that solute.

$$\text{Hildebrand solubility parameter, } \delta = \sqrt{\frac{E_{coh}}{V}} \qquad (1)$$

Although the Hildebrand solubility theory has since been refined to give Hansen solubility [22], it will be used for this discussion due to its simplicity and relevance. Based on this theory, solvents with δ values close to 22.5 $MPa^{1/2}$ have been proposed to be good solvents for lignin [23], whereas, Boeriu et al [19] have reported the δ values for five technical lignins to range between 27.8 $MPa^{1/2}$ and 29.3 $MPa^{1/2}$.

1.3. Significance of fractionation on lignin valorization: Both, HMW- and LMW- fractions of lignin have been found suitable for use in various applications. While both fractions offer the added advantage of having uniform solubility and better miscibility in the formulations over unfractionated lignins [24], because of their distinct physicochemical and structural properties, one fraction has been found to be more desirable over the other, depending on the intended application. For example, HMW-fractions are generally more suitable in polymer-based applications of lignin, due to the presence of larger lignin fragments as opposed to the LMW-fractions which predominantly contain smaller molecules formed by fractionation-induced depolymerization [6]. HMW-fractions have thus been used in synthesis of lignin-based phenol-formaldehyde resins [25], thermoset polyurethane films and coatings [26]. Apart from providing a polymeric base in these formulations, HMW-fractions have been found to induce higher thermostability due to their relatively rigid structure and higher glass transition temperatures (Tg) [16]. HMW-fractions have also been reported to be useful in carbon fiber production, due to their higher molecular weights (less depolymerized nature), and higher thermostability [27]. HMW-fractions have also been used in thermoplastic blends. It has been reported that a large content of PhOH groups in thermoplastic blends leads to excessive cross-linking and brittleness; therefore, masking of the PhOH groups by appropriate methods, such as methylation, is required [7]. HMW fractions have been documented to contain a relatively lower amount of PhOH groups

than LMW fractions because of differential partitioning of PhOH groups in organic solvents [7], [9]–[12], [14], [19]. Due to this, HMW-fractions can be advantageous over LMW-fractions in certain formulations for avoiding issues related to excessive crosslinking and incompatibility with hydrophobic components and solvents [28]. LMW-fractions on the other hand, have been found to be good plasticizers in thermoplastics due to their relatively lower Tg and flexible structure [29], [30]. This plasticizing ability has also been found to improve the mechanical properties of blends [30]. Similar effect of LMW-fractions has been observed for lignin-based cellulose nanofiber-starch composite films [31]. LMW-fractions have also been associated with relatively higher antioxidant activities, as compared to the unfractionated lignins and HMW-fractions, possibly due to their relatively higher PhOH content [9], [32]. However, medium and high molecular weight fractions have also been found to be good antioxidants as compared to unfractionated lignin [13], [32].

Considering the reported utility of fractionation in valorization of predominantly technical lignins, and the relative lack of fractionation literature on biorefinery lignins, our aim was to study the effects of fractionation on lignins recovered from hot-water extracts of angiosperms. Keeping in mind potential polymer-based applications of the isolated fractions in synthesis of lignin-based hydrogels (Chapter 3), it was desired to retain the polymeric nature of lignin, minimize depolymerization and maintain relatively higher molecular weights after fractionation. Two different fractionation approaches (organic solvent-mediated and mild alkali-mediated) were selected to obtain two different fractions of lignin with distinct physicochemical properties relative to each other and the original unfractionated lignins. Alkali-purification was employed to isolate fractions with relatively higher lignin content, while preserving most of the starting lignin features, and organic solvent-fractionation was employed to isolate fractions with relatively

higher carbohydrate content, more condensed character, and higher molecular weights, as the first step to gain better understanding of beneficial characteristics of lignin in polymeric applications.

2. Experimental Materials and Methods:

2.1. Chemicals and materials: All chemicals were used as received without further purification (Table 2).

Table 2: Chemicals used in this study

Chemical	Vendor
Acetic anhydride	EMD Millipore
Acetone	PHARMCO-AAPER
Acetyl bromide	Alfa Aesar
Citric acid	Fisher Scientific
Diethyl ether	PHARMCO-AAPER
Dimethyl sulfoxide-d_6 (DMSO-d_6)	Cambridge Isotope Laboratories, Inc.
2,2-diphenyl-1-picrylhydrazyl (DPPH)	Sigma-Aldrich
Dioxane	TCI
Glacial acetic acid	EMD Millipore
Hydrochloric acid	EMD Millipore
Pyridine	EMD Millipore
Sodium Hydroxide	Macron Fine Chemicals
Sulfuric acid	EMD Millipore
Tetrahydrofuran (THF)	PHARMCO-AAPER
Trisodium citrate	Fisher Scientific

2.2. Recovery of lignins from hot-water extracts of angiosperms (RecL): The biorefinery lignins studied in this work were recovered from autohydrolyzates produced at the end of hot-water extraction of the following angiosperms: sugar maple (*Acer saccharum,* Family: *Sapindaceae*; harvested from Heiberg Forest, Tully, NY), willow with bark (*Salix sp.,* Family:

Salicaceae; mixed commercial cultivars, donated by SUNY ESF Tully station), miscanthus (*Miscanthus* sp. Family: *Poaceae/Graminae;* harvested from Bono, AK), wheat straw (*Triticum* sp. Family: *Poaceae/Graminae;* harvested from Central NY), and a mix of various angiosperms (maple, aspen, red oak, and wheat straw). Miscanthus and wheat straw were milled at ¾" screen size. Sugar maple, willow and mixed angiosperm were chipped to ¾" in length. The pilot-scale hot-water extraction of the biomass was carried out in a 65 ft^3 Struthers-Wells stainless lined batch digester, at 160 ºC for 2 hours. Further treatment of the hot-water hydrolyzate for the different biomass types differed as follows:

Sugar maple hydrolyzate was subjected to ultra-filtration on a 0.01 µm ceramic membrane filter (Hilco HM634-01). The retentate was recovered, the pH was dropped to 2 with dilute sulfuric acid, and the precipitated sugar maple lignin was recovered by centrifugation. Willow, miscanthus, and wheat straw hydrolyzates were collected in separate experiments and were acidified to pH 2 with dilute sulfuric acid. The lignins were allowed to precipitate for a week at room temperature. The respective lignins were recovered by decanting the supernatant and were air-dried. The hydrolyzate of mixed angiosperms was mixed with hydrolyzate of wheat straw (prepared in a separate run). This mixed extract was ultra-filtered on a 0.01 µm ceramic membrane filter (Hilco HM634-01) and was acidified to pH 2 with concentrated sulfuric acid. The precipitated lignin was recovered by decanting the supernatant and was air-dried. All recovered lignins were eventually vacuum dried (~40 °C) before performing further characterization and fractionation. These lignins were collected as recovered lignins (RecL) for each of the biomass and were referred to as sugar maple RecL (SM), willow RecL (W), miscanthus RecL (MS), wheat straw RecL (WS), miscanthus RecL (MS), and mixed angiosperms RecL (MA).

2.3. Determination of lignin content: The acid insoluble lignin content of all lignin samples were determined by the Tappi Method T 222 om-02, Acid-insoluble lignin in wood and pulp. Acid soluble lignin content is determined by measuring UV absorbance at 205 nm on a Genesys 10 Series Spectrophotometer (Thermo Fisher Scientific, Waltham, MA, USA) [37]. Duplicates were measured, and the average value was calculated. Experiments were performed at the United States Department of Agriculture - Forest Products Lab (USDA-FPL) (Madison, WI).

2.4. Carbohydrate analysis: Carbohydrates composition was analyzed from acid-hydrolysate resulting from Klason lignin determination at the United States Department of Agriculture - Forest Products Lab (USDA-FPL) (Madison, WI) [33]. Duplicates were measured, and the average value was calculated.

2.5. Determination of ash content: Ash content was determined according to Tappi method T 211-om-02, Ash in wood, pulp, paper and paperboard: combustion at 900 °C, Test Method. 2 g of moisture free sample was weighed and ignited in a muffle furnace at 900 °C, for at least 4 hours. The end weight was recorded as the ash content. Duplicates were measured, and the average value was calculated. Experiments were performed at the United States Department of Agriculture - Forest Products Lab (USDA-FPL) (Madison, WI).

2.6. Free Phenolic Hydroxyl Group Content (PhOH): Free phenolic hydroxyl content of all lignin samples was determined by the UV differentiation method [34]. About 10 mg samples of the lignin were separately dissolved in 5 mL of dioxane and 5 mL 0.2 M NaOH. From each lignin solution, 2 mL was further diluted to 25 mL using either a pH 6 citrate buffer solution, or a 0.2 M NaOH solution. The PhOH content was calculated from the differential UV-spectra of the 0.2 M sodium hydroxide solution recorded on a Genesis 10s UV-Vis spectrophotometer (Thermo

Scientific, MA, USA) at 300 nm and 350 nm, against the pH 6 lignin solution as reference. Four observations were made for each sample, and the average value was calculated.

2.7. Fourier-transform infrared (FT-IR) spectroscopy: FT-IR of lignin samples were conducted on a PerkinElmer Frontier FT-IR/NIR Spectrometer. Calibration was done with an empty sample cell, and the spectra were averaged over 16 readings. Sample analysis was conducted by loading the sample evenly over the beam and recording the baseline-corrected spectra from 4000cm^{-1} to 650cm^{-1} in MIR mode. Absorbance values were normalized based on the band from 1515-1505cm^{-1}, which represents aromatic skeletal vibrations.

2.8. Thermogravimetric Analysis (TGA): Thermogravimetric analysis (TGA) was performed using TA instruments Q500. Approximately 20 mg of the samples were heated under an inert (N_2) nitrogen atmosphere up to 600 °C at a rate of 10 °C/min **[35]**.

2.9. Determination of acetyl bromide extinction coefficient (EC): Extinction coefficients were calculated from standard curves constructed by dissolving 10 mg of lignin in 5 ml dioxane, and pipetting aliquots of 0.2, 0.3, 0.4, 0.5, and 0.6 mL were pipetted into centrifuge tubes, and were vacuum dried **[36]**. To each tube 0.5 mL of 25% acetyl bromide in glacial acetic acid was added. A blank was included to correct for reagent background absorbance. Tubes were tightly capped and put in a 50 °C water bath for 30 min. After cooling, all tubes received 2.5 mL of acetic acid, 1.5 ml of 0.3 M NaOH, and 0.5 mL of 0.5 M hydroxylamine hydrochloride solution. Tubes were shaken and further glacial acetic acid was added to give a final volume of 10.0 ml. Solutions were read on a Genesis 10s UV-Vis spectrophotometer (Thermo Scientific, MA, USA) at 280 nm.

2.10. Estimation of antioxidant activity (AOA): Antioxidant activity was measured by determining the amount of sample needed to quench 50% of the DPPH free radicals present in the solution (DPPH•) **[37]**. 4 mL of 6 x 10^{-5} mol/L DPPH• in methanol was added to 500 µl of sample lignin solution made in dioxane:water (9:1), at various lignin concentrations. The absorbance was immediately measured at 517 nm using a Genesys 10 Series Spectrophotometer at room temperature as the zero-time reading. The solutions were allowed to reach steady-state for 2 hours. The decrease in the percentage of DPPH• in solution over various lignin concentrations was measured as the decrease in the absorbance at 517 nm, and was plotted as the function of lignin concentration. The resulting equation was utilized to determine the concentration of the antioxidant that would be required to quench 50% of the free radicals from DPPH•. This value was recorded as the 50% inhibitory concentration (IC_{50}) for each antioxidant. Lower the IC_{50} indicates higher antioxidant activity. Five data points were used to compute the IC_{50} for each sample.

2.11. Alkali-purification: In order to prevent excessive depolymerization of lignin, a mild alkali-purification method was selected [38]. Lignin was dissolved in 125 mL 0.05 M NaOH and 25 mL dioxane per gram of lignin. Fractionation was allowed to proceed under an inert (N_2) atmosphere. After 24 hours the solution was acidified with 0.1 M hydrochloric acid to a pH of 2, ending the reaction, and inducing precipitation of lignin (Figure 2). Hydrochloric acid was preferred over sulfuric acid since precipitations induced by use of sulfuric acid have been reported to result in lower yields [6]. The solution was stored in the cold room (≤8 °C) overnight and the resulting precipitate was vacuum filtered in a Buchner funnel. Subsequently, the lignin precipitate was washed with cold water until the filtrate reached a pH of 5. It was then dried under vacuum. The residues produced in this step were collected as alkali-purified lignin (AH)

for each of the biomass and were referred to as sugar maple alkali-purified lignin (SMAH), willow alkali-purified lignin (WAH), miscanthus alkali-purified lignin (MSAH), wheat straw alkali-purified lignin (WSAH), miscanthus alkali-purified lignin (MSAH), and mixed angiosperms alkali-purified lignin (MAAH). Duplicates were performed and the average yield was calculated.

2.12. Organic solvent-fractionation (Solvent fractionation): The solvents used in these experiments were desired to be safe, environmentally-friendly, and industrially-accepted. Hence, popular bench-scale solvents such as hexane, DCM and THF were rejected due to the regulatory issues they pose. Solvents with high boiling points such as DMSO and dioxane/water (b.p. > 100 ºC) were also deemed undesirable due to the high energy costs involved in their recovery. Considering these factors, a solvent system of diethyl ether and acetone was found suitable (Table 3) [39].

Table 3: Properties of organic solvents selected for fractionation

Solvent	**Hildebrand Solubility Parameter (HSP)** [40] **(δ, $MPa^{1/2}$)**	**Boiling Point (ºC)**	**Relative Polarity** [33]
Diethyl ether; $(C_2H_5)_2O$	15.4	34.6	0.117
Diethyl ether/Acetone (4:1 v/v)	16.26[a]	nd	0.165[b]
Acetone; C_3H_6O	19.7	56.2	0.355

[a] Value calculated as (15.4*4 + 19.7)/5
[b] Value calculated as (0.117*4 + 0.355)/5

The sequential fractionation was performed with diethyl ether, diethyl ether/acetone (4:1 v/v) and acetone, at a lignin/solvent ratio 1 g lignin/10 ml solvent (Figure 2). In each step, lignin was

suspended in the respective solvent, and was stirred at room temperature for 2 hours. The insoluble residue was filtered over oven dried Whatman GF/B filter (1µm), vacuum dried, weighed and then used for the next step [39]. The insoluble residues from the final step were collected as a higher molecular weight solvent-insoluble fraction (FR) for each of the biomass and were referred to as sugar maple fraction (SMFR), willow fraction (WFR), miscanthus fraction (MSFR), wheat straw fraction (WSFR), miscanthus fraction (MSFR), and mixed angiosperms fraction (MAFR). Duplicates were performed and the average yield was calculated.

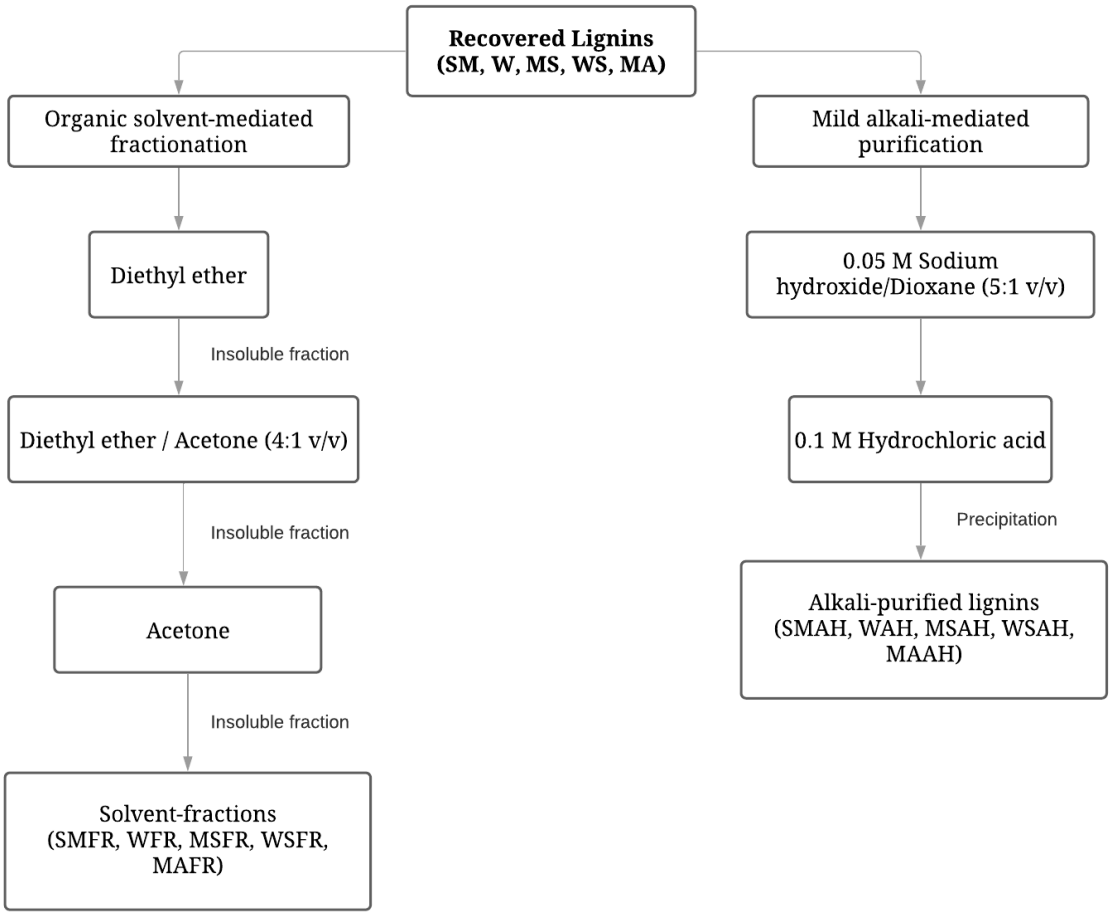

Figure 2: Fractionation scheme for recovered lignins

3. Results and Discussion:

3.1. Lignin solubility in organic solvents and fractionation yields: Although the exact yields for each RecL varied considerably (Figure 3), in general, RecLs showed higher solubilities in solvents with higher HSPs, with the highest dissolution seen in acetone (Figure 3). The higher solubility of lignin in acetone could be explained by its higher HSP (δ = 19.7 $MPa^{1/2}$; Table 3) as compared to diethyl ether, and diethyl ether / acetone mixture. As stated earlier, solvents with δ values close to 22.5 $MPa^{1/2}$ have been proposed as good solvents for lignin. Along with the HSP, a high hydrogen bonding capacity (high polarity) has also been proposed to play an important role in lignin dissolution [14], [41]. The decreasing solubility of RecLs in the other two solvents in the same order of their δ values and polarity also supports this reasoning. After acetone, diethyl ether/acetone (4:1 v/v) dissolved the most mass of lignin except in the case of W, which showed higher solubility in diethyl ether instead. The anomalous behavior of W could be arising from the presence of unidentified bark compounds.

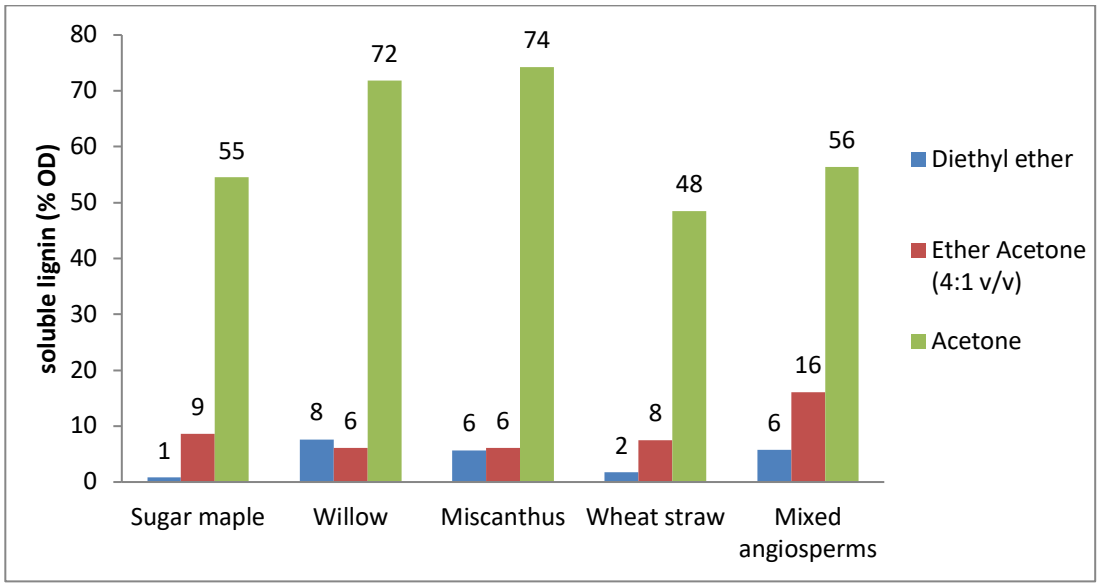

Figure 3: Solubility of recovered lignins in organic solvents

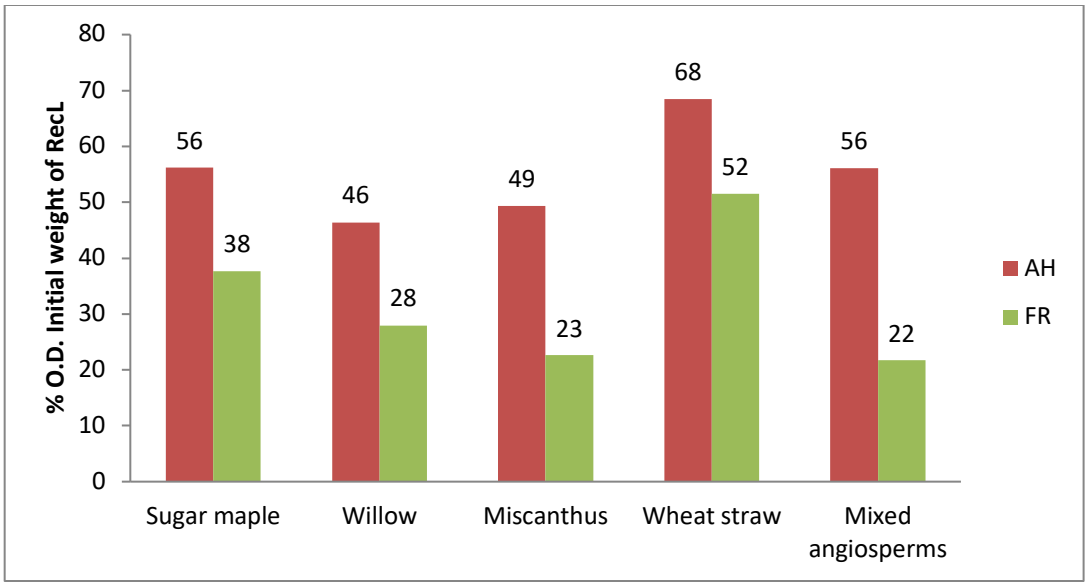

Figure 4: Comparison of yields during alkali-purification (AH) and solvent-fractionation (FR)

As compared to solvent-fractionation, significantly higher yields of insoluble residues were obtained for alkali-purification (Figure 4). The lower yields of insoluble residues in solvent-fractionation suggest extensive partitioning of lignin in organic solvents.

3.2. Composition analysis: The total lignin content in RecLs varied between 81% and 86% OD (Figure 5). All of the RecLs were contaminated with carbohydrates (between 3% and 8% OD), probably in the form of lignin-carbohydrate complexes (LCCs) to some extent, with xylans being the major carbohydrate impurity (Figure 6). This is as expected, since xylans constitute a major portion of hemicelluloses in angiosperms, and are the target for selective removal during hot-water extraction [42], [43]. They are also the major hemicelluloses bound to lignin in the form of LCCs. The benzyl ester and phenyl glycosidic bonds in LCCs are relatively acid stable, while benzyl ether is acid susceptible [44]. The mildly acidic conditions during hot-water extraction (pH > 3; [45]) probably retained a few LCC-type linkages resulting in RecLs contaminated with carbohydrates.

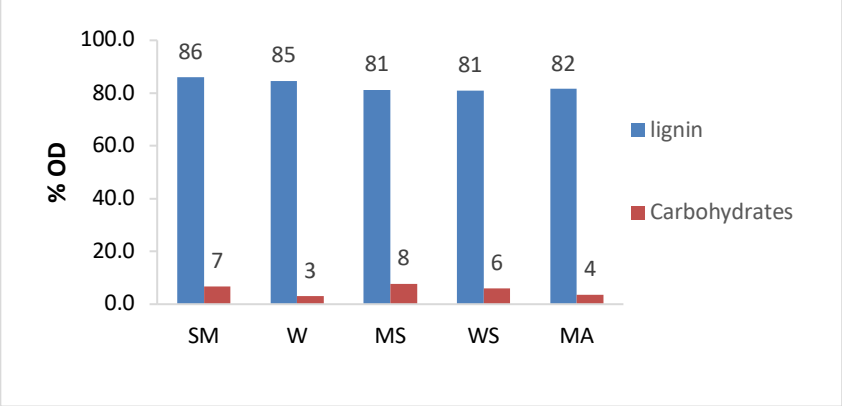

Figure 5: Composition analysis of recovered lignins

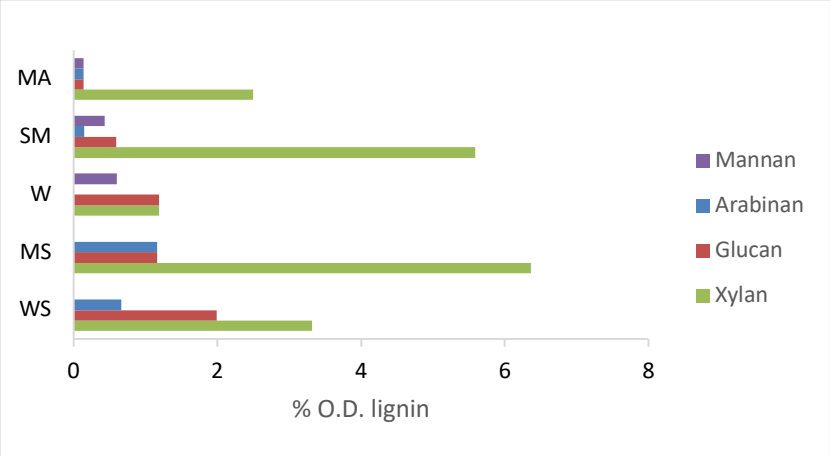

Figure 6: Carbohydrate make-up of recovered lignins

The two different fractionation methods *viz.* alkali-purification and solvent-fractionation were found to produce two distinct fractions from the same starting lignins, as evidenced from the lignin contents (Figure 7), carbohydrate contents (Table 4) and the lignin/carbohydrate ratio obtained for each fraction (Figure 8). As compared to RecLs, AHs were more lignin-enriched, most likely due to the mild-alkali catalyzed cleavage of LCC bonds (lignin/carbohydrate ratios ~2 to 4 times higher than RecLs, Figure 8, red). On the other hand, FRs were more carbohydrate-enriched, due to the preferential partitioning of lignin into organic solvents of similar HSPs (Lignin/carbohydrate ratios up to 7 times lower than RecLs, Figure 8, green). Alkali-purification

was found to affect the composition of lignins slightly differently based on their lignocellulosic origin (hardwoods vs grasses; Figure 8, red). The lignin/carbohydrate ratios for hardwood AH (sugar maple, willow) were slightly higher, and more homogenous within this group. Whereas, the lignin/carbohydrate ratios for graminae AH (miscanthus, wheat straw) were slightly lower than hardwoods. Solvent-fractionation (Figure 8, green) gave very homogenous results for graminae FR (miscanthus and wheat straw), but the effect wasn't as pronounced in hardwood FR (sugar maple and willow). Figure 8 shows the ash content of RecLs, AHs, and FRs. The amount of ash in RecLs varied between 0.1% and 1.2% OD lignin (Figure 9, blue). Solvent-fractionation was found to increase ash content in all FR (Figure 9, green). This might be the result of favorable partitioning of the inorganic compounds in the solvent-insoluble fraction of lignin, due to the generally poor solubility of minerals in organic solvents.

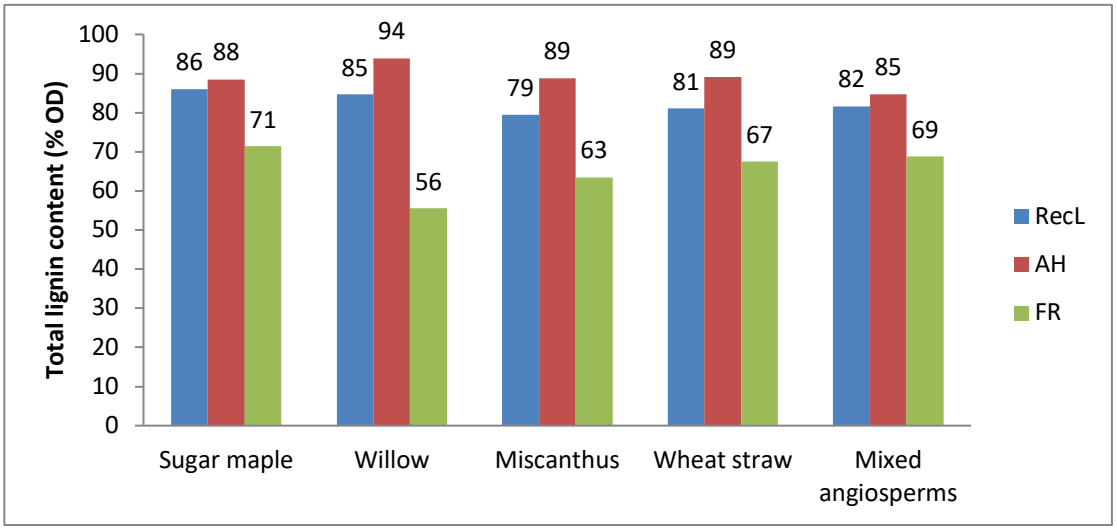

Figure 7: Lignin content of recovered (RecL) and alkali-purified (AH) lignins, and solvent-insoluble fractions (FR)

Table 4: Carbohydrate composition of lignins

Lignin	Arabinan (% OD)	Galactan (% OD)	Glucan (% OD)	Xylan (% OD)	Mannan (% OD)	Tot. Carb. (% OD)
SM	0.15	NA	0.59	5.59	0.43	6.33
SMAH	0.00%	0.00%	0.58%	0.58%	0.35%	1.51%
SMFR	0.00%	0.45%	1.11%	3.67%	0.95%	6.18%
W	NA	1.19	NA	1.19	NA	2.38
WAH	0.00%	0.00%	0.53%	0.87%	0.11%	1.50%
WFR	0.39%	1.54%	3.21%	8.68%	1.35%	15.17%
MS	1.16%	NA	1.16%	6.36%	NA	8.68%
MSAH	0.10%	0.05%	0.52%	1.14%	0.10%	1.92%
MSFR	1.36%	0.36%	2.15%	13.77%	NA	17.63%
WS	0.66%	NA	1.99%	3.32%	NA	5.97%
WSAH	0.17%	0.12%	1.17%	1.09%	0.06%	2.60%
WSFR	1.10%	0.62%	5.51%	8.56%	0.21%	16.00%
MA	0.14%	0.14%	0.69%	2.50%	0.14%	3.61%
MAAH	0.00%	0.00%	0.62%	0.62%	0.06%	1.30%
MAFR	0.26%	0.26%	1.97%	6.15%	0.33%	8.97%

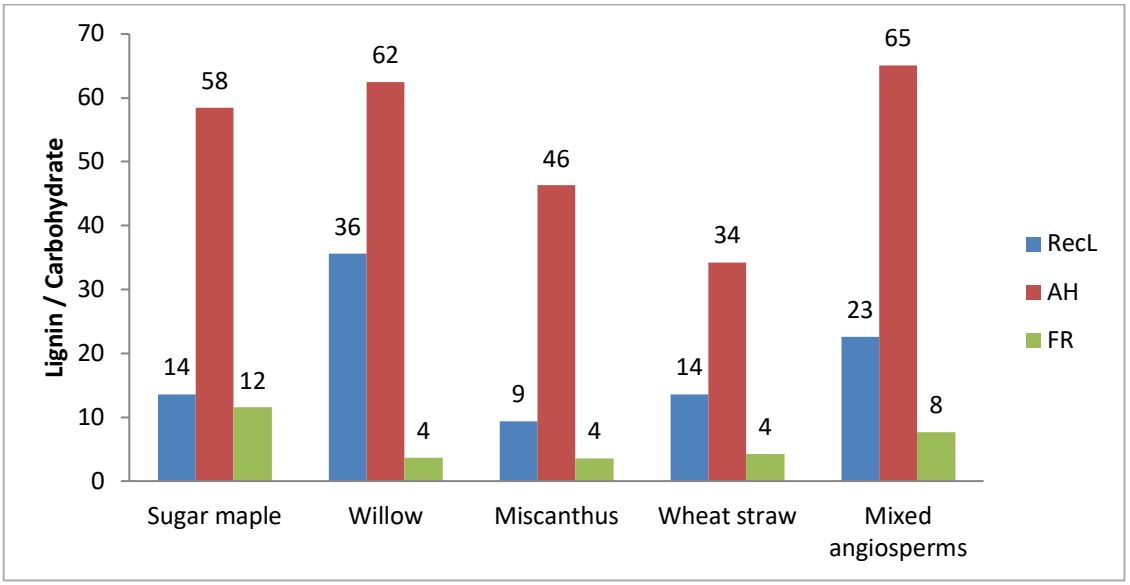

Figure 8: Effect of alkali-purification (AH) and solvent-fractionation (FR) on lignin/carbohydrate ratio

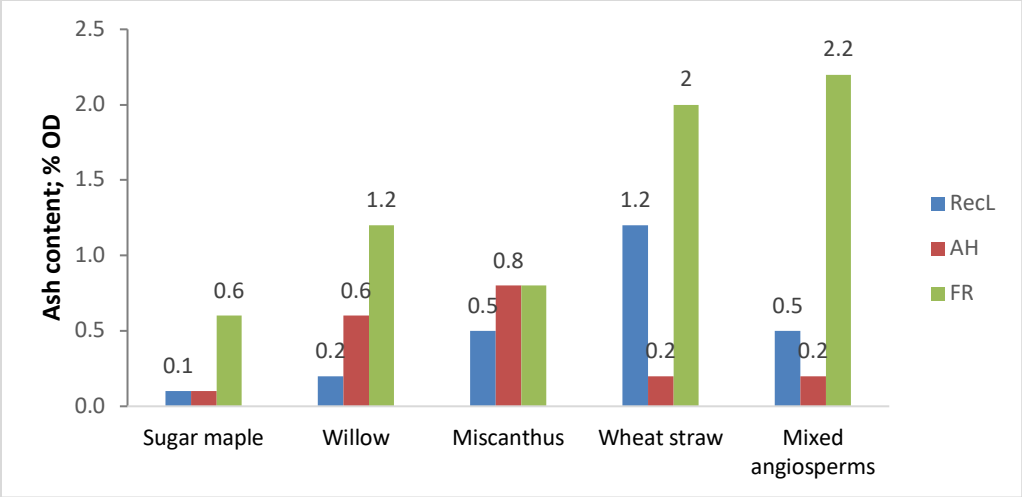

Figure 9: Effect of alkali-purification (AH) and solvent-fractionation (FR) on ash content of lignins

These changes in the composition indicate that fractionation has the potential to be explored as a means to tailor lignin/carbohydrate composition of lignins. They further imply that alkali-purification resulted in the cleavage of some lignin-carbohydrate linkages - thus enriching the precipitated fractions with lignin, while solvent-fractionation caused partitioning of lignin in organic solvents, probably leaving a few higher molecular weight lignin fragments bound to carbohydrates in the form of LCCs in the insoluble residue.

3.3. Free phenolic hydroxyl group (PhOH) content: The PhOH content for RecLs ranged between 0.99 mmol/g and 2.47 mmol/g (Figure 10, blue). MAAH and MAFR were excluded from this analysis due to the restrictions on sample availability. While the average range reported for native lignins is 0.5-0.7 mmol/g hardwood lignin [46], and ~1.5 mmol/g graminae lignin [47], slightly higher PhOH content is observed in hot-water extracted lignins due to the acid-catalyzed cleavage of aryl ether bonds [48]. Alkali-purification was found to cause a slight increase (< 10%) in the PhOH content of AHs (Figure 10, red), as compared to RecLs. This again indicates that alkali-purification was a relatively mild fractionation method, which did not

cause significant cleavage of interunit lignin linkages, and did not modify the original structure of RecLs to a large extent. On the other hand, solvent-fractionation caused a marked increase in the PhOH content of FRs (up to ~100%, Figure 10, green), indicating that the lignin fraction associated with LCCs is rich in the PhOH content.

Due to the higher PhOH content, FRs might be more reactive as compared to RecLs and AHs when the reaction involves PhOH groups [12]. It might be worthy to recall that willow biomass was not debarked prior to hot-water extraction, and the presence of bark compounds in W might have contributed to the overall higher values of PhOH content in W, WAH and WFR.

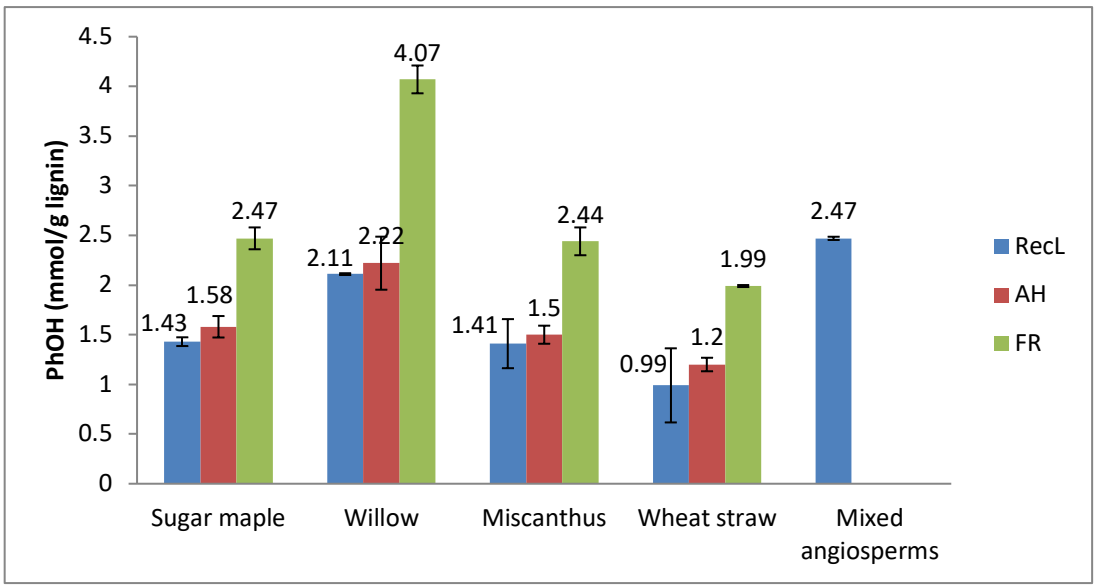

Figure 10: Free phenolic hydroxyl group content of recovered (RecL) and alkali-purified (AH) lignins and solvent (FR) fractions

3.4. FT-IR analysis: RecLs, AHs, and FRs all showed FT-IR spectra typical of angiosperm lignins (Willow lignins are discussed below as an example, Table 4, Figure 11; spectra for other biomass species can be found in Appendix, Figure 15).

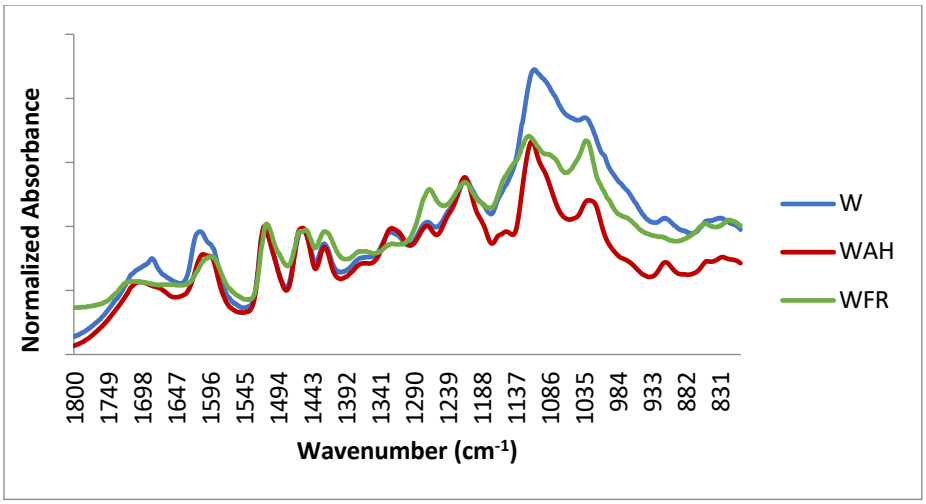

Figure 11: FT-IR spectra of recovered (W), alkali (WAH) and solvent (WFR) fractionated lignins

Table 5: FT-IR band assignment in the mid-infrared region

Wavenumber (cm^{-1})	**Band Origin** [12], [49]
1713-1678	C=O stretch in ketones, carbonyls, and esters (carbohydrates and aryl ketones). C=O stretch in carboxylic acids and aldehydes.
1620-1592	Aromatic skeletal vibrations plus C=O stretch; S > G
1515-1505	Aromatic skeletal vibrations; G > S
1466-1446	C-H deformations (methyl and methylene groups)
1430-1416	Aromatic skeletal vibrations, aromatic ring stretching, C-H in-plane deformation
1330-1312	Rings of S-units and condensed G-units
1260-1257	Rings of G-unit plus C=O stretch
1220-1207	C-C plus C-O stretch
1124-1110	Aromatic C-H in-plane deformation of S-units plus secondary alcohol and C=O stretch
1038-1025	Aromatic C-H in plane deformation, G- > S-units; C-O deform in primary alcohols; C=O stretch
908-804	C-H out-of-plane

W, WAH and WFR all showed typical absorption bands for aromatic vibrations (1620-1592 cm^{-1} and 1515-1505 cm^{-1}), and bands at 1508 cm^{-1}, 1454 cm^{-1}, and 1426 cm^{-1} typical of SG type lignin [49]. Alkali-purification was found to retain most of the bands seen in RecLs, thus corroborating the assumption that most of the lignin structures were preserved during alkali-purification. Solvent-fractionation on the other hand caused some noticeable changes. WFR showed flattening of the band at 1318 cm^{-1} (Vibrations on the rings of S-units), prominently present in W and WAH. Instead, it showed a prominent absorption band 1264 cm^{-1} (Rings of G-unit), as compared to W and WAH. Additionally, it showed a more prominent band at 1030 cm^{-1} (Aromatic C-H in plane deformation, G- > S-units). This band was almost equal in intensity to the band at 1115 cm^{-1} (Aromatic C-H in-plane deformation of S-units) in WFR, whereas in W and WAH, it was much smaller. These results indicate that during solvent-fractionation, the less condensed and more soluble lignin fractions (higher S/G ratio) were partitioned into the organic solvents, while more condensed lignin fractions (lower S/G ratio) were accumulated in the solvent-insoluble portion (WFR). Similar results were observed in SMFR, MSFR, and WSFR (Appendix, Figure 15). This finding is in line with literature reports that solvent-fractionation results in fractions with more condensed character, and lower S/G ratio [6], [16], [19]. This might be the result of an easier accessibility of the less condensed fractions by the solvents, and their favorable HSPs / hydrogen bonding interactions with the solvents, as compared to the more condensed fractions. Reported S/G ratios as measured by HSQC for W, MS, WS, and MA are 1.25, 2.86, 1.9, and 0.52 [35]. It should be noted, that neither FT-IR nor HSQC are quantitative methods, and the changes observed in the FT-IR must be corroborated by standard quantitative methods for S/G ratio determination such as nitrobenzene oxidation and pyrolysis.

3.5. Thermogravimetric analysis (TGA): TGA analysis echoed the findings of FT-IR analysis, where the AHs were largely unmodified as compared to the RecLs, while FRs were found to be significantly modified (Figure 12). The trends seen in TGA analysis of AHs were not as harmonious for all biomass species as those seen in FT-IR analysis, and each biomass is addressed below. Mixed angiosperms were excluded from this analysis due to restrictions on sample availability. In all cases, RecLs displayed a degradation shoulder between ~200 ºC and 300 ºC, which was significantly diminished in SMAH, WAH and MSAH. This region is generally indicative of thermal degradation of carbohydrate impurities in lignin, which are converted to volatile compounds such as methane and carbon dioxide [16]. Its diminished appearance in AHs is in line with the removal of carbohydrates during alkali-purification, as observed in the compositional analysis of AHs (Figure 8, Table 4). The carbohydrate-degradation shoulder was still visible in the thermogram of WSAH, probably due to its relatively higher carbohydrate content as compared to the other AHs (lignin/carbohydrate ratio = 34, lowest of all AHs; Figure 8). As expected, appearance of the carbohydrate-degradation shoulder was enhanced in thermograms of FRs, in line with their carbohydrate content (Figure 8). The temperature of maximum mass loss rate for all AHs remained almost unchanged from that of RecLs, between ~338 ºC and ~363 ºC, within the typical range for cleavage of carbon-carbon linkages and degradation of polymeric structure of lignin [16] (Figure 12). On the other hand, solvent-fractionation was found to affect this temperature variably. SMFR showed two prominent degradation temperatures (341 ºC and 398 ºC), as did MSFR (354 ºC and 475 ºC). WFR and WSFR showed single degradation peaks (382 ºC and 338 ºC respectively). Hence, with the exception WSFR, FRs were found to contain some components with higher thermostability than RecLs and AHs. This thermostability further corroborates the FT-IR

findings of more condensed nature and lower S/G ratio of FRs, as a higher G-unit content has been reported to contribute to the higher thermostability by restricting the polymer chain movement due to their relatively rigid nature as compared to S units [12]. It also indicates toward the higher molecular weights of FRs, as HMW fractions of lignin have been found to possess higher Tg [7], [8], [12], [15]–[17]. Lastly, the presence of multiple peaks in the thermograms of FR indicates their relatively heterogenous composition. All FRs showed acetone evaporation peak around 56 ºC, from the trace solvent remaining in the samples even after extensive vacuum drying.

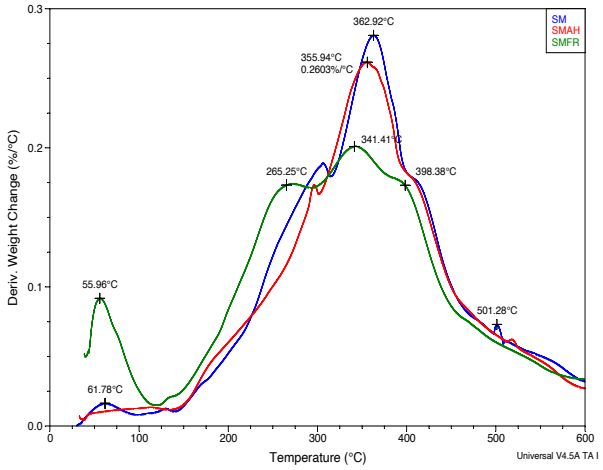

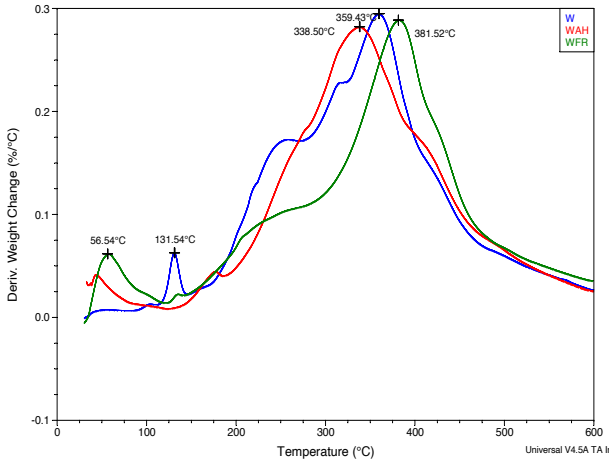

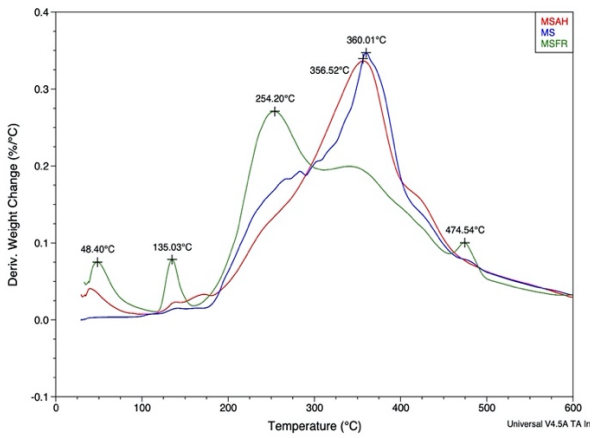

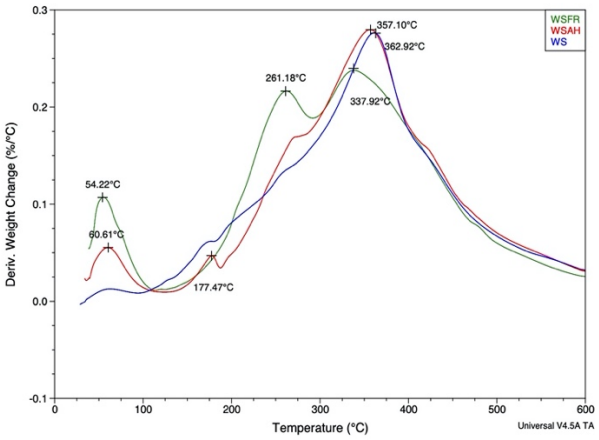

Figure 12: Derivative thermogravimetry spectra of recovered and alkali-purified lignins and solvent-insoluble fractions

3.6. Acetyl Bromide coefficient determination: The acetyl bromide extinction coefficient values (EC) for RecLs ranged between 18 $lg^{-1}cm^{-1}$ (W) and 27 $lg^{-1}cm^{-1}$ (WS; Figure 13, blue). The value for W was slightly higher than the typical range reported (hardwoods ~23.6 $lg^{-1}cm^{-1}$, kenaf ~34 $lg^{-1}cm^{-1}$) [50]. Alkali-purification was found to increase the EC values for AHs (Figure 13, red). Increased purity of AHs might be the possible reason behind the increase in EC values, but more studies are needed. Some of the small-molecular weight aromatic fragments atypical for lignin have been documented to possess notably different ECs from typical lignin (higher and lower both, depending on the molecule) [51]. The variability in their interaction with the mild alkali might also have contributed to the variability in the EC values of AHs. For example, ferulates and coumarates, which are a characteristic feature of graminae lignins (as described in the introduction) have been documented to possess significantly higher EC values as compared to lignin [51]. Although the ester linkages between ferulates and xylans can be expected to be cleaved during alkali-purification, ether linkages between ferulate and lignin might have been retained, thus increasing the relative amount of ferulates in AHs, leading to their overall higher EC values. FRs and MA were excluded from this analysis due to their high carbohydrate content and heterogenous origins respectively.

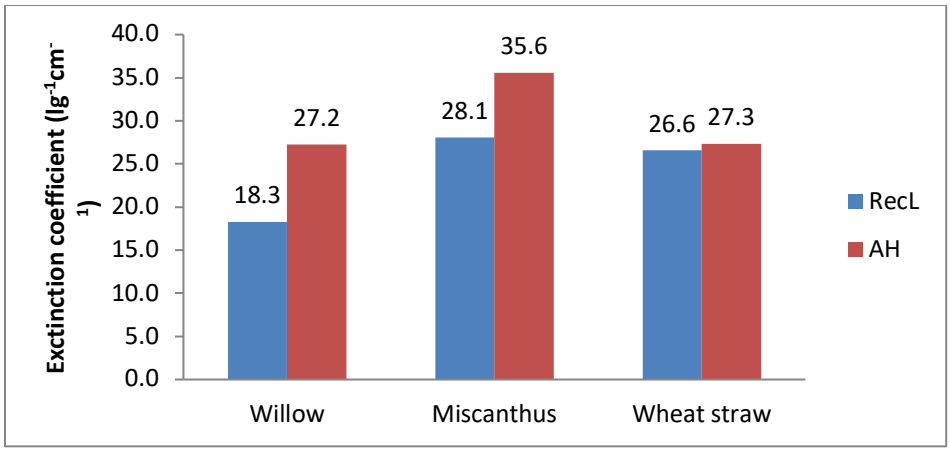

Figure 13: Acetyl bromide coefficients of recovered (RecL) and alkali-purified (AH) lignins

3.7. Antioxidant activity (AOA): Antioxidant activity of RecLs and AHs was analyzed to determine effect of lignin purity on AOA. Higher lignin purity produced by alkali-purification was found to affect the AOA of lignins variably. The trends observed for changes in EC after alkali-purification were not reflected in the trends observed for changes in AOA. The activities of SMAH and MSAH (lower IC_{50}) were found to be superior to SM and MS (higher IC_{50}) respectively, while the activities of WAH and WSAH were found to be inferior to W and WS (Figure 14). This indicates that during alkali-purification, W and WS lost some small-molecular weight compounds which were contributing to the AOA of these lignins. All lignins were found to be superior to the reference commercial antioxidant 3,5-di-tert-butyl-4-hydroxytoluene (BHT). The two natural antioxidants used as standards- ferulic acid, and vitamin C were found to be very effective antioxidants. Free phenolic hydroxyl groups are reported to contribute to the AOA of lignins [52], and it is expected that higher the PhOH content, better the AOA, and lower the IC_{50}. The PhOH content of RecLs (Figure 10, blue) correlated well with their AOA (Figure 14, blue), where decreasing PhOH content (W > SM = MS > WS) matched with increasing IC_{50} and decreasing AOA (W < MS = SM < WS). However, this correlation was not observed for AHs.

This indicates that AOA might be mediated by other moieties in addition to PhOH, and more studies are needed to explain this result.

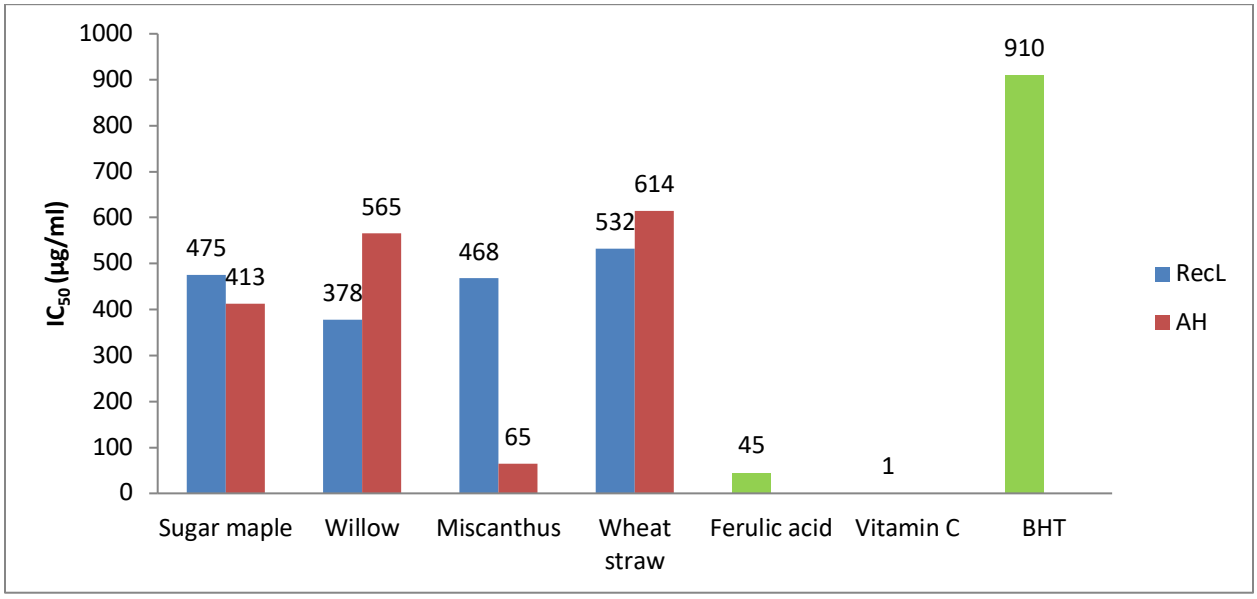

Figure 14: Antioxidant activities of recovered (RecL) and alkali-purified (AH) lignins, along with ferulic acid and vitamin C (natural antioxidant) and BHT* (butylated hydroxytoluene; commercial standard) *Literature value; Pan et al, 2006 [52]

4. Conclusions: Our results indicated that mild alkali-mediated and organic solvent-mediated fractionation are viable methods for differentiating hot-water extracted angiosperm lignin into fractions with distinct physicochemical properties. Alkali-purified lignins were found to possess higher lignin content, lower carbohydrate content, lower PhOH content, less condensed structures, and relatively lower thermostability. The effects on acetyl bromide extinction coefficient and antioxidant activity were variable. On the other hand, solvent-insoluble fractions were found to possess lower lignin content, higher carbohydrate content, higher PhOH content, more condensed structures, and partially higher thermostability. These results suggest that alkali-purification probably preserves most of the initial lignin structure in the final residue, while solvent-fractionation probably accumulates more condensed lignin fragments in the final residue.

Overall, both methods were successful in producing fractions that can be explored in polymeric applications for lignin valorization, such as in synthesis of lignin-based hydrogels described Chapter 3.

Appendix:

A. FT-IR Spectra of lignins:

Mixed angiosperms were excluded from this analysis due to their heterogenous origins and restrictions on sample availability.

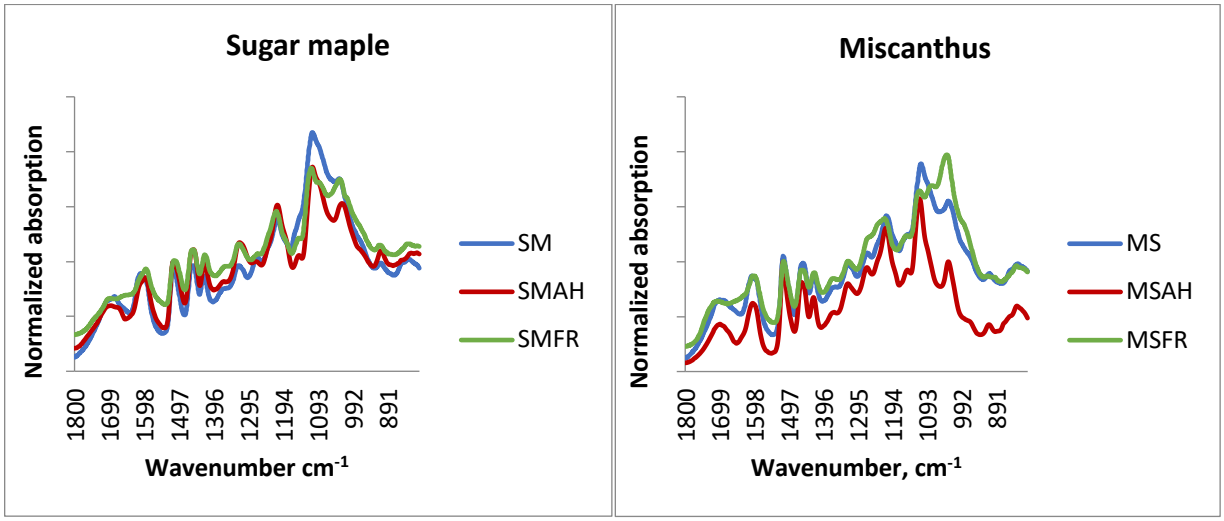

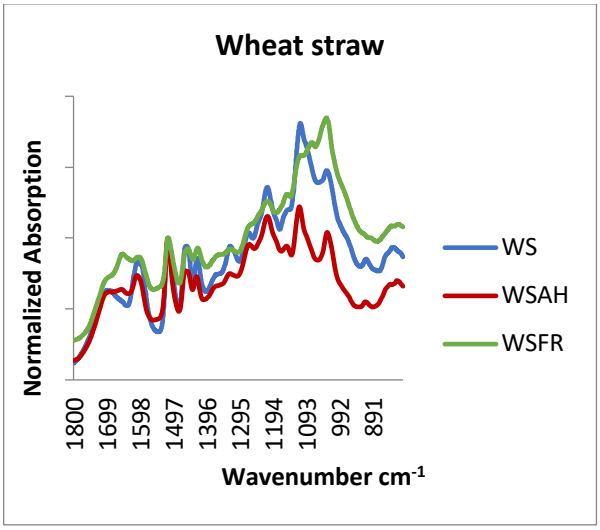

Figure 15: FT-IR spectra of recovered (RecL) and alkali-purified lignins (AH) and solvent-insoluble fraction (FR)

B. Nuclear Magnetic Spectroscopy (NMR): All 2D heteronuclear single quantum correlation nuclear magnetic resonance spectroscopy (HSQC NMR) experiments were acquired at 30°C on a Bruker AVANCE III 600 spectrometer (600MHz ^{1}H frequency, Bruker Biospin Corporation, Billerica, MA, USA) equipped with a 5 mm triple resonance *z*-gradient probe. Data was processed in Topspin v. 3.2 from Bruker Biospin. The samples were dissolved in deuterated dimethyl sulfoxide (DMSO-d_6) without acetylation. Mixed angiosperms were excluded from this analysis due to their heterogenous origins, while FRs were excluded since they were significantly contaminated with carbohydrate to a much higher extent than RecLs and AHs.

As compared to RecLs, the HSQC spectra of AHs showed a marked decrease in the correlation integral areas for lignin-carbohydrate linkages (hardwoods and graminae lignins) and ferulates (graminae lignins). However, it should be noted that HSQC is not a quantitative method and the results obtained by this method are not precise. It should also be noted that due to the presence of significant impurities resulting in overlapping of individual correlations, the correlations integrals are not well-defined, introducing further imprecision.

Table 6: Comparison between HSQC integrals for recovered (RecL) and alkali-fractionated (AHs). Semiquantitative, calibrated to solvent integral area

Biomass	Unit	δ_C / δ_H, ppm [56, 57]	Integral area[a] (abs) RecL	Integral area[a] (abs) AH
Sugar maple	LCC (β-D-Xylp), C1	103-99 / 4.7-4.1	0.09	0.03
Willow	LCC (β-D-Xylp), C1	103-92 / 4.8-4.1	0.11	0.05
Miscanthus	LCC (β-D-Xylp), C1	102-92 / 4.9-4.2	0.03	0.02
	Ferulate, Cα	145-144 / 7.6-7.4	0.04	0.036
	Ferulate, Cβ	116-114 / 6.4-6.2	0.04	0.1
Wheat straw	LCC (β-D-Xylp), C1	102-100 / 5.1-4.2	9.48	8.73
	Ferulate, Cα	145 / 7.6-7.2	4.74	3.79
	Ferulate, Cβ	115-113 / 6.9-6.2	5.69	5.22

[a]: Calibrated to DMSO integral area (39.7-40, 2.4 ppm)

References:

[1] S. Gillet *et al.*, "Lignin transformations for high value applications: towards targeted modifications using green chemistry," *Green Chem.*, vol. 19, no. 18, pp. 4200–4233, Sep. 2017, doi: 10.1039/C7GC01479A.

[2] E. Sjöström, "Chapter 4 - LIGNIN," in *Wood Chemistry (Second Edition)*, E. Sjöström, Ed. San Diego: Academic Press, 1993, pp. 71–89.

[3] "Supercritical water-induced lignin decomposition reactions: A structural and quantitative study :: BioResources." https://bioresources.cnr.ncsu.edu/ (accessed Jul. 10, 2020).

[4] N. Sun, M. Rahman, Y. Qin, M. L. Maxim, H. Rodríguez, and R. D. Rogers, "Complete dissolution and partial delignification of wood in the ionic liquid 1-ethyl-3-methylimidazolium acetate," *Green Chem.*, vol. 11, no. 5, pp. 646–655, May 2009, doi: 10.1039/B822702K.

[5] C. Li, X. Zhao, A. Wang, G. W. Huber, and T. Zhang, "Catalytic Transformation of Lignin for the Production of Chemicals and Fuels," *Chem. Rev.*, vol. 115, no. 21, pp. 11559–11624, Nov. 2015, doi: 10.1021/acs.chemrev.5b00155.

[6] M. Gigli and C. Crestini, "Lignin fractionation: Opportunities and Challenges," *Green Chem.*, 2020, doi: 10.1039/D0GC01606C.

[7] C. Cui, R. Sun, and D. S. Argyropoulos, "Fractional Precipitation of Softwood Kraft Lignin: Isolation of Narrow Fractions Common to a Variety of Lignins," *ACS Sustain. Chem. Eng.*, vol. 2, no. 4, pp. 959–968, Apr. 2014, doi: 10.1021/sc400545d.

[8] A. P. Dodd, J. F. Kadla, and S. K. Straus, "Characterization of Fractions Obtained from Two Industrial Softwood Kraft Lignins," *ACS Sustain. Chem. Eng.*, vol. 3, no. 1, pp. 103–110, Jan. 2015, doi: 10.1021/sc500601b.

[9] J. Domínguez-Robles, T. Tamminen, T. Liitiä, M. S. Peresin, A. Rodríguez, and A.-S. Jääskeläinen, "Aqueous acetone fractionation of kraft, organosolv and soda lignins," *Int. J. Biol. Macromol.*, vol. 106, pp. 979–987, Jan. 2018, doi: 10.1016/j.ijbiomac.2017.08.102.

[10] A.-S. Jääskeläinen, T. Liitiä, A. Mikkelson, and T. Tamminen, "Aqueous organic solvent fractionation as means to improve lignin homogeneity and purity," *Ind. Crops Prod.*, vol. 103, pp. 51–58, Sep. 2017, doi: 10.1016/j.indcrop.2017.03.039.

[11] J.-Y. Kim, S. Y. Park, J. H. Lee, I.-G. Choi, and J. W. Choi, "Sequential solvent fractionation of lignin for selective production of monoaromatics by Ru catalyzed ethanolysis," *RSC Adv.*, vol. 7, no. 84, pp. 53117–53125, Nov. 2017, doi: 10.1039/C7RA11541E.

[12] H. Li and A. G. McDonald, "Fractionation and characterization of industrial lignins," *Ind. Crops Prod.*, vol. 62, pp. 67–76, Dec. 2014, doi: 10.1016/j.indcrop.2014.08.013.

[13] A. Arshanitsa *et al.*, "Fractionation of technical lignins as a tool for improvement of their antioxidant properties," *J. Anal. Appl. Pyrolysis*, vol. 103, pp. 78–85, Sep. 2013, doi: 10.1016/j.jaap.2012.12.023.

[14] V. Passoni, C. Scarica, M. Levi, S. Turri, and G. Griffini, "Fractionation of Industrial Softwood Kraft Lignin: Solvent Selection as a Tool for Tailored Material Properties," *ACS Sustain. Chem. Eng.*, vol. 4, no. 4, pp. 2232–2242, Apr. 2016, doi: 10.1021/acssuschemeng.5b01722.

[15] T. Saito *et al.*, "Methanol fractionation of softwood Kraft lignin: impact on the lignin properties," *ChemSusChem*, vol. 7, no. 1, pp. 221–228, Jan. 2014, doi: 10.1002/cssc.201300509.

[16] K. Wang, F. Xu, and R. Sun, "Molecular Characteristics of Kraft-AQ Pulping Lignin Fractionated by Sequential Organic Solvent Extraction," *Int. J. Mol. Sci.*, vol. 11, no. 8, Art. no. 8, Aug. 2010, doi: 10.3390/ijms11082988.

[17] T. V. Lourençon, F. A. Hansel, T. A. da Silva, L. P. Ramos, G. I. B. de Muniz, and W. L. E. Magalhães, "Hardwood and softwood kraft lignins fractionation by simple sequential acid precipitation," *Sep. Purif. Technol.*, vol. 154, pp. 82–88, Nov. 2015, doi: 10.1016/j.seppur.2015.09.015.

[18] X. Du, G. Gellerstedt, and J. Li, "Universal fractionation of lignin–carbohydrate complexes (LCCs) from lignocellulosic biomass: an example using spruce wood," *Plant J.*, vol. 74, no. 2, pp. 328–338, 2013, doi: 10.1111/tpj.12124.

[19] C. G. Boeriu, F. I. Fiţigău, R. J. A. Gosselink, A. E. Frissen, J. Stoutjesdijk, and F. Peter, "Fractionation of five technical lignins by selective extraction in green solvents and characterisation of isolated fractions," *Ind. Crops Prod.*, vol. 62, pp. 481–490, Dec. 2014, doi: 10.1016/j.indcrop.2014.09.019.

[20] E. Stefanis and C. Panayiotou, "Prediction of Hansen Solubility Parameters with a New Group-Contribution Method," *Int. J. Thermophys.*, vol. 29, no. 2, pp. 568–585, Apr. 2008, doi: 10.1007/s10765-008-0415-z.

[21] J. H. Hildebrand, “A Critique of the Theory of Solubility of Non-Electrolytes.,” *Chem. Rev.*, vol. 44, no. 1, pp. 37–45, Feb. 1949, doi: 10.1021/cr60137a003.
[22] C. M. Hansen, “The Universality of the Solubility Parameter,” *Prod. RD*, vol. 8, no. 1, pp. 2–11, Mar. 1969, doi: 10.1021/i360029a002.
[23] A. Duval, F. Vilaplana, C. Crestini, and M. Lawoko, “Solvent screening for the fractionation of industrial kraft lignin,” *Holzforschung*, vol. 70, no. 1, pp. 11–20, Jan. 2016, doi: 10.1515/hf-2014-0346.
[24] J. Y. Jung, C.-H. Park, and E. Y. Lee, “Epoxidation of Methanol-Soluble Kraft Lignin for Lignin-Derived Epoxy Resin and Its Usage in the Preparation of Biopolyester,” *J. Wood Chem. Technol.*, vol. 37, no. 6, pp. 433–442, Nov. 2017, doi: 10.1080/02773813.2017.1310901.
[25] M. Olivares, J. A. Guzmán, A. Natho, and A. Saavedra, “Kraft lignin utilization in adhesives,” *Wood Sci. Technol.*, vol. 22, no. 2, pp. 157–165, Jun. 1988, doi: 10.1007/BF00355851.
[26] M. N. Vanderlaan and R. W. Thring, “Polyurethanes from Alcell® lignin fractions obtained by sequential solvent extraction,” *Biomass Bioenergy*, vol. 14, no. 5, pp. 525–531, May 1998, doi: 10.1016/S0961-9534(97)10058-7.
[27] Q. Li *et al.*, “Non-Solvent Fractionation of Lignin Enhances Carbon Fiber Performance,” *ChemSusChem*, vol. 12, no. 14, pp. 3249–3256, Jul. 2019, doi: 10.1002/cssc.201901052.
[28] T. Saito *et al.*, “Turning renewable resources into value-added polymer: development of lignin-based thermoplastic,” *Green Chem.*, vol. 14, no. 12, pp. 3295–3303, Nov. 2012, doi: 10.1039/C2GC35933B.
[29] H. Sadeghifar and D. S. Argyropoulos, “Macroscopic Behavior of Kraft Lignin Fractions: Melt Stability Considerations for Lignin–Polyethylene Blends | ACS Sustainable Chemistry & Engineering,” *ACS Sustain. Chem. Eng.*, vol. 4, no. 10, pp. 5160–5166, May 2016, doi: https://doi.org/10.1021/acssuschemeng.6b00636.
[30] X. Yue, F. Chen, X. Zhou, and G. He, “Preparation and Characterization of Poly (vinyl chloride) Polyblends with Fractionated Lignin,” *Int. J. Polym. Mater. Polym. Biomater.*, vol. 61, no. 3, pp. 214–228, Mar. 2012, doi: 10.1080/00914037.2011.574659.
[31] Y. Zhao, A. Tagami, G. Dobele, M. E. Lindström, and O. Sevastyanova, “The Impact of Lignin Structural Diversity on Performance of Cellulose Nanofiber (CNF)-Starch Composite Films,” *Polymers*, vol. 11, no. 3, Art. no. 3, Mar. 2019, doi: 10.3390/polym11030538.
[32] H. Sadeghifar, T. Wells, R. K. Le, F. Sadeghifar, J. S. Yuan, and A. Jonas Ragauskas, “Fractionation of Organosolv Lignin Using Acetone:Water and Properties of the Obtained Fractions,” *ACS Sustain. Chem. Eng.*, vol. 5, no. 1, pp. 580–587, Jan. 2017, doi: 10.1021/acssuschemeng.6b01955.
[33] M. W. Davis, “A Rapid Modified Method for Compositional Carbohydrate Analysis of Lignocellulosics by High pH Anion-Exchange Chromatography with Pulsed Amperometric Detection (HPAEC/PAD),” *J. Wood Chem. Technol.*, vol. 18, no. 2, pp. 235–252, May 1998, doi: 10.1080/02773819809349579.
[34] A. Gärtner, G. Gellerstedt, and T. Tamminen, “Determination of phenolic hydroxyl groups in residual lignin using a modified UV-method,” *Nord. Pulp Pap. Res. J.*, vol. 14, no. 2, pp. 163–170, May 1999, doi: 10.3183/npprj-1999-14-02-p163-170.
[35] P. Dongre, “Characterization and utilization of hot-water extracted lignin for formaldehyde-free resin applications," *Diss. Theses*, Apr. 2018, [Online]. Available: https://digitalcommons.esf.edu/etds/58.
[36] R. S. Fukushima and R. D. Hatfield, “Comparison of the Acetyl Bromide Spectrophotometric Method with Other Analytical Lignin Methods for Determining Lignin Concentration in Forage Samples,” *J. Agric. Food Chem.*, vol. 52, no. 12, pp. 3713–3720, Jun. 2004, doi: 10.1021/jf035497l.
[37] T. Dizhbite, G. Telysheva, V. Jurkjane, and U. Viesturs, “Characterization of the radical scavenging activity of lignins--natural antioxidants,” *Bioresour. Technol.*, vol. 95, no. 3, pp. 309–317, Dec. 2004, doi: 10.1016/j.biortech.2004.02.024.
[38] K. Lundquist, R. Simonson, and K. Tingsvik, “Studies on lignin carbohydrate linkages in milled wood lignin preparations,” *Sven. Papperstidning*, vol. 83, no. 16, pp. 452–454, 1980.
[39] J. Ropponen *et al.*, “Solvent extraction as a means of preparing homogeneous lignin fractions: 11th EWLP, Hamburg, Germany, August 16–19, 2010,” *Holzforschung*, vol. 65, no. 4, pp. 543–549, Jun. 2011, doi: 10.1515/hf.2011.089.
[40] J. K. Fink, “Chapter 12 - Terpene Resins,” in *Reactive Polymers Fundamentals and Applications (Second Edition)*, J. K. Fink, Ed. Oxford: William Andrew Publishing, 2013, pp. 303–315.
[41] C. Schuerch, “The Solvent Properties of Liquids and Their Relation to the Solubility, Swelling, Isolation and Fractionation of Lignin,” *J. Am. Chem. Soc.*, vol. 74, no. 20, pp. 5061–5067, Oct. 1952, doi: 10.1021/ja01140a020.
[42] I. Demuner, J. Colodette, and A. Demuner, “Biorefinery review: Wide-reaching products through kraft lignin :: BioResources,” *BioResources*, vol. 14, pp. 7543–7481, 2019.

[43] T. E. Amidon, C. D. Wood, A. M. Shupe, Y. Wang, M. Graves, and S. Liu, "Biorefinery: Conversion of Woody Biomass to Chemicals, Energy and Materials," Jun. 2008. https://www.ingentaconnect.com/content/asp/jbmb/2008/00000002/00000002/art00002 (accessed May 07, 2020).
[44] Y. Zhao, U. Shakeel, M. Saif Ur Rehman, H. Li, X. Xu, and J. Xu, "Lignin-carbohydrate complexes (LCCs) and its role in biorefinery," *J. Clean. Prod.*, vol. 253, p. 120076, Apr. 2020, doi: 10.1016/j.jclepro.2020.120076.
[45] C. Gong and B. M. Bujanovic, "Impact of Hot-Water Extraction on Acetone-Water Oxygen Delignification of Paulownia Spp. and Lignin Recovery," *Energies*, vol. 7, no. 2, Art. no. 2, Feb. 2014, doi: 10.3390/en7020857.
[46] E. Sjöström, *Wood Chemistry*, 2nd ed. Elsevier, 1993.
[47] C. Crestini and D. S. Argyropoulos, "Structural Analysis of Wheat Straw Lignin by Quantitative 31P and 2D NMR Spectroscopy. The Occurrence of Ester Bonds and α-O-4 Substructures," *J. Agric. Food Chem.*, vol. 45, no. 4, pp. 1212–1219, Apr. 1997, doi: 10.1021/jf960568k.
[48] M. J. Goundalkar, D. B. Corbett, and B. M. Bujanovic, "Comparative Analysis of Milled Wood Lignins (MWLs) Isolated from Sugar Maple (SM) and Hot-Water Extracted Sugar Maple (ESM)," *Energies*, vol. 7, no. 3, Art. no. 3, Mar. 2014, doi: 10.3390/en7031363.
[49] O. Faix, "Fourier Transform Infrared Spectroscopy," in *Methods in Lignin Chemistry*, S. Y. Lin and C. W. Dence, Eds. Berlin, Heidelberg: Springer, 1992, pp. 83–109.
[50] S. Y. Lin and C. W. Dence, Eds., *Methods in Lignin Chemistry*. Berlin Heidelberg: Springer-Verlag, 1992.
[51] C. Jing, "Lignin content in xylan-rich lignocellulosic species (angiosperms) before and after hot-water extraction: Klason lignin and acetyl bromide methods," Masters Thesis, SUNY-ESF, Syracuse, 2017.
[52] X. Pan, J. F. Kadla, K. Ehara, N. Gilkes, and J. N. Saddler, "Organosolv ethanol lignin from hybrid poplar as a radical scavenger: relationship between lignin structure, extraction conditions, and antioxidant activity," *J. Agric. Food Chem.*, vol. 54, no. 16, pp. 5806–5813, Aug. 2006, doi: 10.1021/jf0605392.

Chapter III

Synthesis and Characterization of Lignin-based gels

1. Introduction:

Gels are three dimensional polymeric networks that are chemically or physically cross-linked with each other and have the intrinsic ability to swell in aqueous solvents, increasing in weight from 10-20% to up to thousands of times their dry weight [1]. The balance between the hydrophilicity of the polymers and the extensive cross-linking between polymers allows them to interact with aqueous solutions or biological fluids, while preventing them from dissolving and losing form. The most common type of gels are hydrogels, which primarily interact with aqueous solutions. Hydrogels are versatile, relatively modern materials that have been a subject of interest since the early reports of hydrogel synthesis in 1960s [2], [3], due to their amenability to a myriad applications Figure 1.

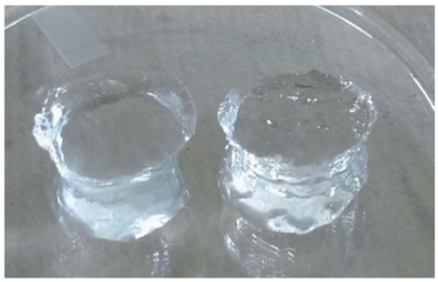

Figure 1: Typical appearance of hydrogels used in biomedical field. Reprinted with permission from [194]

When manufactured from the aptly called ‘smart polymers’, they are capable of altering their physicochemical properties in response to stimuli (e.g. magnetic field, radiation, ultrasound, and ionic concentration) in their external environment [4]–[8]. Hydrogels have been employed in hygiene, agriculture, waste management, coal dewatering, sealing, food additives,

pharmaceutical drug delivery, biomedical, biosensor, wound dressing, tissue engineering and regenerative medicine, and diagnostic fields, to name a few [9]. Hydrogel sizes can vary from a few nanometers to a few centimeters, depending on the method of preparation and intended application, and they have a tendency to adapt the shape of any space they are confined to during synthesis [10]. A model hydrogel is generally expected to have most of the following features [9]:

- High sorption capacity at a desired rate, as demanded by the intended application,
- Low solubility in aqueous solutions,
- High mechanical and chemical stability during application and storage,
- High biodegradability after use, without formation of toxic degradation products,
- Functionality over a wide range of pH and temperature, and
- Rewetting capability.

In addition, it is also preferred to be easy and economical to manufacture. Hydrogels have traditionally been made from synthetic monomers/polymers. Common examples of these are shown in Figure 2 [11]–[17].

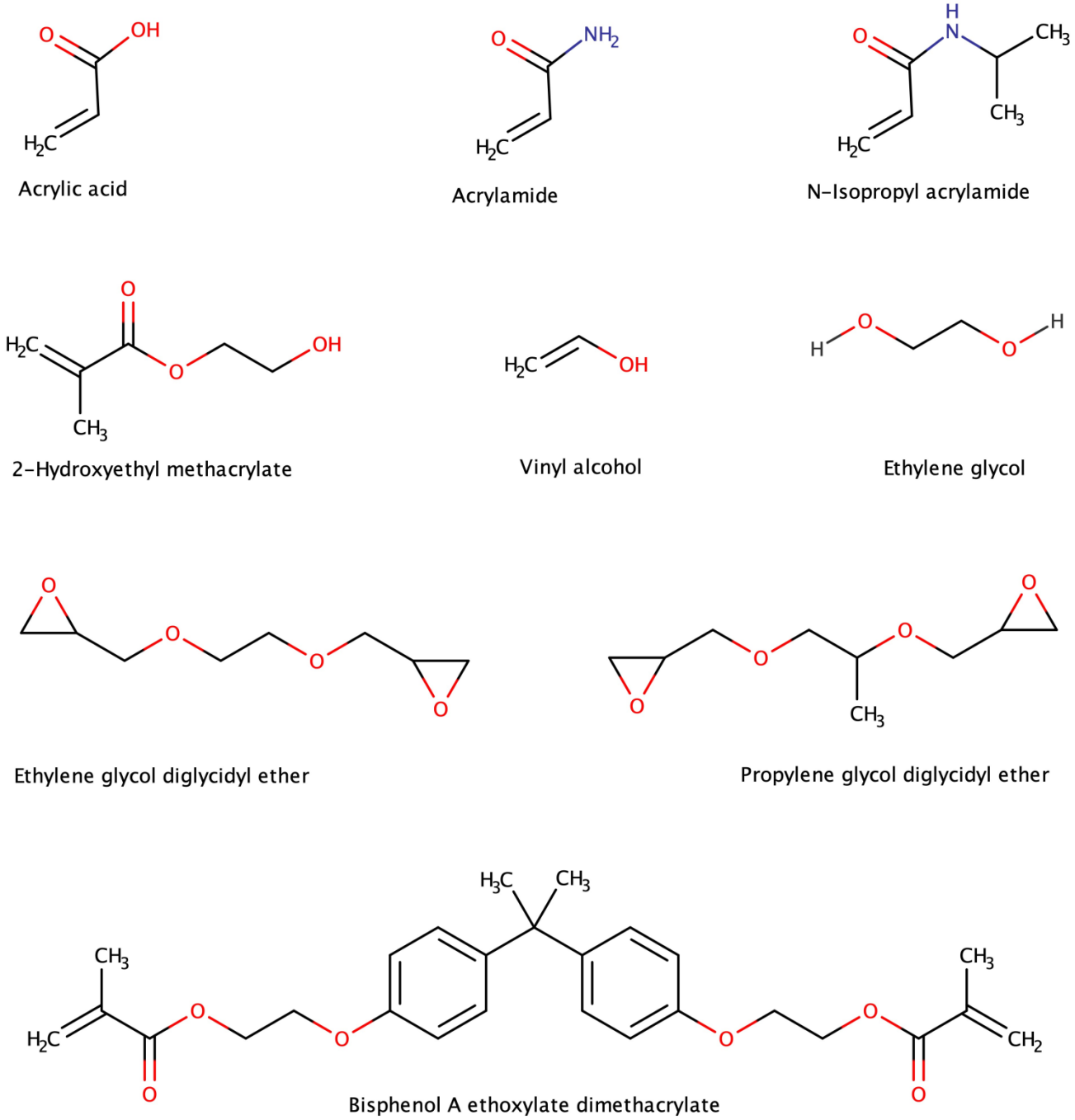

Figure 2: Common monomers and cross-linkers used in synthesis of hydrogels [11-17]

Recently biopolymers have also been explored for hydrogel synthesis, either by themselves, or in combination with synthetic components. Incorporation of a biopolymer in a hydrogel offers several additional advantages to the hydrogel, such as eco-friendliness by reducing energy

consumption and pollution associated with synthetic polymers, relatively higher biodegradability, lower procurement costs and greater biocompatibility [10]. The most common biopolymers used in hydrogel synthesis are polysaccharides such as cellulose, xylan, alginates, starch, chitosan, and gelatin, due to their high hydrophilicity [18]–[23]. Lignin can also serve as a polymer component for hydrogels, typically in combination with other synthetic or natural polymers [10]. Synthesis of lignin-based hydrogels is a relatively nascent research area, with oldest reports originating only in the last few decades [24]–[26].

1.1. Common techniques of hydrogel synthesis:

The starting components of a hydrogel can be a) monomers b) pre-polymers or c) existing hydrophilic polymers (Figure 3) [27]:

a) Synthesis of hydrogels from monomers: This involves copolymerization of monomers and polyfunctional co-monomers which act as cross-linkers to create a gel network. Acrylates and acrylamides are common monomers used in this method, cross-linked by N,N'-Methylenebisacrylamide (NMBA, Figure 4). Radical polymerization is initiated by heat, a redox initiator such as ammonium/potassium persulfate (APS; $(NH_4)_2S_2O_8$ / KPS; $K_2S_2O_8$), a photoinitiator such as AIBN or by a high-energy irradiation. For example, synthesis of gel membranes from dimethacrylate monomers has been reported for application in lithium-based batteries [15].

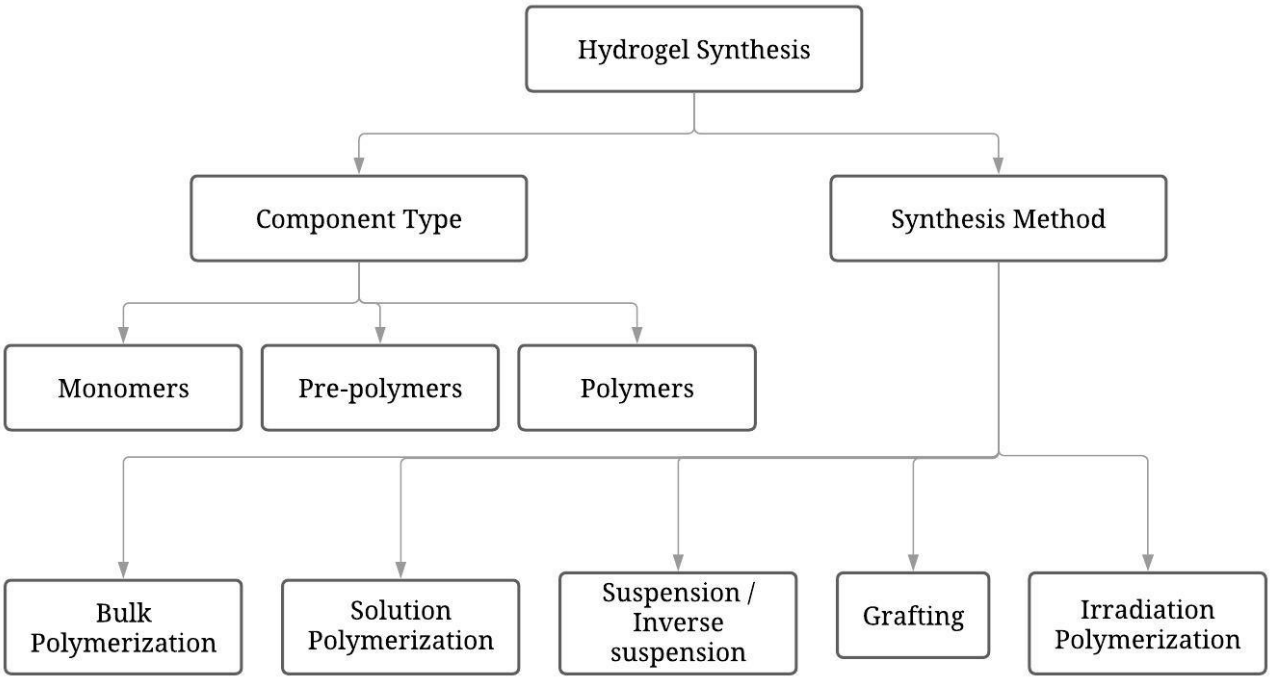

Figure 3: Hydrogel synthesis techniques showing possible component types and possible synthesis methods [9], [27]

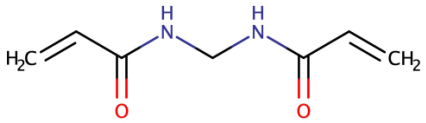

Figure 4: Cross-linker N,N'-Methylene bisacrylamide (NMBA). Redrawn from [28]

b) Synthesis of hydrogels from pre-polymers: This involves cross-linking hydrophilic polymers or oligomers of lower degree of polymerization to form a hydrogel network. An example is cross-linking of poly(ethylene) glycol with β-cyclodextrin (Figure 5) in presence of dibutyltin dilaurate catalyst to produce poly(ethylene glycol-β-cyclodextrin) hydrogels for temperature resistant applications [16] (Figure 6).

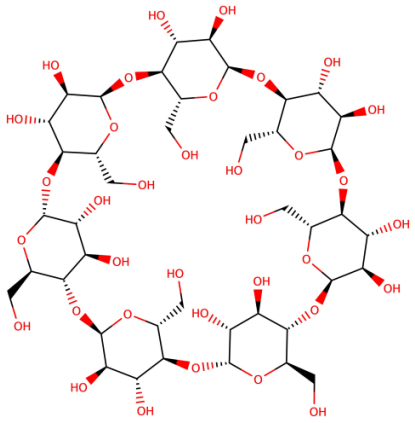

Figure 5: β-cyclodextrin. Redrawn from [29]

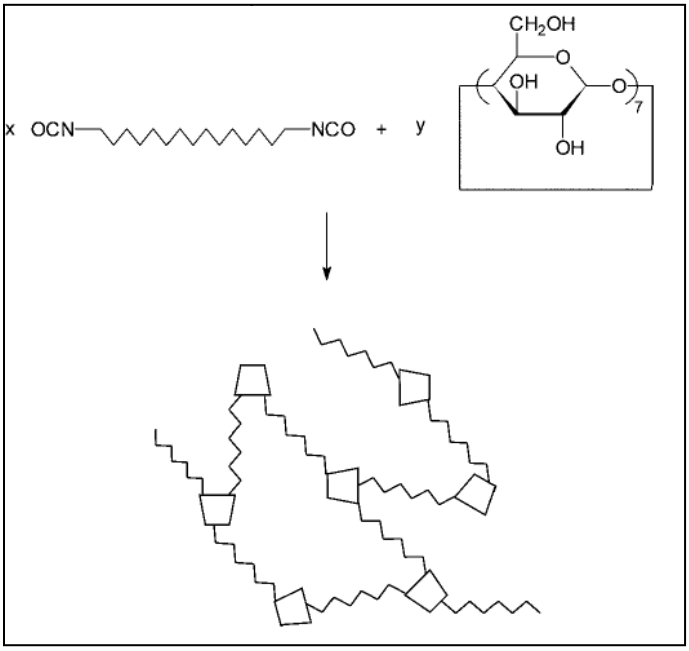

Figure 6: Synthesis of poly(ethylene glycol-β-cyclodextrin) hydrogels from end-capped poly(ethylene glycol) and β-cyclodextrin. Reprinted with permission from [16]

c) Synthesis of hydrogels from existing polymers: This method involves chemical or physical cross-linking of existing polymers. Examples are gelation of alginate with Ca^{+2} ions due to ionic interactions (Figure 7)[30]. Alginates are linear copolymers composed of (1 → 4)-linked α-L-guluronic acid and β-D-mannuronic acid residues of varying sequences, depending on the

organism and tissue that they are isolated from. Alginate gelation results from interactions between Ca^{2+} ions and the carboxyl groups on α-L-guluronic acid, which lead to chain–chain association and to the formation of junction zones [31].

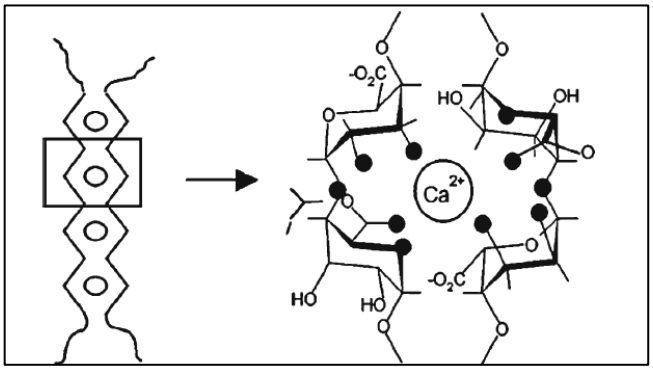

Figure 7: Development of cross-linked network of calcium alginate gel through ionic interaction of Ca^{+2} ions with oxygen atoms on the guluronic acid residues, resulting in an 'egg box' structure. Reprinted with permission from [30]

Polymerization of the starting hydrogel components occurs by one of the following ways (Figure 3) [9]:

a) Bulk polymerization: This simple technique involves addition of a monomer-soluble initiator into a pure liquid monomer. Usually a small amount of a cross-linking agent is also added into the mix. Instead of an initiator, irradiation, ultraviolet light or chemical catalysts can also be used. Due to the high concentration of the monomer, this method is characterized by high rate of polymerization, leading to generation of polymers of high-molecular weight and high purity [86]. For example, bulk polymerization of 2-hydroxyethyl methacrylate has been reported to produce glassy nonporous hydrogels in biomaterial applications [17].

b) Solution polymerization / cross-linking: In this technique, the monomer(s) is (are) mixed with a multifunctional cross-linking agent in presence of a solvent, which serves as a heat sink during polymerization. The polymerization is initiated thermally or by a redox initiators such as

peroxides (e.g. hydrogen peroxide) and persulfates (e.g. ammonium/potassium persulfate) [32]. Common solvents are water, ethanol, water/ethanol mixtures, and benzyl alcohol. The formed gel is washed with the solvent to remove unreacted components. The solvent is then removed from the gel network after the gel has formed (e.g. by lyophilization). Solution polymerization of 2-hydroxyethyl methacrylate with water as diluent produced porous hydrogels in studies carried out by the same group as in the earlier example [17].

c) Suspension / inverse suspension polymerization: This method is used to prepare spherical gel particles. The monomers and the initiator are dispersed in a non-solvent under continuous agitation, forming fine droplets [33]. The final product is obtained in the form of a powder, beads or a resin-like substance. Polyacrylate superabsorbent polymers are generally synthesized by this method [34].

d) Grafting on a support: This involves generation of free radicals on a mechanically stronger support, onto which the monomer is directly polymerized. The support and the polymer are covalently linked to each other. Cellulose-supported 2-hydroxyethyl methacrylate hydrogels have been reported, formed by graft polymerization of 2-hydroxyl methacrylate in the pores of cellulose [35]. Grafting of methacrylic acid on gelatin (product of denaturation and chemical degradation of collagen, containing a protein backbone [36]), with NMBA cross-linker has also been carried out (Figure 8) [37].

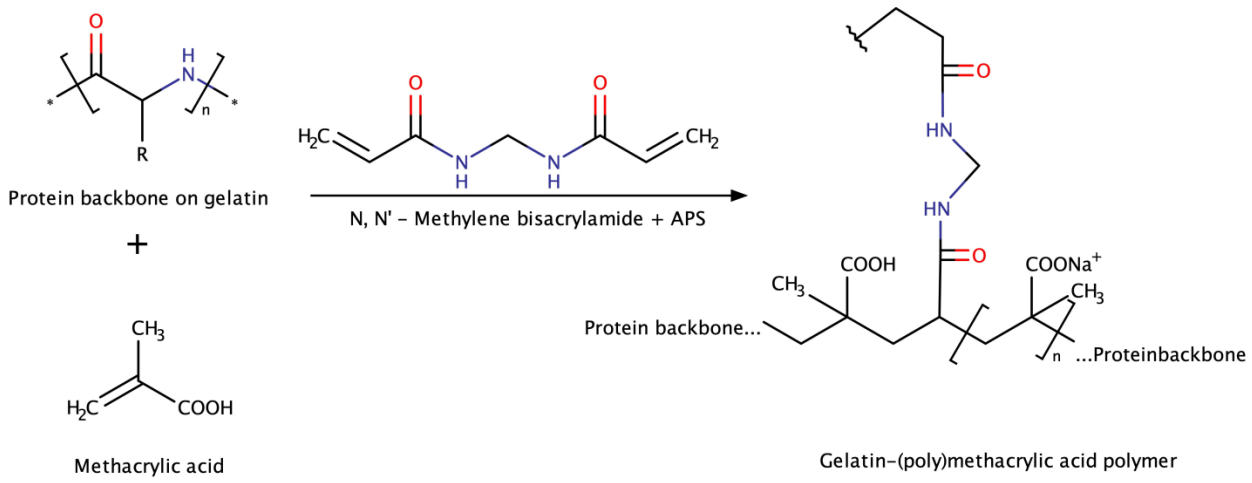

Figure 8: Grafting of methacrylic acid on gelatin, cross-linked with NMBA. Redrawn from [37]

e) Polymerization by irradiation: This method is generally employed for preparation of hydrogels from unsaturated compounds. It involves irradiation of gamma rays and electron beams onto aqueous polymer solutions leading to generation of free radicals on the polymers chains. Further, radiolysis of water produces hydroxyl free radicals which attack the polymer chains, resulting in relatively pure and initiator-free hydrogels. Poly(vinyl alcohol), poly(ethylene glycol) and poly(acrylic acid) are the most common examples of hydrogels produced by this method [33].

1.2. Lignin-based hydrogels:

Lignin has a tremendous potential to replace traditional petroleum-based polymers. As opposed to petroleum-based polymers used in the production of hydrogels, apart from being cost-efficient, lignin is biodegradable and CO_2 neutral, and shows little to no cytotoxicity [38]. Due to the variety of functional groups present on its structure, it offers flexibility to be incorporated with several copolymers. It is not prone to undergo explosive chemical reactions, and is safer to store and handle [10]. As compared to other biopolymers explored in hydrogel synthesis, it is

relatively more resistant to biological attacks than the polysaccharides, due to its antioxidant and antimicrobial properties, and hence can have a longer shelf-life [38], [39]. Additionally, the relative hydrophobicity of lignin can be advantageous for hydrogels. Inclusion of hydrophobic components in a hydrogel is expected to confer additional mechanical stability to the hydrogel and durability in aqueous solutions, thereby prolonging its functional life [11]. Lignin has been used in combination with different synthetic polymers as well as biopolymers to produce hydrogels which are applicable in a range of fields (Table 1).

Most of the applications of these hydrogels are sorption based. **Sorption** is a universal term used to define removal of compounds from a solution, and includes absorption and adsorption [40]. **Absorption** is a bulk phenomenon involving accumulation of atoms, molecules or ions within solids or liquids, while **adsorption** is a surface phenomenon involving accumulation of atoms, molecules or ions at a solid interface [40]–[42]. The moiety being absorbed is 'absorbate', and the matrix into which it is absorbed is called 'absorbent'. Similarly, the moiety being adsorbed is called 'adsorbate' and the surface onto which it is adsorbed is called 'adsorbent'. Adsorption can be further classified as physical adsorption and chemical adsorption or chemisorption. Physical adsorption involves non-specific, weaker intermolecular interactions (such as van der Waals interactions), between the adsorbate and the adsorbent, and occurs according to the size and nature of adsorbent-adsorbate interactions [43]. Chemisorption involves stronger interactions (such as covalent or ionic bonds) between the adsorbent and the adsorbate. The bond energies involved here are much higher than in physical adsorption, and the adsorption tends to be localized at particular sites where the bond formation occurs [43].

Table 1: Summary of selected reports on lignin-based hydrogels

Abbreviations: APS: Ammonium persulfate, ATRP: Atom transfer radical polymerization, CAS: Ceric ammonium sulfate, KPS: Potassium persulfate, LCST: lower critical solution temperature, NMBA: N,N'-methylenebisacrylamide, NIPAM: N-isopropyl acrylamide, PAM: polyacrylamide; PEGDGE: poly(ethylene glycol) diglycidyl ether, PVA: polyvinyl alcohol, t-BHP: t-butyl hydroperoxide

Lignin origin	**Copolymer/s**	**Hydrogel synthesis method**	**Hydrogel property / Application**
Banana pseudostem Soda lignin from banana pseudostem [44]	PVA, acrylamide	Radical initiated solution polymerization, KPS initiator	Absorption, Swelling degree ~484%
Kraft lignin [44]			~147%
Black liquor from alkaline pulping of rice straw, ~5% solid content [45]	Polyacrylamide, PVA	Radical initiated polymerization, ceric ammonium sulfate ($(NH_4)_4Ce(SO_4)_4$) initiator, NMBA cross-linker	Absorption, Swelling degree ~60%
Eucalyptus acetic acid lignin [46]	NIPAM	Graft copolymerization, initiated by hydrogen peroxide, NMBA cross-linker	Temperature sensitive, LCST ~31 ºC
LignoBoost (Softwood) [47]	Phenol and formaldehyde	Concentrated alkali	Aerogels and cryogels

	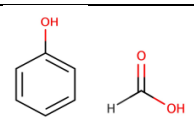		
Acetic acid lignin [48]	isocyanate (-NCO) terminated polyurethane ionomers		Absorption and slow release of ammonium sulfate fertilizer
Spruce organosolv lignin [49]	PEGDGE	Cross-linking in concentrated alkali, initiated by hydrogen peroxide	Absorption Swelling degree ~1600%
Steam explosion lignin from Aspen wood [50]	Microcrystalline cellulose	Chemical cross-linking in alkali with epichlorohydrin and heat	Absorption and controlled release of grape seed polyphenols and vanillin
Unspecified lignin from black liquor [51]	Acrylamide	Cross-linking in presence of APS and NMBA	Adsorption of Cu^{+2} and Ni^{+2} ions from simulated wastewater
Various lignins - Pine, Aspen, annual plants [52]	Xanthan gum	Cross-linking in presence of epichlorohydrin in alkali	Absorption
Birch acetic acid lignin [25]	PEGDGE	Cross-linking in alkali	Absorption
Softwood kraft lignin [53]			Separation of Ethanol and 1-Butanol from aqueous solutions
Unspecified lignin	Acrylamide, NIPAM,	Radical initiated graft	Sorption of

[54]	montmorillonite	polymerization on lignin in presence of APS, with NMBA as cross-linker, assisted by ultrasound	methylene blue dye from wastewater
Alkali lignin from wheat straw [55]	Acrylic acid	Radical initiated cross-linking in alkali, with APS initiator and NMBA cross-linker	Moisture retention in soils
Unspecified lignosulfonate [56]	Acrylic acid	Grafting on lignosulfonate initiated by laccase/t-BHP with NMBA cross-linker	Sorption of cationic dye from wastewater
Poplar lignin-carbohydrate complex (LCC) [57]	PEGDGE	Dissolution in alkaline medium	Cell carrier for human hepatocytes
LignoBoost (softwood) [58]	Tannin	Dissolution in alkaline medium in presence of formaldehyde	Aerogel for environmental and biomedical applications
Liquid hot-water extracted lignin from wheat straw, 200 ºC [59]	Oligo(ethylene)glycol- and oligo(propylene)glycol-α,ω-diglycidyl ether	Cross-linking in alkaline medium	Aerogel for thermal insulation
Lignosulfonate (sulfite pulping) [60]	Polyoxazoline conjugated with triazole	Graft polymerization on tosylated lignin[a] in organic solvent	Anti-infective ointment to control chronic inflammation

	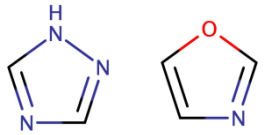		
Hardwood kraft lignin [61]	NIPAM	ATRP, with lignin macroinitiator created by modifying the PhOH groups	Thermoresponsive hydrogel, LCST ~32 ºC
Unspecified kraft lignin [62]	Poly(ethylene) glycol methyl ether methacrylate (PEGMA)	Grafting onto lignin by ATRP	Self-healing smart hydrogel for biomedical applications
[a]: The free aliphatic and aromatic hydroxyl groups on lignin were replaced by a tosyl group (Ts; $CH_3C_6H_4SO_2$) to produce a more active Lignin-OTs oligomer as a macroinitiator for ring-opening polymerization, and to increase hydrophilicity and compatibility of lignin with hydrophilic polymers.			

1.3. Applicability of hydrogels in wastewater remediation and sustained release systems:

Dyes are one of the most visible and easy to detect pollutants and wastewater contaminants due to their brilliant colors even at low concentrations (e.g. 0.005 mg/l) in industrial effluents [63]. Release of dye in wastewater occurs as a direct result of dye production, as well as through its subsequent use in pertinent industries. Apart from the intolerable coloring of wastewater streams, dyes hinder the photosynthetic abilities of aquatic ecosystems due to their ability to absorb and reflect sunlight. Additionally, not only can dyes themselves exert acute and chronic effects on the aquatic life, their degradation products can also be carcinogenic and mutagenic. Methyl violet dyes are water-soluble cationic dyes, mainly used in textile, paint and ink industries to impart deep purple color to materials (Figure 9) [64].

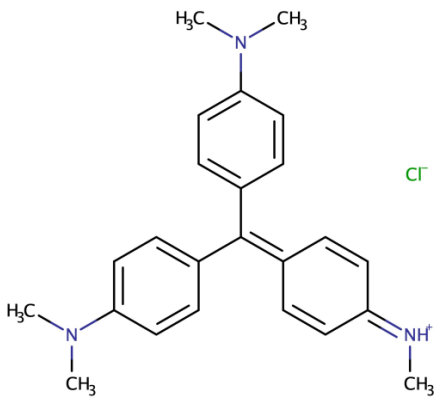

Figure 9: Methyl violet dye. Redrawn from [64]

Several different strategies have been used in removal of dyes, such as coagulation and precipitation, ozonation, ion exchange treatment, and selective adsorption using hydrogels, sawdust, and bagasse fly ash [63], [65], [66]. The advantages of selective adsorption using hydrogels over other strategies include high dye removal efficiency, absence of harmful byproducts released into water, and relative ease of separation of adsorbent from water stream [65]. Similar to dyes, metallic cations such as Cu^{+1}, Ni^{+1}, Zn^{+2}, Cd^{+2}, Cr^{+2}, Pb^{+2}, Hg^{+2} in wastewater streams pose serious biological hazards, and can find their way into humans through bioaccumulation [20], [67]. If ingested in excessive amounts, they can deposit in liver, brain, and pancreas, resulting in vomiting, cramps, convulsion and even death [20]. Hydrogels can be applied for selective adsorption and removal of these toxic metal ions, in similar fashion as dyes.

Hydrogels are also instrumental in sustained delivery of suitable agents in agricultural, pharmaceutical and fragrance industry. Incorporation of a bioactive agent or fragrance into the polymeric network of hydrogel results in a sustained release of the agent from the hydrogel matrix over an extended time [20]. Apart from bioactive agents and fragrances, water (moisture) can also be delivered to arid soils in this manner. Use of hydrogels for sustained release offers the advantage of targeting the release site by strategic placement of the hydrogel, and achieving

greater dose efficiency by avoiding non-productive release of the active agent. The ability of hydrogels to imbibe large amounts of aqueous solutions allows administration of fewer doses to target site, without the harmful effects of overdosing.

Keeping in mind these two different applications based on adsorption and absorption phenomena respectively, it was desired in this study to synthesize two types of lignin-based hydrogels. Lignin- poly(acrylamide)-kaolin hydrogels were developed with intended applications in wastewater remediation via selective adsorption of cationic dyes and metal cations, and lignin-poly(ethylene glycol) diglycidyl ether hydrogels were developed with intended applications in agriculture and fragrance delivery via absorption and subsequent release of aqueous solutions (e.g. Chaga-silver nanoparticles; Chapter 4) and fragrances.

1.4. Lignin as a partial replacement of poly(acrylamide) (PAM): Acrylamide (2-propenamide; C_3H_5NO; 71.08 g/mol; Figure 2) is a colorless and odorless crystalline solid, with a melting point of 84.5 ºC. It is a biodegradable molecule [68]. Acrylamide is derived from acrylonitrile by either catalytic hydrolysis or bioconversion. It has a favorable reactivity with many co-monomers, and it can be readily polymerized to form PAM gels with the help of initiators such as persulfates and suitable bifunctional crosslinking agents such as NMBA (Figure 10) [28], [69]. Solution polymerization in aqueous solvents is a commonly used technique for acrylamide polymerization [69]. Acrylamide has competitive prices as compared to other common monomers such as vinyl chloride and acrylic acid ($800-$1000/ton), and acrylamide-based polymeric materials are some of the most widespread materials used in the modern technologies - traditionally in applications such as flocculants, dewatering aids and as filtration enhancers in wastewater treatments [70], and centrifuges, and as wet-end additives in paper production [71]. PAM has recently emerged as an important polymer in hydrogel synthesis.

PAM hydrogels in combination with natural and synthetic polymers have been used in drug delivery, tissue engineering, and in removal of heavy metal cations. Although PAM polymers have been found to be generally safe [69], the acrylamide monomer has been known to cause neurotoxicity in humans, and has a high mobility in soil and in groundwater [72]. Hence, in this study, an attempt was made to partially replace PAM with lignin to synthesize greener hydrogels with retained functionality. The free phenolic hydroxyl groups on lignins recovered from hot-water hydrolyzate were expected to provide polymerization sites for acrylamide [44]–[46], [51], [54], [61], forming an effective polymeric network.

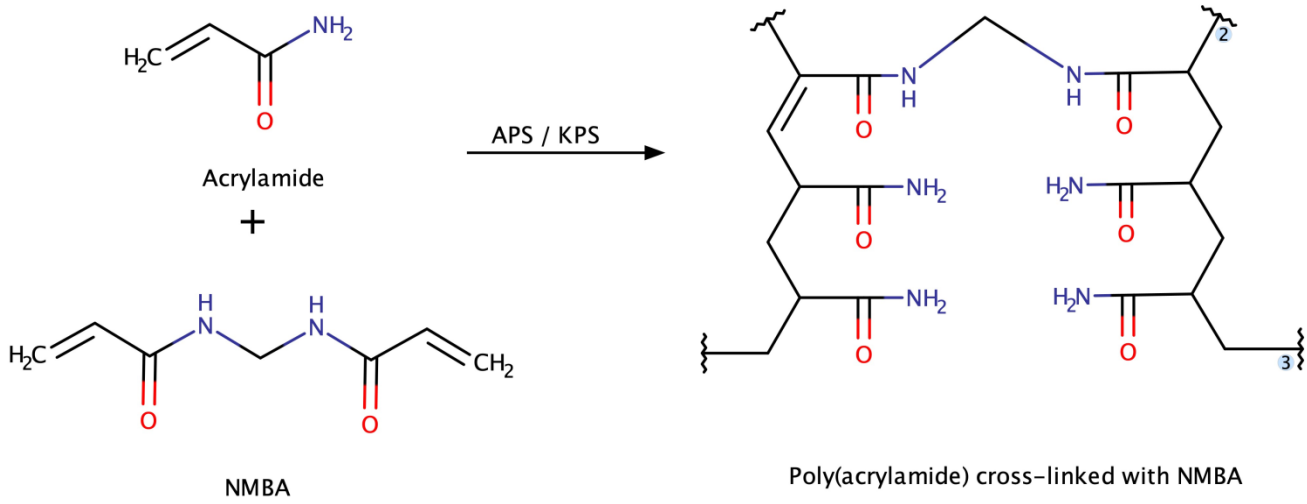

Figure 10: Polymerization of acrylamide with N,N'-methylenebisacrylamide (NMBA) as cross-linker, and ammonium/potassium persulfate as initiator

1.5. Incorporation of kaolin in lignin-poly (acrylamide) hydrogels: The term kaolin encompasses a group of naturally occurring aluminum silicate minerals, one of which is kaolinite ($Al_2O_3.2SiO_2.2H_2O$). Since kaolinite is the dominant mineral in kaolin group, the two terms are sometimes used interchangeably in the industry. Kaolinite consists of an alumina octahedral sheet, which is bound to a silica tetrahedral sheet on one side, making the theoretical composition 46.3% SiO_2, 39.8% Al_2O_3 and 13.9% H_2O. The two sheets are stacked alternately,

with the oxygen atoms forming the link between the two layers (Figure 11). This arrangement gives rise to a plate-like morphology (Figure 11). The 'plate' structure has an oxygen surface on one side and a hydroxyl surface on the other (Figure 11). Hence, the individual plates can stack upon each other through strong hydrogen bonding in the lamella, forming 'booklets' (Figure 12) [73]. It takes a considerable energy to separate the plates due to the strong hydrogen bonding, but booklets can be separated into thinner stacks of plates by milling with fine ceramic media, in a process called delamination [74]. The plate surfaces are primarily negatively charged, allowing them to interact with positive ions (cations) through cation exchange. The surface charges of kaolin and its cation exchange capacity fluctuate with changes in pH [74], [75].

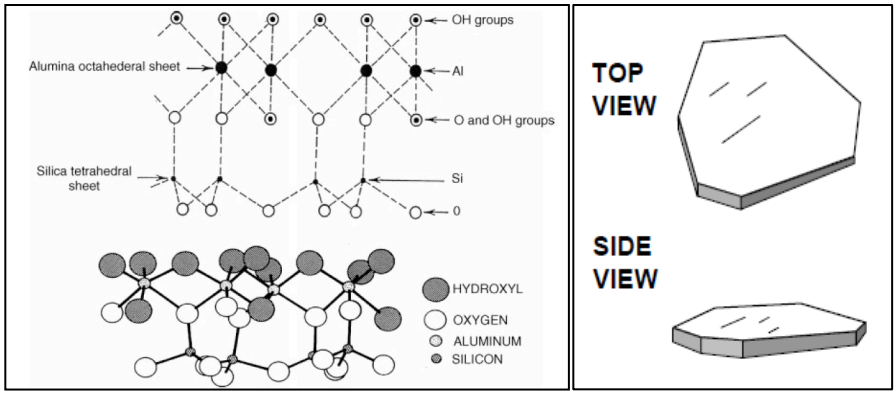

Figure 11: Plate-like structure of kaolinite showing alumina octahedral sheet bound to silica tetrahedral sheet in 1:1 layer; with hydroxyl groups on one side and oxygen groups on the other [73], [74]

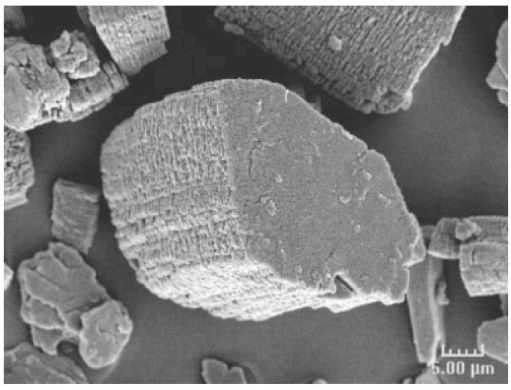

Figure 12: 'Booklets' of kaolin as seen in by SEM imaging [73]

Typical properties of kaolin are summarized in Table 2. Kaolin is mostly used as a filler with applications in paper coating, paints, plastics, rubber and inks. It is also applicable in ceramics and as a catalyst in cracking processes in petroleum refineries. Kaolin has also been reported to be incorporated in poly(acrylic acid) hydrogels, aiding in dispersion of reactants and leading to improvement in various properties of hydrogels, including mechanical strength, cationic dye and metal ion removal efficiency and gelling capacity [76]–[80]. Hence, in this study kaolin was incorporated in lignin-poly(acrylamide) hydrogels to aid in cation adsorption capacity and for improving the mechanical strength of the hydrogels [54]. The hydroxyl groups on kaolin surface and the ionic groups on its edges were expected to increase the hydrophilicity of the formulation, aid in uniform dispersion of the hydrogel components in water during synthesis and contribute to cation exchange processes involved in adsorption of dyes and metals.

Table 2: Typical properties of kaolin [74], [81]

Density (g/cm^3)	2.6
Hardness (Moh's scale)	2
Loss on ignition, 900^oC (%)	12 to 14
Mean diameter (μm)	0.3-5
Surface area (m^2/g)	10-20
Aspect ratio (length/width)	4-30

1.6. Use of Poly(ethylene) glycol diglycidyl ether (PEGDGE) as a cross-linker in lignin-based hydrogels: PEGDGE is a derivative of poly(ethylene glycol). It is a biocompatible, highly water soluble polymer which readily undergoes hydrolysis resulting in ring cleavage (Figure 13), making it a popular choice as a cross-linker to form hydrogels with natural polymers [82]–[84].

The relative hydrophilic nature of PEGDGE was expected to balance the relative hydrophobic nature of lignin, resulting in a hydrogel that is able to adequately interact with solutions and still maintain mechanical stability [25], [57], [62].

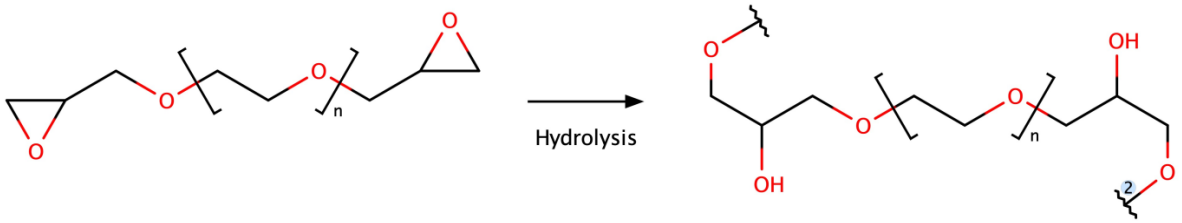

Figure 13: Ring-opening of poly(ethylene glycol) diglycidyl ether (PEGDGE; Mn = 500 Da) to form reactive groups useful in cross-linking. Redrawn from [49]

2. Experimental Materials and Methods:

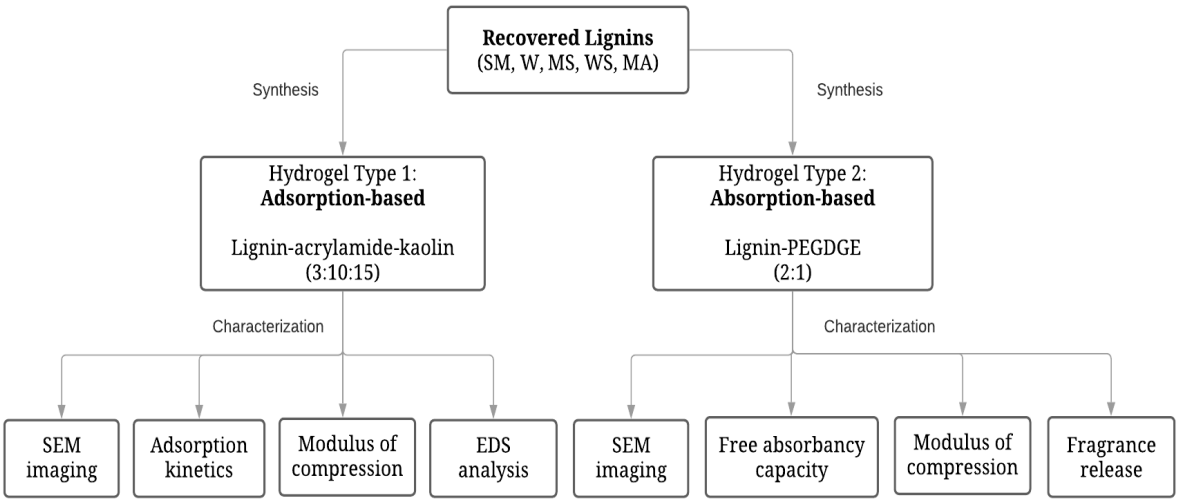

Figure 14: Schematic showing the main experiments carried out in this study

2.1. Chemicals and materials:

Lignins recovered from hot-water extracts (RecLs, Chapter 2) of angiospermic biomass (Sugar maple RecL, SM; willow RecL, W; miscanthus RecL, MS; wheat straw RecL, WS; and mixed

angiosperm lignin, MA) were used (Chapter 2). Kraft lignin (K) was obtained from Sigma-Aldrich, MO, USA as a reference lignin, being the most abundant technical lignin.

Acrylamide, kaolin, and poly(ethylene glycol) diglycidyl ether (PEGDGE; average *M*n 500 Da, DP ~3) were purchased from Alfa Aesar, MA, USA, Fisher scientific Inc., MA, USA and Sigma-Aldrich, MO, USA, respectively. Commercial hydrogels made of acrylamide/potassium acrylate ('TW' and 'CG') were purchased as a commercial control (Tasty Worms Nutrition Inc., FL, USA; eBoot Clear Gel Crystal Beads). Other chemicals utilized, and their respective vendors are as listed (Table 3). Deionized water (pH ~5) was used in all experiments.

Table 3: Chemical Compounds Used in this Study

Chemical	Vendor
Ammonium persulfate (APS)	Sigma-Aldrich
Chloroform	J.T. Baker
Dioxane	TCI
Ferulic acid	Sigma-Aldrich
Hydrogen peroxide	Fisher Scientific
Methylene violet	MP Biochemicals
N, N-dimethylformamide	VWR
N, N'-Methyelenbisacrylamide (NMBA)	Beantown Chemicals
Poly(ethylene) oxide	Sigma-Aldrich
Silica, fumed	Sigma-Aldrich
Sodium Hydroxide	Macron Fine Chemicals

2.2. Synthesis of gels: Lignin-acrylamide-kaolin gels were prepared by graft polymerization of acrylamide on lignin in presence of initiator APS, cross-linker NMBA, and kaolin [54]. During the initial scouting studies, fumed silica was explored as an alternative aluminosilicate to kaolin, because of its larger surface area (generally 1.6 to 7 times higher than kaolin [81]). Additionally, different lignin:acrylamide ratios (ranging between 0.05 and 0.4) were tried out during the

formulation. As the result of these studies (described in later sections), the procedure below was finalized: 1.5 g of kaolin was dispersed in deionized water under constant stirring in vacuum for 1 hour. 1 g of acrylamide and 300 mg (10.7% w/w) of lignin were then incorporated into the kaolin-water dispersion for 20 minutes, followed by addition of 150 mg of APS and 50 mg of NMBA. In this way, lignin was used to partially replace 23% of the acrylamide (lignin:acrylamide = 0.3). The reaction mixture was then immediately immersed into a bath sonicator maintained at 50°C to aid gelation (40 kHz, Branson 3510 Ultrasonic Cleaner, Branson Ultrasonics Corp, CT, USA), for 90 minutes (Figure 15). Similar method was employed to synthesize control gels with K (K-AAm) and without lignin (Blank; kaolin-acrylamide hydrogels). Synthesis of gels was performed at least five times for each lignin. Weight of lyophilized gel was noted, and the yield was calculated as percent of dry ingredient weight.

In a separate set of experiments for graminae lignins (MS, WS, and MA), additional reaction parameters were tested, such as RecL particle size (finely ground vs coarsely ground), Lignin:acrylamide ratio (0.05, 0.1, 0.2, 0.24, and 0.3), ultrasonication time (1.5 to 3 hours) and reaction atmosphere (air, nitrogen, under vacuum). Further, MS was replaced by lignin recovered after soda-anthraquinone pulping of miscanthus biomass (MS-SAQ) during independent experiments. Additionally, effect of addition of ascorbic acid, and certain small-molecular weight aromatic residues such as ferulic acid and *p*-coumaric acid (replacing 3% w/w total lignin) on gelation of K-acrylamide-kaolin gels was also tested.

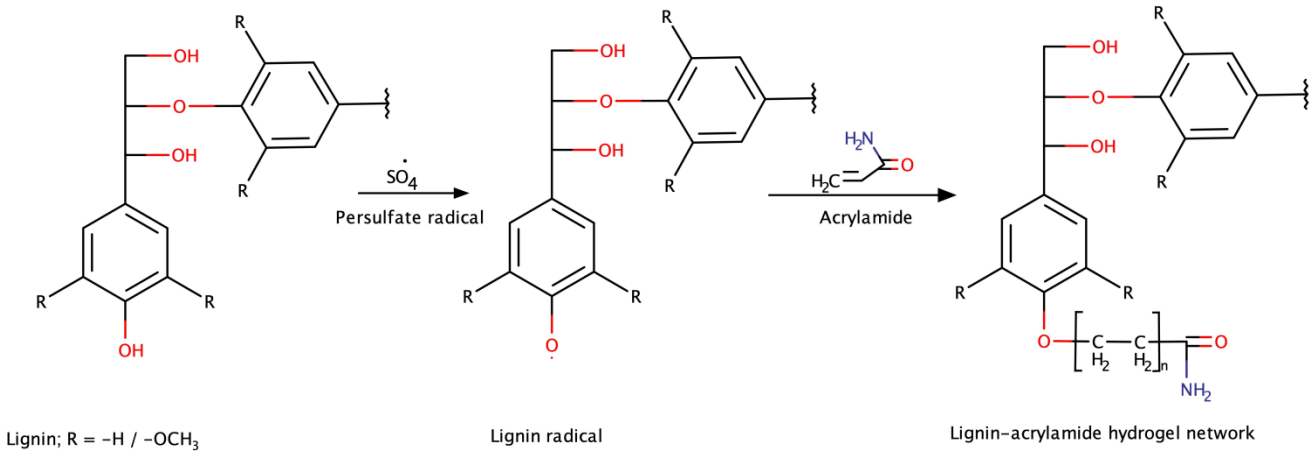

Figure 15: Proposed radical-initiated reaction for grafting of acrylamide on lignin. Kaolin particles disperse into the resulting polymeric matrix

Lignin-PEGDGE gels were made by cross-linking PEGDGE grafted lignin units in presence of alkali and hydrogen peroxide (Figure 16) [49]. During the initial scouting studies, poly(ethylene) oxide (PEO, Mn = 100,000 Da, a higher molecular weight variety of PEG) was explored as an alternative to PEGDGE due to its cheaper price and partial similarity to PEGDGE, and different concentrations of alkali (ranging between 0.2 M and 2 M) were tried out during the formulation. Additionally, higher lignin:PEGDGE ratios were explored. As the result of these studies (described in later sections), the procedure below was finalized: 1 g (66.7% w/w) of lignin was dissolved in 1.6ml of 3.3 M sodium hydroxide solution overnight under constant stirring, and was activated with 5% v/v hydrogen peroxide. 500 mg PEGDGE was then grafted onto activated lignin units, with overnight stirring (lignin:PEGDGE = 2). The stirring was continued until the reaction mixture polymerized into the hydrogel. Similar method was used to synthesize K-PEGDGE control hydrogel. PEGDGE by itself did not form a gel, and hence a blank gel without lignin was not synthesized in this case. Synthesis of gels was performed at least five times for each lignin.

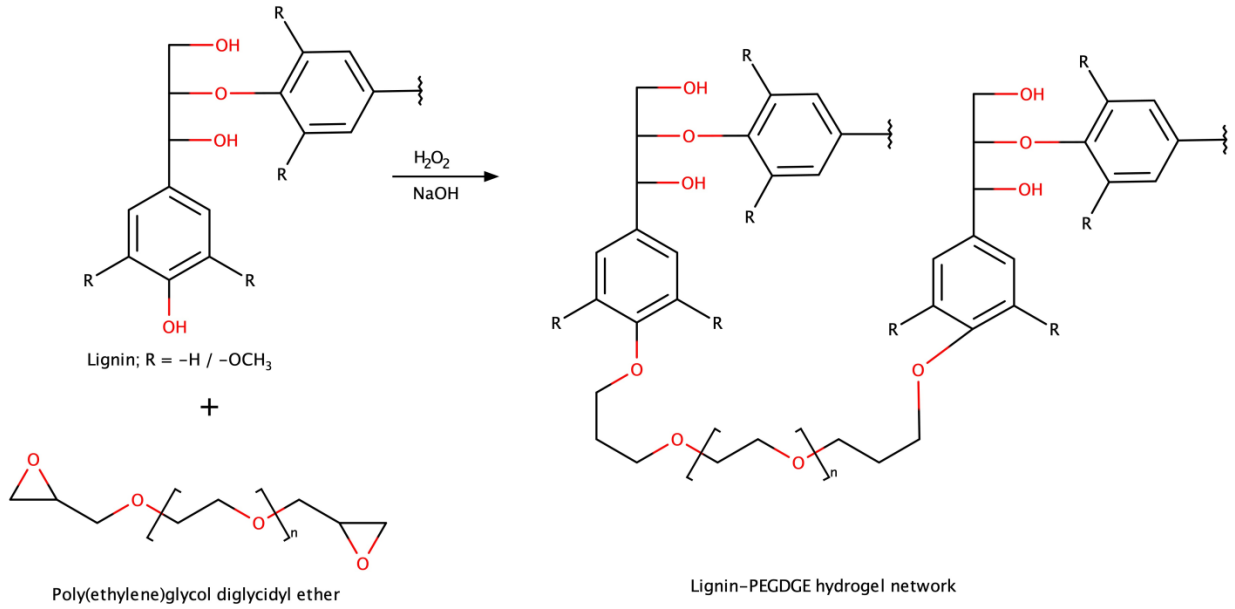

Figure 16: Proposed reaction for synthesis of lignin-PEGDGE gels. Redrawn from [49]

Both types of gels were repeatedly washed with deionized water at pH 5 after synthesis to remove unreacted material if any, and lyophilized to remove water without inducing shrinkage and associated pore deformities (Labconco FreeZone 4.5 liter freeze dry system, Labconco Corporation, MO, USA). After lyophilization, the weights and dimensions of the gels were noted using a Mettler-Toledo precision balance (AE200, Mettler-Toledo, USA) and Vernier calipers, and the approximate density was calculated arithmetically.

2.3. Scanning electron microscopy (SEM) characterization of gels [44], [51]**:** A JEOL scanning electron microscope (JEOL JSM IT100LA InTouch Scanning Electron Microscope, JEOL USA Inc, MA, USA) was used to observe the morphological characteristics of both types of gels and the accumulation of metallic cations on lignin-acrylamide-kaolin gels. Several different techniques were used to observe the surface characteristics, such as secondary electron imaging, backscattered electron (atomic number contrast) imaging, low kV and low vacuum imaging with or without Au/Pd sputter coating as appropriate. Changes in the gel morphology

after sorption were observed by cryofracturing the gels in their swollen state. To observe the accumulation of metallic cations, approximately 100 mg of moisture-free gel was allowed to remain in contact with an aqueous solution of silver nitrate ($AgNO_3$; 0.01 N) for two hours. Accumulation of silver ions on the air-dried and uncoated gel surface was then observed low-vacuum BEC mode (backscattered electron composition / atomic number contrast) and was further studied by energy dispersive X-ray spectroscopy spot analysis (EDS).

2.4. Estimation of dye adsorption kinetics on lignin-acrylamide-kaolin gels: Approximately 100 mg of moisture-free gel was allowed to remain in contact with 10 ml of 12.5 μM aqueous solution of methylene violet dye for two hours with intermittent shaking at room temperature, at pH ~5. Concentration of dye in the solution was measured every 30 minutes by measuring the absorbance of the solution at 530 nm, on a Genesis 10s UV-Vis spectrophotometer (Thermo Scientific, MA, USA). A final measurement was made after 18 hours, after which no change in absorbance was detected. The amount of dye adsorbed on the gel was then calculated as:

$$q_t = (C_0\text{-}C_t)\ V / W_0 \quad (1)$$

where C_0 and C_t (μg/ml) are concentrations of adsorbate (dye) at 0 minute and after t minutes respectively, W_0 (g) is the weight of the adsorbent (gel), and V is the volume of the adsorbate solution (ml) [85]. The percentage removal of the adsorbate was calculated as:

$$\%\ \text{Removal} = (C_0\text{-}C_t) \times 100 / C_0 \quad (2)$$

The dye adsorption kinetics were evaluated by fitting the experimental data into the pseudo-first (Eqn. 3) and pseudo-second (Eqn. 4) order kinetic models [85].

Lagergren's pseudo-first order kinetic model: $\frac{dq_t}{dt} = k_1(qe\text{-}qt)$ (3)

Ho and McKay's pseudo-second order kinetic model: $\frac{dq_t}{dt} = k_2(qe\text{-}qt)^2$ (4)

where qt (μg/g) is the amount of dye adsorbed at time t, qe (μg g^{-1}) is the amount of dye adsorbed at equilibrium, and k_1 (min^{-1}) and k_2 ($g\mu g^{-1}min^{-1}$) are pseudo-first order and pseudo-second order adsorption rate constants. The constants k_1, k_2 and the initial adsorption rate constant $h = k_2qe^2$ (g/μg min) were derived graphically by plotting the experimental data according to the linearized forms of the equations (Eqn. 5 and 6) [63].

First order kinetic model: $\log (qe-qt) = \log (qe) - k_1t/2.303$ (5)

Second order kinetic model: $\frac{t}{q_t} = \frac{1}{k_2qe^2} + \frac{t}{qe}$ (6)

Hence, the pseudo-first order kinetic parameters were obtained by plotting $\log (q_e-q_t)$ versus t and the pseudo-second order parameters were obtained by plotting t/qt versus t. For the first model, the rate constant k_1 was obtained from the slope, and q_e from the intercept. For the second model, the rate constant k_2 was obtained from the intercept, while q_e was obtained from the slope. The advantage of pseudo-second order model over the former is that it allows for the estimation of kinetic parameters without knowing qe beforehand [86]. Validity of the models was confirmed by comparing the qe value obtained from the model (qe_{calc}) to that obtained experimentally (qe_{exp}). Gels synthesized from K and without any lignin (acrylamide-kaolin) were used as two separate controls. Duplicate experiments were performed.

2.5. Assessment of reusability of lignin-acrylamide-kaolin gels: To test the practicality of the gels, the gels used in the above experiment were vacuum-dried and were again allowed to come in contact with a fresh dye solution. The kinetic parameters obtained after repeat use were compared to those obtained for the first use. Duplicate experiments were performed.

2.6. Measurement of free-absorbency capacity of lignin-PEGDGE gels: This parameter measures the capacity of the gel to absorb and retain aqueous solutions, when it is freely swollen, i.e. without any load. It was estimated by two different methods, the modified filtration method

and the centrifuge method in triplicates or more, using gel samples ground to #40 mesh (425 μm). K-PEGDGE gel, TW and CG were used as control. Statistical analysis was performed using RStudio version 1.2.1335.

Modified filtration method [87]*:* 50 mg (W_1) of gel was allowed to remain in contact with 50ml of saline solution for 30 minutes at room temperature. The solution was then filtered using a pre-weighed sintered crucible (W_0), which was covered to ensure no liquid evaporated during filtration. The crucible was weighed again (W_2) and the swelling capacity (Se) was calculated using eqn. 7.

$$Se = (W_2 - W_0 - W_1) / W_1 \quad (7)$$

Centrifuge method [88]*:* 50 mg (W_1) of gel was placed into a tea-bag (made of filter paper, with fabric drawstring, 8x10 cm, Tinkee tea-bags, China), which was dipped into 50 ml saline solution for 30 minutes at room temperature. The bag was then removed, and excess solution and inter-particle liquid was removed by centrifuging it for 3 minutes, at 250 g (Centra-8 Centrifuge, International Equipment Company, TN, USA). The weight of the bag plus the gel (W_2) was measured. Same procedure was carried out with an empty bag, and the weight was measured (W_0). The swelling capacity of the gel was calculated again using eqn. 7.

2.7. Study of fragrance emanation from lignin-PEGDGE gel [89]**:** ~600 mg of three industrially used proprietary fragrances A, B, and C were loaded onto three separate gel samples weighing ~200mg at room temperature. The emanation of each of the fragrances was estimated by measuring the weight loss of the samples every day for three weeks. The relative humidity and room temperature ranged between (9% and 36%) and (20 ºC and 24 ºC) respectively, throughout the duration of this experiment. To account for the effect of humidity and effect of moisture absorption on the gel samples during this period, a separate gel sample without any

fragrance loading was used as a control (~200mg). Percent emanation of fragrance from the gel matrix for each day was calculated as:

$$\% \text{ Emanation, Day D} = L / F*100 \quad (8)$$

where L is the cumulative weight loss of gel-fragrance complex on Day D, adjusted for effects of moisture adsorption and F is the original weight of the fragrance loaded onto the gel.

2.8. Determination of modulus of compression: These tests were performed using Model 100P Universal Resting Machine (Xy software version 4.00.08; TestResources, MN, USA), equipped with 25N load cell, at a displacement rate 5mm/min, log rate 2/sec and jog rate 500, at room temperature. A stress-strain curve was obtained, and the compression modulus was calculated from the slope of the linear portion of curve. To prepare the gels for testing, they were cut into disks as soon as they were synthesized, and lyophilized. Because of the sample and instrument constraints, lignin-acrylamide-kaolin gels were cut into disks 6-8mm in thickness and 15-18 mm in diameter as measured by Vernier calipers in at least three places, while lignin-PEGDGE gels were cut into disks 8-10mm in thickness and 25-30mm in diameter. Same controls as described in earlier sections were used for comparison. These tests were performed in order to measure the mechanical integrity of the gels during their intended application, and hence they were conducted on gel samples soaked in deionized water for 2 hours. The tests were continued until the samples showed signs of breaking, indicated by a sharp decrease in the stress. Minimum three replicate measurements were made. Statistical analysis was performed using RStudio version 1.2.1335.

3. Results and Discussion:

3.1. Initial exploratory studies:

3.1.1. Establishing reaction components and conditions: The lignin-acrylamide-silica reaction mixture required twice the amounts of initiator and cross-linking agents for gelation to occur.

The larger surface area presented by silica may lead to non-productive adsorption of these chemicals on silica particles, making them largely unavailable to participate in polymerization reactions. Additionally, lignin-acrylamide-silica gel had lower adsorption rates as compared to lignin-acrylamide-kaolin gel (Appendix, Table 6 and Table 7). Silica is also more expensive as a raw material as compared to kaolin. Due to these reasons, kaolin was deemed more suitable for the process instead of silica. In addition to replacement of kaolin, another parameter explored for these gels was the amount of lignin in the formulation. However, increasing the lignin:acrylamide ratio beyond 0.3 did not result in gel formation.

For lignin-PEGDGE gels, increasing the lignin:PEGDGE ratio from 2 to 2.5 did not result in gel formation. Replacing PEGDGE with an equal amount of PEO and changing the reaction medium from high alkalinity (3.3 M) to a range of lower alkalinity values (between 0.2 M and 2 M) also resulted in failure to form gels. Hence, the reaction parameters were established as noted in the Materials and Methods section.

3.1.2. Ability of lignins to form gels: Kraft lignin and all of the RecLs used in this study (SM, W, MS, WS, MA) were able to form gels with PEGDGE (henceforth referred to as K-PEGDGE, SM-PEGDGE, W-PEGDGE, MS-PEGDGE, WS-PEGDGE, and MA-PEGDGE gels, respectively).

In the case of lignin-acrylamide-kaolin gels, gels with kraft lignin (K-AAm), and without lignin (Blank gels) were able to form. However, out of all the RecLs, only SM and W (hardwood lignins) were able to form gels with acrylamide and kaolin (henceforth referred to as SM-AAm and W-AAm gels), while the latter three (graminae, graminae and a mix of hardwood and graminae lignins, respectively) did not undergo gelation. This trend continued at different

reaction parameters tested, such as RecL particle size, lignin:acrylamide ratio, ultrasonication time (1.5 to 3 hours) and reaction atmosphere (air, nitrogen, under vacuum).

These observations indicated that specific structural features inherent to graminae lignins were probably hindering the polymerization process. An important difference between graminae lignins and hardwood lignins is the presence of *p*-hydroxycinnamates such as ferulates and *p*-coumarates in graminae lignin [90]. To explore the possibility of these residues interfering with polymerization, kraft lignin spiked with ferulic acid (3% w/w) and *p*-coumaric acid (3% w/w) was used for gel synthesis. This was found to render kraft lignin unable to undergo gelation, whereas kraft lignin in its unadulterated form was able to undergo gelation. Similar results were obtained when equal amount of ascorbic acid was added to kraft lignin instead of ferulic and coumaric acid. Further, while MS was unable to undergo gelation, MS-SAQ was able to undergo gelation to form a gel. HSQC analysis showed that MS-SAQ was less contaminated with hydroxycinnamate residues than MS (Appendix, Table 8). These results indicate toward the radical quenching activity of these residues as the contributing factor for hindering polymerization, but detailed experiments are needed to gather conclusive support. Presently, further trials related to lignin-acrylamide-kaolin gels were focused on SM and W, while lignin-PEGDGE gels were made from all available lignins.

Gelation of the liquid reaction mixture occurred in its entirety for both types of gels, i.e. the entire volume of the reaction mixture turned into the gel. The gels were soft when they formed, and took the shape of the reaction vessel they formed in. After lyophilization, the flexible, semi-solid gels turned into low-density rigid solids (Figure 17), and gave a 100% w/w yield on the basis of dry ingredients.

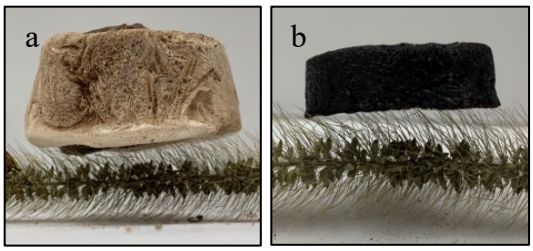

Figure 17: Low-density (ρ ≤ 0.21 g/cm^3) willow lignin-acrylamide-kaolin (a), and willow lignin-PEGDGE (b), gels after lyophilization, balanced on a spike of bristlegrass

3.2. Lignin-acrylamide-kaolin gels:

3.2.1. Estimation of adsorption kinetics: The experimental data established a better overall fit into the pseudo-second order model, with correlation coefficients closer to 1, as compared to the pseudo-first order model (Table 4). Both models were effective in predicting the $q_{e\ calc}$ values close to the observed $q_{e\ exp}$ values. A pseudo-first order adsorption is controlled by diffusion and mass transfer of the adsorbate to the adsorption site. A pseudo-second order adsorption is usually controlled by chemisorption [85]. In the present case, the higher correlation coefficients of the pseudo-second order model indicate that the chemisorption was probably the rate-limiting step in adsorption of methylene violet on the gels. This finding is in line with the reports that the pseudo-second order kinetics have generally been found to be more suitable to describe adsorption processes, than the pseudo-first order kinetics [86]. It also fits well with literature reports of pseudo-second order adsorption kinetics between cationic dyes and silanol containing composites, such as kaolin [77], montmorillonite [65], and attapulgite [65]. It is hypothesized that adsorption mechanisms mainly involve ion-exchange reactions between the charged groups on the edges of kaolin platelets. Additionally, π-π interactions between the aromatic rings on both lignin and the dye have also been suggested to occur [65]. Both models indicated that W-AAm hydrogel had the highest rate of adsorption (k_1 and k_2, Table 4). The amounts of dye adsorbed at equilibrium ($q_{e\ exp}$) by W-AAm and SM-AAm hydrogels were comparable, and

higher than K-AAm and blank gels (Table 4). Inclusion of lignin into the formulation (W, SM or K) was found to result in overall higher adsorption rates, and higher equilibrium dye adsorption amounts, when compared to a blank formulation. This result was also in accord with the percent dye removal for the hydrogels at the end of the adsorption period. SM-AAm and W-AAm gels (67.28% w/w and 67.08% w/w original dye amount, Figure 18, blue) were found to be more effective in removing the dye, as compared to K-AAm and blank gels (59% w/w and 56% w/w original dye amount, Figure 18, blue).This beneficial effect of lignin has also been observed in studies on lignin-based gels with poly (methyl vinyl ether co-maleic acid) which showed overall superior dye removal behavior than the control gel without lignin [91]. The individual differences in adsorption efficiencies between different lignin-containing gels might be arising from the inherent differences in the nature of these lignins, leading to differences in the resulting polymer network between lignin and acrylamide. These in turn would induce differences in the permeability and adsorption behavior of the gels. As hardwood lignins, SM and W are less condensed S/G lignins, with more β-O-4 linkages, while as a softwood lignin, K is more condensed, predominantly G lignin, with less β-O-4 linkages [92]–[94]. Additionally, we found that the free phenolic hydroxyl group content (PhOH) of K was much higher (4.93 mmol/g K) as compared to SM (1.43 mmol/g SM; Chapter 2) and W (2.1 mmol/g W; Chapter 2). The more condensed nature and the excessive polymerization sites (PhOH) on K could most likely have resulted in the formation of a highly cross-linked, denser polymeric network in K-AAm gel, which is less permeable to solutions, and hence provides less accessible surface for dye molecules to adsorb onto [95].

Overall, these results show that incorporation of lignin into the gels as a partial substitute for acrylamide could improve the adsorption capacity of the formulation, with willow lignin being more effective than kraft lignin.

Table 4: First use kinetic parameters for the pseudo-first and pseudo-second order models for adsorption of methylene violet on lignin-kaolin-acrylamide gels, synthesized from sugar maple RecL (SM-AAm), willow RecL (W-AAm), kraft lignin (K-AAm) and without lignin (Blank)

Gel	$q_{e\ exp}$	Pseudo-first order			Pseudo-second order			
		$q_{e\ calc}$	k_1	R^2	$q_{e\ calc}$	k_2	h	R^2
	(μg g^{-1})	(μg g^{-1})	(min^{-1})		(μg g^{-1})	(g μg^{-1} min^{-1})	(μg g^{-1} min^{-1})	
SM-AAm	319. 01	336.05	8.06E-03	0.979	357.14	1.98 E-05	2.52	0.989
W-AAm	323.32	322.92	1.24E-02	0.924	344.83	4.96 E-05	5.89	0.998
K-AAm	280.59	235.45	5.30E-03	0.998	303.03	3.17 E-05	2.91	0.999
Blank	264.38	262.30	5.3E-03	0.962	312.5	1.59 E-05	1.55	0.996

The commercial hydrogels TW and CG were not found to be suitable for this application, as they absorbed the dye solution in its entirety, instead of selectively adsorbing the dye molecules. This result highlights the versatility of lignin as a multi-functional polymer.

Reusability - Changes in adsorption kinetics on repeat use: Although the gels were still effective in dye removal, the adsorption rates for all were found to decrease with repeat use as expected (Table 5). The amount of dye adsorbed at equilibrium ($q_{e\ exp}$) was found to unexpectedly increase for W-AAm hydrogel on repeat use (~ 323μg g^{-1}; Table 4 to ~ 445 μg g^{-1};Table 5), remain unaffected for SM-AAm, and decrease for K-AAm and Blank gels. This trend was also seen for dye removal behavior of the gels (Figure 18, red). The amount of dye removed by W-AAm gel on repeat use was found to be unexpectedly higher than on first use. The dye removal efficiency was found to decrease as expected for all other gels, with the most noticeable

decrease occurring for blank gels (from 56% w/w dye removal on first use to 31% w/w dye removal on repeat use). More experiments including dye desorption studies are necessary to understand the puzzling results for W-AAm gels.

Table 5: Repeat use kinetic parameters for the pseudo-first and pseudo-second order models for adsorption of methylene violet on lignin-kaolin-acrylamide gels, synthesized from sugar maple RecL (SM-AAm), willow RecL (W-AAm), kraft lignin (K-AAm) and without lignin (Blank)

Gel	$q_{e\ exp}$	Pseudo-first order			Pseudo-second order			
		$q_{e\ calc}$	k_1	R^2	$q_{e\ calc}$	k_2	h	R^2
	(μg g^{-1})	(μg g^{-1})	(min^{-1})		(μg g^{-1})	(g μg^{-1} min^{-1})	(μg g^{-1} min^{-1})	
SM-AAm	319.29	298.33	3.68E-03	0.986	384.61	1.13E-05	1.67	0.996
W-AAm	445.02	423.05	4.38E-03	0.994	526.32	9.49E-06	2.63	0.998
K-AAm	251.75	230.25	3.22E-03	0.924	303.03	1.42E-05	1.31	0.999
Blank	147.38	141.97	2.07E-03	0.972	222.22	8.24E-06	0.40	0.996

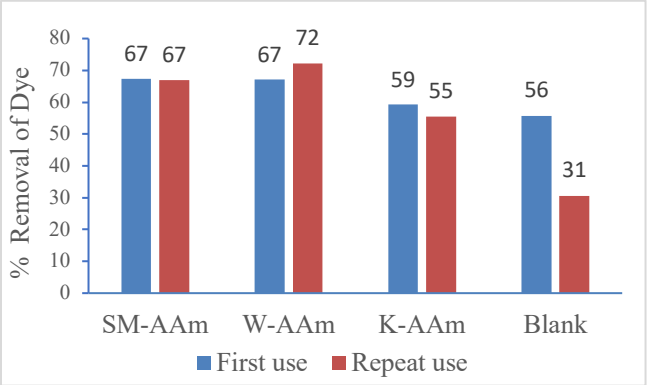

Figure 18: Removal of dye from the solution by lignin-kaolin-acrylamide gels after first use (blue) and repeat use (red), synthesized from sugar maple (SM-AAm), willow (W-AAm), kraft (K-AAm) lignins and without lignin (Blank)

3.2.2. SEM characterization – Gel morphology: Low-vacuum secondary electron images of the lignin-acrylamide-kaolin gel showed a porous, irregular surface with sharp edges and microscopic channels ranging from tens to hundreds of micrometers (Figure 19). The presence of pores and channels might provide a large surface area for the sorption to occur and aid in

increasing permeability and application performance of the gel. A closer inspection of the surface revealed a rough and grainy pattern (Figure 20). The grainy surface might be the result of the kaolin particles suspended into the lignin-acrylamide matrix. Further observations in the atomic number contrast mode (Figure 22) showed that the kaolin particles (appearing brighter than the rest of the matrix due to their aluminosilicate composition) were uniformly dispersed into the gel matrix.

The microstructure of the gel was observed to be distended while in contact with the aqueous metal ion solution, as seen in the Au/Pd-coated secondary electron image of a gel cryofractured during metal-ion adsorption (Figure 21). Post contact and subsequent drying, the microstructure was observed to be damaged (Figure 23), possibly due to the surface tension and hydrogen bonding effects of water. This might result in decreased surface area available for adsorption, and might be one of the factors contributing to the decrease in the adsorption rate on repeat use of the gels as described in Section 3.2.2.

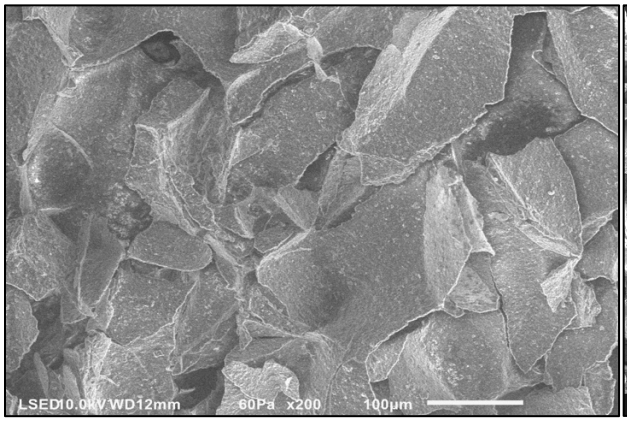

Figure 19: SE micrograph of sugar maple lignin-acrylamide-kaolin gel showing a porous, irregular surface. LSED, 10kV, P.C. 52, 200x

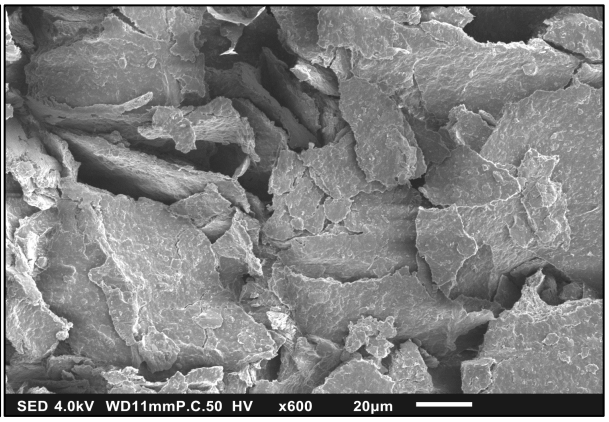

Figure 20: Low-kV micrograph of Au/Pd sputter coated sugar maple lignin-acrylamide-kaolin gel showing surface details. SED, 4kV, P.C. 50, 600x

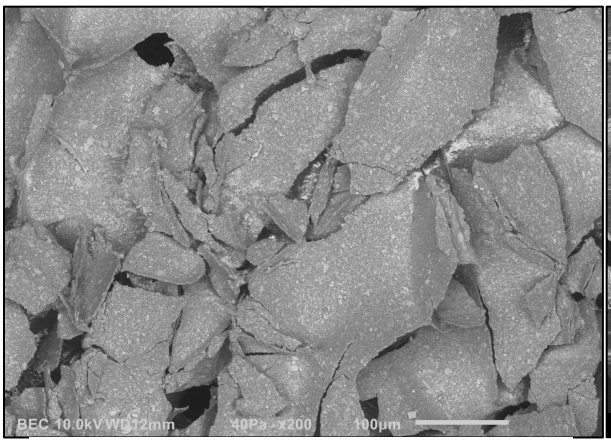

Figure 22: Low-vacuum atomic number contrast micrograph of sugar maple lignin-acrylamide-kaolin gel showing uniform dispersion of kaolin (appearing as bright spots) in the hydrogel matrix. BEC, 10 kV, P.C. 52, 200x

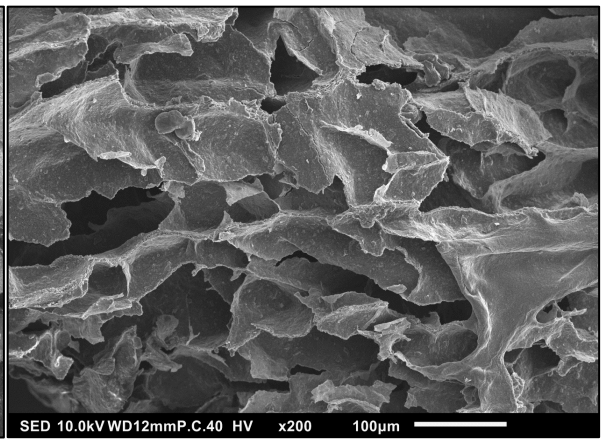

Figure 21: SE micrograph of cryofractured, Au/Pd sputter-coated sugar maple lignin-acrylamide-kaolin gel during adsorption of silver (Ag^{+1}) cations, showing distended channels. SED, 10kV, P.C. 40, 200x

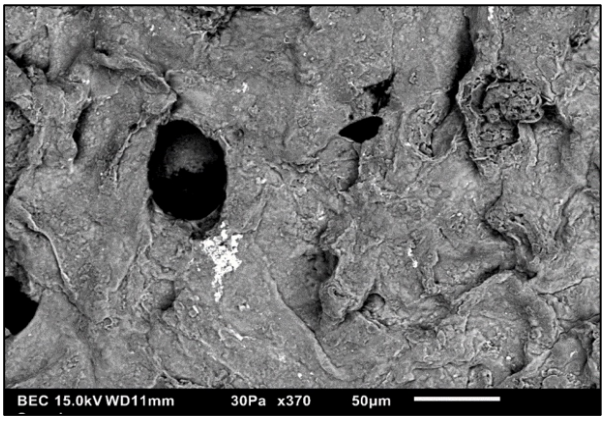

Figure 23: Atomic number contrast image of willow lignin-acrylamide-kaolin gel showing collapse microstructure after adsorption of silver (Ag^{+1}) cations, seen as a bright spot toward the center. BEC, 15 kV, 370x

Observation of the accumulated metal on the gel: The post-adsorption atomic number contrast image also showed clusters of adsorbed silver (Ag^{+1}) cations, on the gel surface (Figure 23). The adsorption of silver on the gel matrix was further validated by comparing the energy dispersion spectra of the gel pre- and post-adsorption (Figure 24).

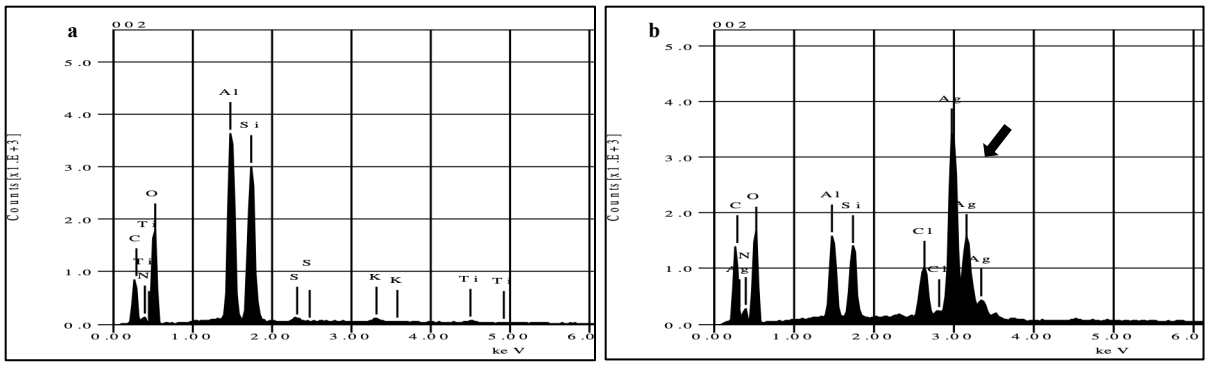

Figure 24: Energy dispersion spectra of willow lignin-kaolin-acrylamide gel before (a) and after (b) Adsorption of silver (Ag^{+1}) cations

3.2.3. Determination of modulus of compression: The sigmoidal stress strain curve obtained for the gels was typical of porous materials [96], showing a linear elasticity at lower stresses, followed by a collapse phase, truncated by a sharp rise in stress (Figure 26). The compression modulus was found to steeply decrease with addition of lignin to the formulation (Blank vs K-AAm, W-AAm and SM-AAm gels; Figure 25). Within the lignin-containing gels, SM-AAm and W-AAm gels were found to have very similar compression moduli, while K-AAm gel was found to have a slightly higher value. Although the differences within the lignin-containing group were not statistically significant (*p*-value 0.8), the overall trend correlates well with the adsorption performance of the gels (Section 3.2.1.), where lignin-containing gels performed better than the blank gel, and SM-AAm and W-AAm gels performed better than K-AAm gel (Table 4, Figure 18). Higher porosity materials have been reported to result in lower compression modulus, because of the faster wall collapse of porous materials [96], [97]. This suggests that the lignin-containing gels probably had a higher porosity than the blank gel, and that addition of lignin might have resulted in increased porosity of the gel matrix and higher accessible surface areas. This might explain the improved adsorption performance of lignin-containing gels over the blank hydrogel. This conclusion also supports the conjecture made earlier that K-AAm gel probably

consists of a denser, less porous network compared to SM-AAm and W-AAm gels, and explains the relatively better adsorption kinetics of the latter two.

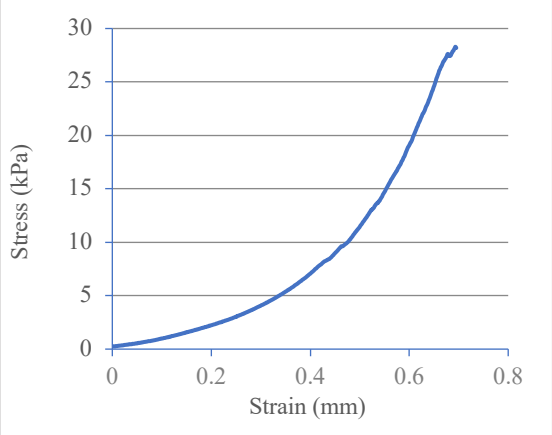

Figure 26: Stress-strain curve for willow lignin-acrylamide- kaolin gel showing a sigmoidal shape typical of porous materials

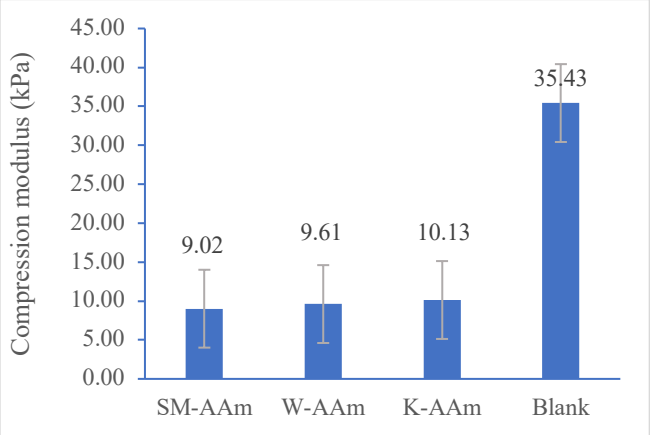

Figure 25: Compression moduli of lignin-acrylamide-kaolin gels. From left to right: gels containing sugar maple lignin, willow lignin, kraft lignin, and no lignin

3.3. Lignin-PEGDGE gels:

3.3.1. Measurement of free-absorbency capacity: The two methods employed for the measurement of swelling capacity, the modified filtration method and the centrifuge method gave fairly congruent results for most gels (*p*-values >> 0.05). However, they gave significantly different results for SM-PEGDGE and MS-PEGDGE gels, and most noticeably for the commercial controls, TW and CG (Figure 27). The values obtained from the centrifuge method are generally expected to be lower and more accurate, since this method is more effective in removing loosely bound water from the hydrogel particles.[48] This was true for TW and CG, which showed a swelling capacity measured by the filtration method more than twice the values measured by the centrifuge method. However, the centrifuge method gave a larger standard deviation between the replicates, possibly due to the variation in the absorption behavior of the tea bags used in the experiment, unavoidable due to the method constraints. Although both

methods showed that the swelling capacities of lignin-containing hydrogels were inferior to that of the commercial hydrogels, it should be noted that TW and CG are composed of an entirely synthetic material, much different in composition (acrylamide/potassium acrylate) than our hydrogels. Between the lignin-containing gels, K-PEGDGE gel was found to have a swelling capacity equal to that of W-PEGDGE gel, and slightly lower than those of SM-PEGDGE, MS-PEGDGE, WS-PEGDGE, and MA-PEGDGE gels as measured by the modified filtration method. However, these differences were not found to be statistically significant (*p*-value 0.068). Overall, the swelling degrees observed for the lignin-PEGDGE gel were in line with the reported values for gels containing lignin in combination with other natural and synthetic polymers [44], [45], [49], [98]. There also have been some reports of lignin-based gels reaching much higher swelling capacities (ranging from 30 to 389) than the numbers found in our studies [55], [98]. These differences are likely originating from the types of lignin and the nature of the copolymers used in the synthesis of the gels, and also from the various methods used to measure the swelling capacities by different authors.

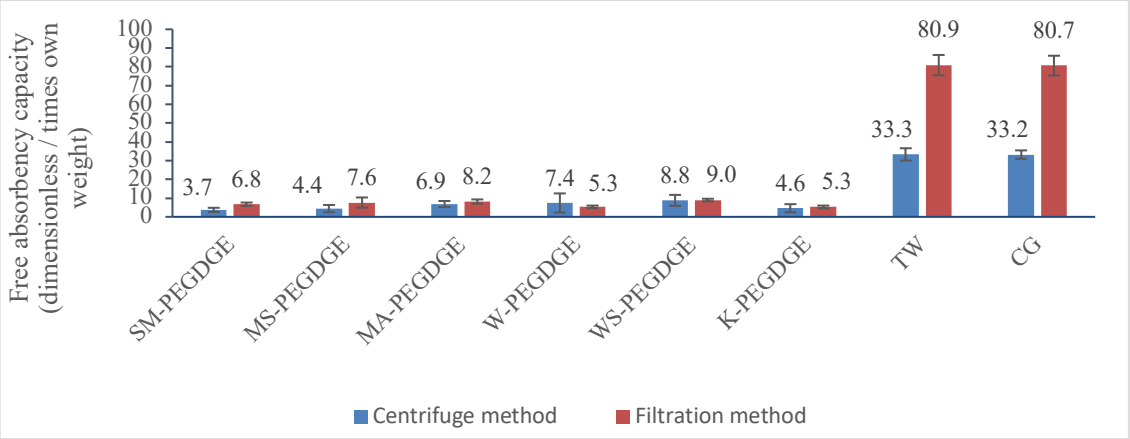

Figure 27: Swelling capacities of lignin-PEGDGE gels compared with commercial control, as measured by the centrifuge method and the modified filtration method. From left to right, gels containing sugar maple, miscanthus, mixed angiosperm, willow, wheat straw, and kraft lignin, and commercial controls TW, CG

3.3.2. SEM characterization – Gel morphology: Similar to the lignin-acrylamide-kaolin gels, the secondary electron images of lignin-PEGDGE gel also showed a porous, irregular surface; however, much larger pores were observed than in lignin-acrylamide-kaolin type (Figure 29). Closer inspection of the surface showed the presence of an etch-like pattern, which might contribute to increased surface area (Figure 28).

Absorption of aqueous solution by the gel resulted in a significant distention of the internal structure of the gel (Figure 30), elucidating the ability of the gel matrix to swell to accommodate the additional volume.

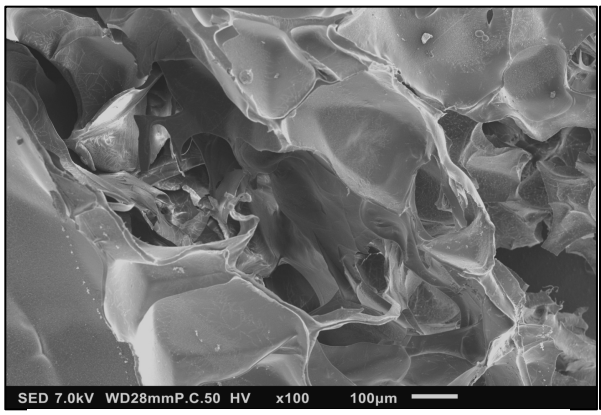

Figure 29: SE micrograph of Au/Pd sputter-coated sugar maple lignin-PEGDGE gel showing a porous, irregular surface. SED, 7 kV, P.C. 50, 100x

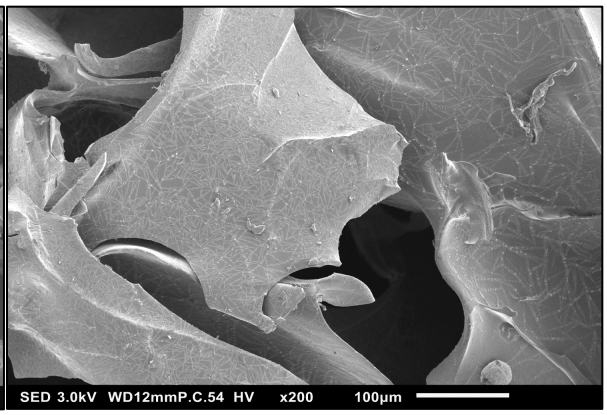

Figure 28: Low-kV micrograph of Au/Pd sputter-coated sugar maple lignin-PEGDGE gel showing surface details. SED, 3 kV, P.C. 54, 200x

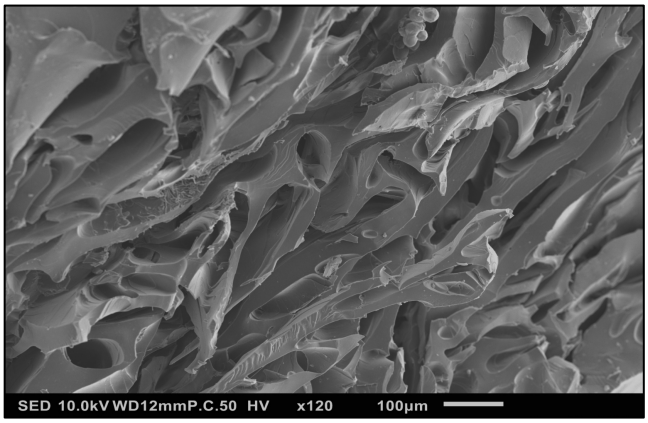

Figure 30: SE micrograph of cryofractured, Au/Pd sputter-coated sugar maple lignin-PEGDGE gel during absorption of ascorbic acid aqueous solution (10mg/ml). SED, 10 kV, P.C. 50, 120x

3.3.3. Determination of modulus of compression: Between the lignin-containing gels, MS-PEGDGE gel was found to have the lowest modulus of compression, which is significantly lower than the values observed for SM-PEGDGE, W-PEGDGE and K-PEGDGE gels (*p*-value 0.03; Figure 31). Although the commercial reference hydrogels TW and CG exhibited similar swelling capacities (Section 3.3.1, Figure 27), this equality was not reflected in their moduli of compression, which varied widely (Figure 31). The overall trend observed for swelling capacities was also not reflected in the compression moduli results. A large sampling variability introduced

into the calculation by the nature of the samples might be one of the reasons behind these differing results.

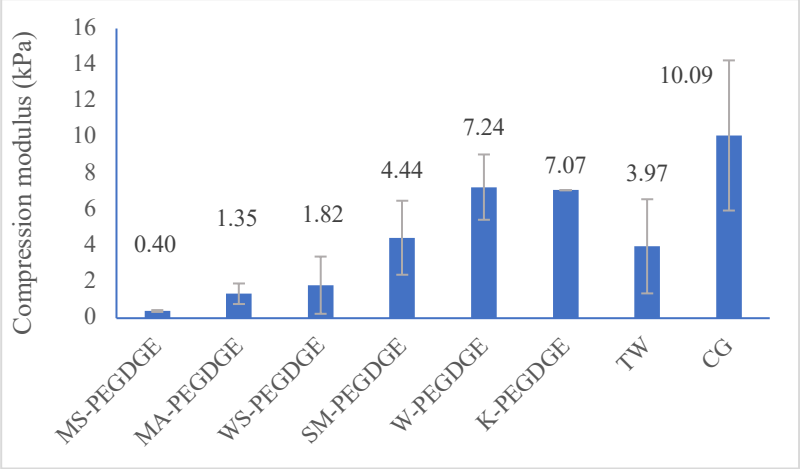

Figure 31: Compression moduli of lignin-PEGDGE gels. From left to right: miscanthus, mixed angiosperm, wheat straw, sugar maple, willow, and kraft lignin, and commercial controls TW, CG

3.3.4. Study of fragrance emanation from W-PEGDGE gel: Based on the results obtained for the free absorbency capacity, W-PEGDGE was chosen to further study fragrance-related applications of the synthesized gels. The emanation rate and cumulative amount of emanation of the fragrances from the hydrogel matrix was found to vary with fragrance composition (Figure 32). Fragrance A was largely made of readily volatile, low molecular weight compounds, and hence had the highest percent cumulative emanation at the end of the experiment. Fragrances B and C were made of compounds with higher molecular weights, and accordingly showed a lower emanation from the gel matrix. This trend and the cumulative percent emanation values for the three fragrances were found to be in line with the internal studies conducted by the proprietor on frequently used matrices in the fragrance application industry, such as natural fiber, paper, and synthetic fiber-based matrices (in-house study conducted by proprietor). The conformity of these results with the industrial materials suggests that W-PEGDGE gel does not undergo any

undesirable interactions with the industrial fragrances, and does not hinder their release from the matrix. Hence, it is a suitable material for fragrance release applications. The commercial hydrogel TW was unable to retain any amount of fragrance and hence was not found adaptable for this application, again highlighting the versatility of our gel in regard to diverse potential applications. This air freshener-related application is a relatively unexplored avenue for lignin-based gels, and these findings are encouraging for further studies.

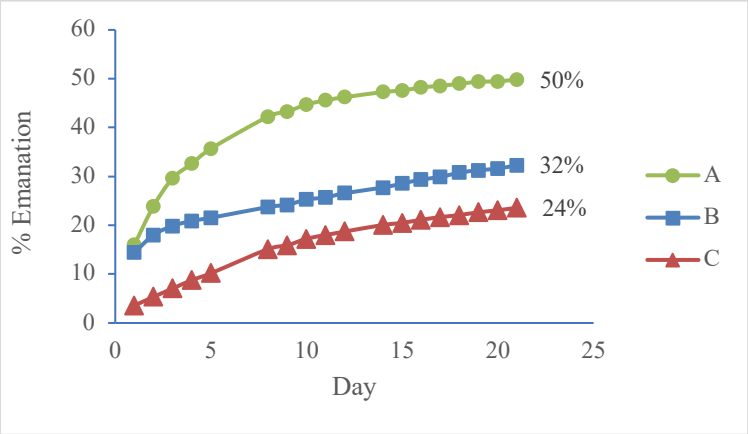

Figure 32: Percent cumulative emanation of proprietary fragrances A, B and C from willow Lignin-PEGDGE gel

3.4. Effect of fractionation of lignin on gel synthesis and performance: The results described above indicated that lignin recovered after hot-water extraction is a suitable partial substituent of synthetic polymers in production of lignin-acrylamide-kaolin and lignin-PEGDGE gels. It was further desired to explore the effects of fractionation on the applicability of this lignin. Since SM and W were the only lignins able to form both types of gels (lignin-acrylamide-kaolin and lignin-PEGDGE), and since W-based gels had comparatively better sorption performance, fractionated willow RecL (WFR, solvent-fractionated; and WAH, alkali-purified; Chapter 2) was selected for further studies.

Lignin-acrylamide-kaolin gel: Similar to W-acrylamide-kaolin gel, WFR-acrylamide-kaolin gel also produced a better fit for second-order adsorption kinetics (R^2 0.99 for second-order fit vs R^2 0.01 for first-order fit). It was found to have slightly higher equilibrium adsorption amounts ($q_{e\ exp}$ 326 μg g^{-1} and $q_{e\ calc}$ 357 μg g^{-1}), but slower adsorption rates (k_2 3E-05 g μg^{-1} min^{-1}) as compared to W-acrylamide-kaolin gel ($q_{e\ exp}$ 323 μg g^{-1}, $q_{e\ calc}$ 345 μg g^{-1}, and k_2 5E-05 g μg^{-1} min^{-1}, Section 3.2.1., Table 4). Dye removal efficiency remained unaffected (67% removal for both). These changes in the adsorption behavior stem from the significant difference between the chemical composition of W and WFR as a result of fractionation. WFR has a higher carbohydrate content (~15% OD carbohydrates, Chapter 2) as compared to W (~3% OD carbohydrates, Chapter 2). Additionally, it has a higher PhOH content (~2 mmol/g W vs. ~4 mmol/g WFR). The higher carbohydrate content and higher PhOH content might have imparted more hydrophilic character to WFR, achieving better contact with kaolin and acrylamide, and a more uniform polymerization. This could have resulted in the higher equilibrium adsorption amount. At the same time, the higher PhOH content would provide more polymerization sites and might lead to a higher cross-linking density, which could have resulted in the slower adsorption rates.

WFR-acrylamide-kaolin gel was also found to have a higher compression modulus (~19 ± 5 kPa) as compared to W-acrylamide-kaolin hydrogel (~10 ± 3 kPa; Section 3.2.3., Figure 24). This is a significant (P-value 0.03) and somewhat unexpected change, since decreased lignin purity is expected to cause decrease in the mechanical strength of the resulting gel [11]. However, as mentioned earlier, the possibly higher cross-linking density produced by higher PhOH content might have led to this effect.

WAH was unable to form a useable gel with acrylamide-kaolin. In this case, the higher lignin content of WAH (~94% OD lignin) might have imparted more hydrophobic character to WAH as compared to W (~85% OD lignin), resulting in poor dispersion of WAH in the solution and hampering polymerization.

Lignin-PEGDGE gel: The swelling capacity was found to slightly increase for WAH-PEGDGE gel (6.59 $\pm$ 0.5) and decrease for WFR-PEGDGE gel (5.04 $\pm$ 0.7), as compared to the original W-PEGDGE gel (5.3 $\pm$ 0.7, Figure 26. However, these changes were not found to be statistically significant (P-value 0.0501). The modulus of compression was found to increase for WAH-PEGDGE gel (16.4 $\pm$ 6 kPa), from the original W-PEGDGE gel (7.2 $\pm$ 2 kPa, Section 3.3.3., Figure 31). However, both results displayed a large sampling variation, and the change was not found to be statistically significant (P-value 0.07). This slight increase in mechanical strength could be the result of higher purity (hence higher hydrophobicity) of WAH (~94% OD lignin) as compared to W (~85% OD lignin respectively; Chapter 2) [11].

Due to the large sampling requirements, and limited lignin availability, the compression modulus was not calculated for WFR-PEGDGE gel.

4. Conclusions:

Lignins recovered from hot-water extracts of angiosperms were found to be suitable partial replacements of synthetic polymers in synthesis of lignin-acrylamide-kaolin (SM and W) and lignin-PEGDGE (SM, W, MS, WS, MA) gels. Compared to the previous literature on predominantly technical lignin-based hydrogels and hydrogels synthesized from lignin isolated under harsher conditions, this research shows the applicability of biorefinery lignin isolated under milder conditions at pilot scale for gel synthesis. It also shows the ability of these gels to interact with non-aqueous solutions, and opens up a new application opportunity in lignin

valorization. Gel performance and characteristics were found to depend on a combination of physicochemical and structural features of both; lignin and the co-polymers used for synthesis. This flexibility provides opportunities to tailor the gel properties through deliberate lignin selection with a desirable set of features, including the lignocellulosic origin of lignin (e.g. hardwoods vs grasses), its free phenolic hydroxyl group content, and S/G ratio. Fractionation was explored as one such way to modify gel properties. While it influenced a few of the properties of the resulting gels, it was not found to result in significant improvements. The sorption characteristics of the gels synthesized from recovered lignins were found to be better than or equal to those synthesized from kraft, the most readily available technical lignin. Although the absorption performance of lignin-based gels was inferior to the commercial hydrogels, the commercial hydrogels were limited in functionality. On the other hand, lignin-based gels were applicable in a variety of fields such as selective adsorption of dyes and metal cations, absorption of aqueous solutions and fragrance delivery. This wide applicability of lignin-based gels highlights the utility of lignin as a versatile biopolymer.

Appendix:

A. Adsorption kinetics:

Table 6: Second order adsorption kinetics showing differences in use of silica vs kaolin in willow lignin-acrylamide gels during first use

Parameter	**W-acrylamide-silica gel**	**W-acrylamide-kaolin gel**
qe_{calc} (µg/g)	370.4	333.3
qe_{exp} (µg/g)	319.5	319.5
k_2 (g/µg.min)	1.1E-05	3.5E-05
R^2	0.997	1
H (µg g^{-1} min^{-1})	1.5	3.9

Table 7: Second order adsorption kinetics showing differences in use of silica vs kaolin in willow lignin-acrylamide gels during repeat use

Parameter	W-acrylamide-silica gel	W-acrylamide-kaolin gel
qe $_{calc}$ (µg/g)	370	400
qe $_{exp}$ (µg/g)	335	371
k_2 (g/µg.min)	1.8E-05	2.9E-05
R^2	1	1
h (µg g^{-1} min^{-1})	2.4	4.6

B. TGA and FT-IR analysis showing formation of kraft lignin-acrylamide-kaolin gel:

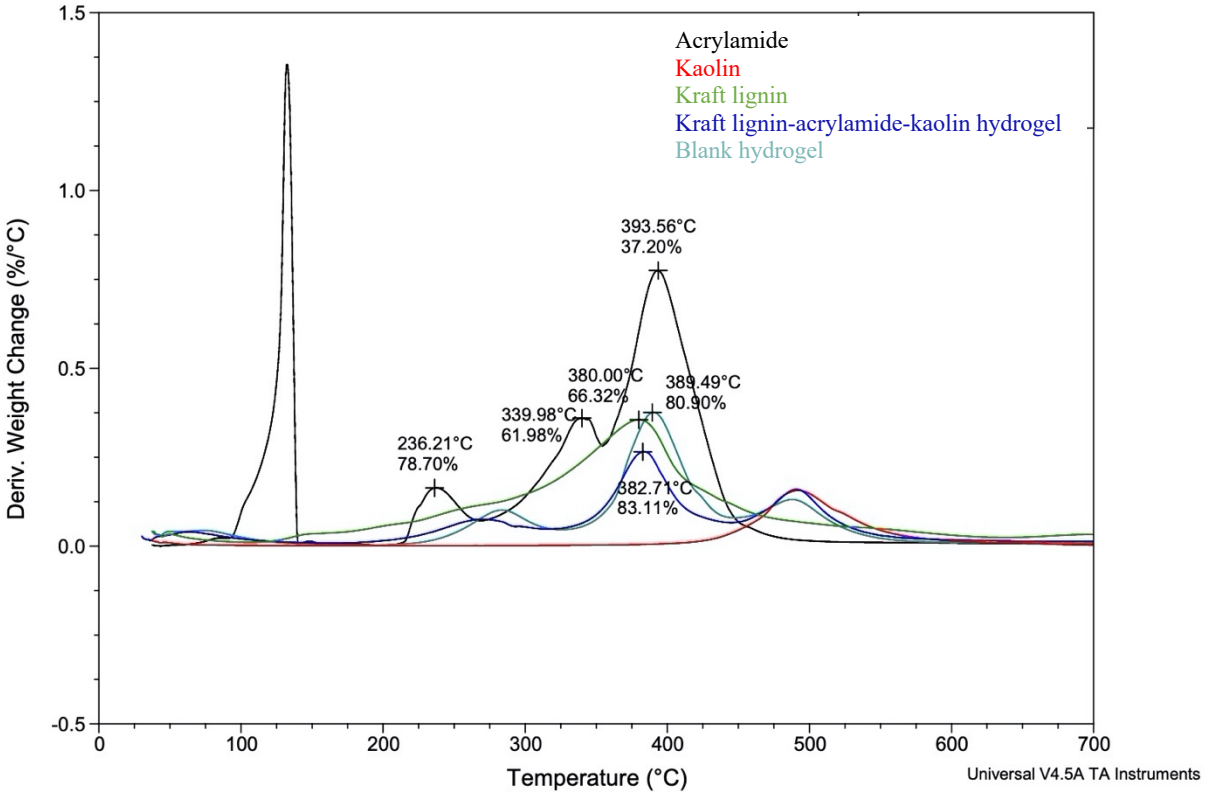

Figure 33: Combined DTG spectra of kraft lignin-acrylamide-kaolin gel showing individual components and the gel. The differences in the DTG curve of the gel as compared to the individual components indicate formation of a structurally different material

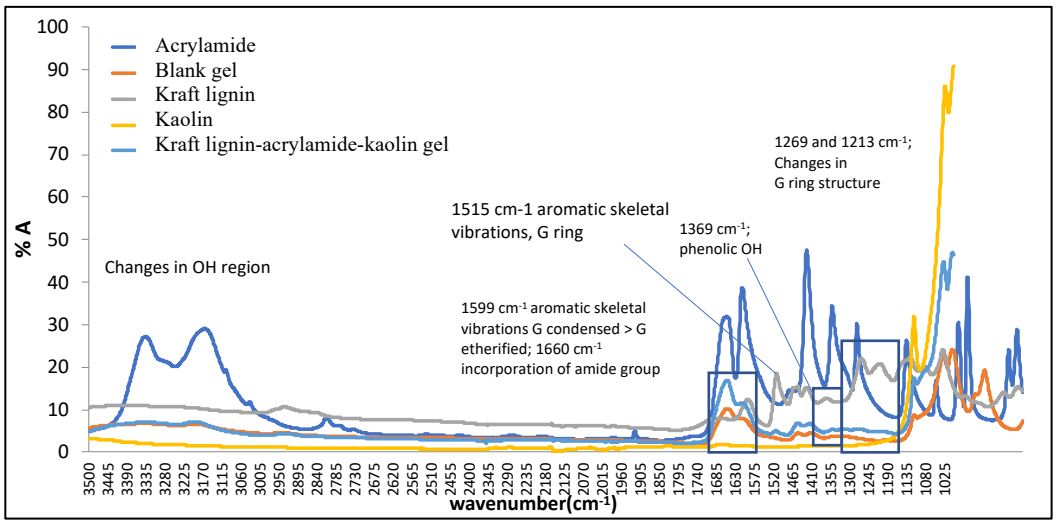

Figure 34: Combined FT-IR spectra of kraft lignin-acrylamide-kaolin gel showing individual components and the gel. The differences in the absorption bands of the gel as compared to the individual components indicate formation of a structurally different material

C. 2D NMR (HSQC analysis)

All 2D heteronuclear single quantum correlation nuclear magnetic resonance spectroscopy (HSQC NMR) experiments were acquired at 30°C on a Bruker AVANCE III 600 spectrometer (600MHz ^{1}H frequency, Bruker Biospin Corporation, Billerica, MA, USA) equipped with a 5 mm triple resonance *z*-gradient probe. Data was processed in Topspin v. 3.2 from Bruker Biospin. The samples were dissolved in deuterated dimethyl sulfoxide (DMSO-d_6) without acetylation.

As compared to MS, the HSQC spectrum of Ms-SAQ showed a marked decrease in the correlation integral areas for ferulate and coumarate residues. However, it should be noted that HSQC is not a quantitative method and the results obtained by this method are not accurate. It should also be noted that due to the presence of significant impurities resulting in overlapping of individual correlations, the correlations integrals are not precise.

Table 8: HSQC analysis of miscanthus lignins recovered from hot-water extract (MS) and from soda-anthraquinone liquor (MS-SAQ)

Unit	δc / δh, ppm	Integral area (MS, total lignin content 80% w/w OD)	Integral area (MS-SAQ, total lignin content 50% w/w OD)
Ferulate Cα	145.2, 7.59	0.02	0.006
Ferulate C_β	115.9, 6.4	0.01	0.006
p-Coumarate Cα	144.11, 7.54	0.03	0.002
p-Coumarate C_β	113.9, 6.2	0.02	0.006
[a]: Calibrated to DMSO integral area (39.7-40, 2.4 ppm)			

R code used for statistical analysis of results using ANOVA.

```
## ABSORBENCY CAPACITY
W_C <- c(2.97005988, 3.532, 16.6798419, 15.76893204, 9.761252446, 4.118908382, 4.756916996, 4.767175573, 4.257197697, 7.733197556)
SM_C <- c(2.678714859,2.904572565,3.538461538,3.167664671,5.596153846,4.446850394)
MS_C <- c(2.644400786,3.157170923,3.620481928,3.542574257,7.46812749,6.125248509)
WS_C <- c(3.222440945,9.495088409,11.52895753,8.690763052,10.25098039,9.716566866)
MA_C <- c(6.337972167,6.73,7.303571429,4.224,9.035928144,7.561507937)
K_C <- c(2.915322581,2.436507937,4.486921529,8.313402062,5.7578125,3.756048387)
WAH_C <- c(3.730097087,4.347992352,9.093253968,5.417647059)
TW_C <- c(28.67131474,35.86912065,33.3006135,35.37621832)
CG_C <- c(31.53846154,32.29674797,35.75050302)
W_F <- c(6.072144289,5.225321888,4.732334047)
SM_F <- c(6.100775194,7.742063492,6.417879418)
MS_F <- c(8.997929607,11.72435897,6.510416667,5.324380165,5.544871795)
WS_F <- c(8.4375,9.739212008,8.745)
MA_F <- c(8.997890295,8.612,6.87664042)
K_F <- c(5.821568627,4.456692913,5.594)
WAH_F <- c(6.257874016,7.187747036,6.340080972)
WFR_F <- c(5.824894515,4.589211618,4.732692308)
TW_F <- c(86.82323232,79.736,76.19917864)
CG_F <- c(74.59837728,83.5625,83.83474576)

W_compare <- data.frame(
  Y=c(W_C, W_F),
  Site =factor(rep(c("W_C", "W_F"), times=c(length(W_C), length(W_F)))))
W_Comp <- aov(Y~Site, data=W_compare)
anova(W_Comp) ## P 0.5

SM_compare <- data.frame(
  Y=c(SM_C, SM_F),
```

```
  Site =factor(rep(c("SM_C", "SM_F"),
times=c(length(SM_C), length(SM_F)))))
SM_Comp <- aov(Y~Site, data=SM_compare)
anova(SM_Comp) ## P 0.004

MS_compare <- data.frame(
  Y=c(MS_C, MS_F),
  Site =factor(rep(c("MS_C", "MS_F"),
times=c(length(MS_C), length(MS_F)))))
MS_Comp <- aov(Y~Site, data=MS_compare)
anova(MS_Comp) ## P 0.048

WS_compare <- data.frame(
  Y=c(WS_C, WS_F),
  Site =factor(rep(c("WS_C", "WS_F"),
times=c(length(WS_C), length(WS_F)))))
WS_Comp <- aov(Y~Site, data=WS_compare)
anova(WS_Comp)## P 0.93

MA_compare <- data.frame(
  Y=c(MA_C, MA_F),
  Site =factor(rep(c("MA_C", "MA_F"),
times=c(length(MA_C), length(MA_F)))))
MA_Comp <- aov(Y~Site, data=MA_compare)
anova(MA_Comp) ## P 0.25

K_compare <- data.frame(
  Y=c(K_C, K_F),
  Site =factor(rep(c("K_C", "K_F"), times=c(length(K_C),
length(K_F)))))
K_Comp <- aov(Y~Site, data=K_compare)
anova(K_Comp)  ## P 0.62

TW_compare <- data.frame(
  Y=c(TW_C, TW_F),
  Site =factor(rep(c("TW_C", "TW_F"),
times=c(length(TW_C), length(TW_F)))))
TW_Comp <- aov(Y~Site, data=TW_compare)
anova(TW_Comp)  ## P 0.000027

CG_compare <- data.frame(
  Y=c(CG_C, CG_F),
  Site =factor(rep(c("CG_C", "CG_F"),
times=c(length(CG_C), length(CG_F)))))
CG_Comp <- aov(Y~Site, data=CG_compare)
anova(CG_Comp)  ## P 0.00014

lignin_compare <- data.frame(
  Y=c(SM_F, WS_F, W_F, MS_F, MA_F, K_F),
  Site =factor(rep(c("SM_F", "WS_F", "W_F", "MS_F",
"MA_F", "K_F"), times=c(length(SM_F), length(WS_F),
length(W_F), length(MS_F), length(MA_F),
length(K_F)))))
lignin_Comp <- aov(Y~Site, data=lignin_compare)
anova(lignin_Comp) ## P 0.068

fr_compare <- data.frame(
  Y=c(W_F, WAH_F, WFR_F),
  Site =factor(rep(c("W_F", "WAH_F", "WFR_F"),
times=c(length(W_F), length(WAH_F),
length(WFR_F)))))
fr_Comp <- aov(Y~Site, data=fr_compare)
anova(fr_Comp)
####################################
## MODULUS OF COMPRESSION: Lignin-acrylamide-
kaolin hydrogels
W <- c(11.535, 10.922, 5.8416, 10.135)
SM <- c(11.15, 6.88, NA, NA)
K <- c(7.1423, 14.786, 8.4747, NA)
Blank <- c(35.984, 34.868, NA, NA)
WFR <- c(24.119,13.614,17.99)
AAM <- data.frame(W, SM, K, Blank)

res.aov <- aov (W ~ K, data = AAM)
res.aov
summary(res.aov)

AAm_compare <- data.frame(
  Y=c(W, WFR),
  Site =factor(rep(c("W", "WFR"), times=c(length(W),
length(WFR)))))
AAm_Comp <- aov(Y~Site, data=AAm_compare)
anova(AAm_Comp) ## P 0.029
```

```
##################################################
####
## Modulus of compression: PEGDGE:
W_PEG <- c(5.347,8.9362,7.4486)
SM_PEG <- c(6.0944,2.1579,5.0786)
K_PEG <- c(7.0744,NA,NA)
MS_PEG <- c(0.4334,0.3616,NA)
WS_PEG <- c(0.2595,3.413,1.7969,NA)
MA_PEG <- c(1.3424,1.92,0.7845)
WAH_PEG <- c(9.2987,19.279,20.722)
WD_PEG <- c(1.2465,1.2562,3.86)
CG_hemi <-
c(7,12.29,6.94,8.59,8.64,13.74,4.61,19.16,12.95,7.01)
TW <- c(7.3904,6.3078,2.1451,4.904,2.0039,1.0409)

Mod_compare <- data.frame(
  Y=c(W_PEG, SM_PEG, K_PEG, MS_PEG, WS_PEG,
MA_PEG, CG_hemi, TW),
  site=factor(rep(c("W_PEG", "SM_PEG", "K_PEG",
"MS_PEG", "WS_PEG", "MA_PEG", "CG_hemi", "TW"),
times=c(length(W_PEG), length(SM_PEG),
length(K_PEG), length(MS_PEG), length(WS_PEG),
length(MA_PEG), length(CG_hemi), length(TW)))))
Mod_Comp <- aov(Y~site, data=Mod_compare)
anova(Mod_Comp) ## P 0.0007641

Mod_compare2 <- data.frame(
  Y=c(W_PEG, SM_PEG, K_PEG),
  site=factor(rep(c("W_PEG", "SM_PEG", "K_PEG"),
times=c(length(W_PEG), length(SM_PEG),
length(K_PEG)))))
Mod_Comp2 <- aov(Y~site, data=Mod_compare2)
anova(Mod_Comp2) ## P 0.28

Mod_compare3 <- data.frame(
  Y=c(W_PEG, SM_PEG, K_PEG, MS_PEG),
  site=factor(rep(c("W_PEG", "SM_PEG", "K_PEG",
"MS_PEG"), times=c(length(W_PEG), length(SM_PEG),
length(K_PEG), length(MS_PEG)))))
Mod_Comp3 <- aov(Y~site, data=Mod_compare3)
anova(Mod_Comp3) ## P 0.03

Mod_compare4 <- data.frame(
  Y=c(MS_PEG, WS_PEG, MA_PEG),
  site=factor(rep(c("MS_PEG", "WS_PEG", "MA_PEG"),
times=c(length(MS_PEG), length(WS_PEG),
length(MA_PEG)))))
Mod_Comp4 <- aov(Y~site, data=Mod_compare4)
anova(Mod_Comp4) ## P 0.4

Mod_compare5 <- data.frame(
  Y=c(W_PEG, WAH_PEG),
  site=factor(rep(c("W_PEG", "WAH_PEG"),
times=c(length(W_PEG), length(WAH_PEG)))))
Mod_Comp5 <- aov(Y~site, data=Mod_compare5)
anova(Mod_Comp5) ## P 0.06
```

References:

[1] A. S. Hoffman, "Hydrogels for biomedical applications," *Adv. Drug Deliv. Rev.*, vol. 64, pp. 18–23, Dec. 2012, doi: 10.1016/j.addr.2012.09.010.

[2] O. Wichterle and D. Lím, "Hydrophilic Gels for Biological Use," *Nature*, vol. 185, no. 4706, Art. no. 4706, Jan. 1960, doi: 10.1038/185117a0.

[3] W. Otto and L. Drahoslav, "Cross-linked hydrophilic polymers and articles made therefrom," US3220960A, Nov. 30, 1965.

[4] X.-F. Sun, Z. Jing, H. Wang, and Y. Liu, "Physical–chemical properties of xylan/PAAc magnetic semi-interpenetrating network hydrogel," *Polym. Compos.*, vol. 36, no. 12, pp. 2317–2325, 2015, doi: 10.1002/pc.23145.

[5] M. Irie and D. Kunwatchakun, "Photoresponsive polymers. 8. Reversible photostimulated dilation of polyacrylamide gels having triphenylmethane leuco derivatives," *Macromolecules*, vol. 19, no. 10, pp. 2476–2480, Oct. 1986, doi: 10.1021/ma00164a003.

[6] C. S. Kwok, P. D. Mourad, L. A. Crum, and B. D. Ratner, "Self-assembled molecular structures as ultrasonically-responsive barrier membranes for pulsatile drug delivery," *J. Biomed. Mater. Res.*, vol. 57, no. 2, pp. 151–164, Nov. 2001, doi: 10.1002/1097-4636(200111)57:2<151::aid-jbm1154>3.0.co;2-5.

[7] I. Roy and M. N. Gupta, "Smart Polymeric Materials: Emerging Biochemical Applications," *Chem. Biol.*, vol. 10, no. 12, pp. 1161–1171, Dec. 2003, doi: 10.1016/j.chembiol.2003.12.004.

[8] B. Kippelen, S. Marder, E. Hendrickx, J. Maldonado, G. Guillemet, and B. Volodin, "Infrared photorefractive polymers and their applications for imaging — University of Arizona," *Science*, vol. 279, no. 5347, pp. 54–57, doi: 10.1126/science.279.5347.54.

[9] E. M. Ahmed, "Hydrogel: Preparation, characterization, and applications: A review," *J. Adv. Res.*, vol. 6, no. 2, pp. 105–121, Mar. 2015, doi: 10.1016/j.jare.2013.07.006.

[10] V. K. Thakur and M. K. Thakur, "Recent advances in green hydrogels from lignin: a review," *Int. J. Biol. Macromol.*, vol. 72, pp. 834–847, Jan. 2015, doi: 10.1016/j.ijbiomac.2014.09.044.

[11] D. A. Gyles, L. D. Castro, J. O. C. Silva, and R. M. Ribeiro-Costa, "A review of the designs and prominent biomedical advances of natural and synthetic hydrogel formulations," *Eur. Polym. J.*, vol. 88, pp. 373–392, Mar. 2017, doi: 10.1016/j.eurpolymj.2017.01.027.

[12] A. Tangri, "Polyacrylamide Based Hydrogels: Synthesis, Characterization and Applications," *Int. J. Pharm. Biol. Sci.*, vol. 4, pp. 951-959, 2014.

[13] J. Sun, J. Chen, L. Yang, S. Wang, Z. Li, and H. Wu, "Synthesis and characterization of a pH-sensitive hydrogel made of pyruvic-acid-modified chitosan," *J. Biomater. Sci. Polym. Ed.*, vol. 18, no. 1, pp. 35–44, 2007, doi: 10.1163/156856207779146132.

[14] E. Marsano, E. Bianchi, and L. Sciutto, "Microporous thermally sensitive hydrogels based on hydroxypropyl cellulose crosslinked with poly-ethyleneglicol diglycidyl ether," *Polymer*, vol. 44, no. 22, pp. 6835–6841, Oct. 2003, doi: 10.1016/S0032-3861(03)00693-1.

[15] C. Gerbaldi, J. R. Nair, G. Meligrana, R. Bongiovanni, S. Bodoardo, and N. Penazzi, "UV-curable siloxane-acrylate gel-copolymer electrolytes for lithium-based battery applications," *Electrochimica Acta*, vol. 55, no. 4, pp. 1460–1467, Jan. 2010, doi: 10.1016/j.electacta.2009.05.055.

[16] L. C. Cesteros, C. A. Ramírez, A. Peciña, and I. Katime, "Poly(ethylene glycol-β-cyclodextrin) gels: Synthesis and properties," *J. Appl. Polym. Sci.*, vol. 102, no. 2, pp. 1162–1166, 2006, doi: 10.1002/app.24390.

[17] J. M. Seidel and S. M. Malmonge, "Synthesis of polyHEMA hydrogels for using as biomaterials. Bulk and solution radical-initiated polymerization techniques," *Mater. Res.*, vol. 3, no. 3, pp. 79–83, Jul. 2000, doi: 10.1590/S1516-14392000000300006.

[18] C. Chang and L. Zhang, "Cellulose-based hydrogels: Present status and application prospects," *Carbohydr. Polym.*, vol. 84, no. 1, pp. 40–53, Feb. 2011, doi: 10.1016/j.carbpol.2010.12.023.

[19] R. Pereira, A. Carvalho, D. C. Vaz, M. H. Gil, A. Mendes, and P. Bártolo, "Development of novel alginate based hydrogel films for wound healing applications," *Int. J. Biol. Macromol.*, vol. 52, pp. 221–230, Jan. 2013, doi: 10.1016/j.ijbiomac.2012.09.031.

[20] N. Bhattarai, J. Gunn, and M. Zhang, "Chitosan-based hydrogels for controlled, localized drug delivery," *Adv. Drug Deliv. Rev.*, vol. 62, no. 1, pp. 83–99, Jan. 2010, doi: 10.1016/j.addr.2009.07.019.

[21] K. Yue, G. Trujillo-de Santiago, M. M. Alvarez, A. Tamayol, N. Annabi, and A. Khademhosseini, "Synthesis, properties, and biomedical applications of gelatin methacryloyl (GelMA) hydrogels," *Biomaterials*, vol. 73, pp. 254–271, Dec. 2015, doi: 10.1016/j.biomaterials.2015.08.045.

[22] X.-W. Peng, L.-X. Zhong, J.-L. Ren, and R.-C. Sun, “Highly Effective Adsorption of Heavy Metal Ions from Aqueous Solutions by Macroporous Xylan-Rich Hemicelluloses-Based Hydrogel,” *J. Agric. Food Chem.*, vol. 60, no. 15, pp. 3909–3916, Apr. 2012, doi: 10.1021/jf300387q.
[23] H. Ismail, M. Irani, and Z. Ahmad, “Starch-Based Hydrogels: Present Status and Applications,” *Int. J. Polym. Mater. Polym. Biomater.*, vol. 62, no. 7, pp. 411–420, Mar. 2013, doi: 10.1080/00914037.2012.719141.
[24] T. Lindström, A. Wallis, J. Tulonen, and F. Kolseth, “The Effect of Chemical Environment on Swelling and Dynamic Mechanical Properties of Milled Wood Lignin Gels,” *Holzforschung*, vol. 42, no. 4, pp. 225–231, Jan. 1988, doi: 10.1515/hfsg.1988.42.4.225.
[25] M. Nishida, Y. Uraki, and Y. Sano, “Lignin gel with unique swelling property,” *Bioresour. Technol.*, vol. 88, no. 1, pp. 81–83, May 2003, doi: 10.1016/S0960-8524(02)00264-X.
[26] X. Li and X. Pan, “Hydrogels Based on Hemicellulose and Lignin from Lignocellulose Biorefinery: a Mini-review,” *J. Biobased Mater. Bioenergy*, vol. 4, no. 4, pp. 289–297, Dec. 2010, doi: 10.1166/jbmb.2010.1107.
[27] E. H. Schacht, “Polymer chemistry and hydrogel systems,” *J. Phys. Conf. Ser.*, vol. 3, pp. 22–28, Jan. 2004, doi: 10.1088/1742-6596/3/1/004.
[28] PubChem, “N,N’-Methylenebisacrylamide.” https://pubchem.ncbi.nlm.nih.gov/compound/8041 (accessed Jul. 24, 2020).
[29] PubChem, “beta-CYCLODEXTRIN.” https://pubchem.ncbi.nlm.nih.gov/compound/444041 (accessed Jul. 24, 2020).
[30] S. Fu *et al.*, “Relevance of Rheological Properties of Sodium Alginate in Solution to Calcium Alginate Gel Properties,” *AAPS PharmSciTech*, vol. 12, no. 2, pp. 453–460, Mar. 2011, doi: 10.1208/s12249-011-9587-0.
[31] H. Hecht and S. Srebnik, “Structural Characterization of Sodium Alginate and Calcium Alginate,” *Biomacromolecules*, vol. 17, no. 6, pp. 2160–2167, Jun. 2016, doi: 10.1021/acs.biomac.6b00378.
[32] A. S. Sarac, “Redox polymerization,” *Prog. Polym. Sci.*, vol. 24, no. 8, pp. 1149–1204, Oct. 1999, doi: 10.1016/S0079-6700(99)00026-X.
[33] S. Kiatkamjornwong, “Superabsorbent Polymers and Superabsorbent Polymer Composites,” *ScienceAsia*, vol. 33(s1), p. 039, 2007, doi: 10.2306/scienceasia1513-1874.2007.33(s1).039.
[34] G. Wang, M. Li, and X. Chen, “Inverse suspension polymerization of sodium acrylate,” *www.paper.edu*, p. 6.
[35] J. O. Karlsson and P. Gatenholm, “Preparation and characterization of cellulose-supported HEMA hydrogels,” *Polymer*, vol. 38, no. 18, pp. 4727–4731, Sep. 1997, doi: 10.1016/S0032-3861(96)01075-0.
[36] P. V. Kozlov and G. I. Burdygina, “The structure and properties of solid gelatin and the principles of their modification,” *Polymer*, vol. 24, pp. 651–666, Jun. 1983.
[37] M. Sadeghi and B. Heidari, “Crosslinked Graft Copolymer of Methacrylic Acid and Gelatin as a Novel Hydrogel with pH-Responsiveness Properties,” *Materials*, vol. 4, no. 3, Art. no. 3, Mar. 2011, doi: 10.3390/ma4030543.
[38] G. J. Gil-Chávez, S. S. P. Padhi, C. V. Pereira, J. N. Guerreiro, A. A. Matias, and I. Smirnova, “Cytotoxicity and biological capacity of sulfur-free lignins obtained in novel biorefining process,” *Int. J. Biol. Macromol.*, vol. 136, pp. 697–703, Sep. 2019, doi: 10.1016/j.ijbiomac.2019.06.021.
[39] M. Witzler *et al.*, “Lignin-Derived Biomaterials for Drug Release and Tissue Engineering,” *Molecules*, vol. 23, no. 8, Art. no. 8, Aug. 2018, doi: 10.3390/molecules23081885.
[40] “Introduction to the Sorption of Chemical Constituents in Soils | Learn Science at Scitable.” https://www.nature.com/scitable/knowledge/library/introduction-to-the-sorption-of-chemical-constituents-94841002/ (accessed Jul. 24, 2020).
[41] “Adsorption,” *Wikipedia*. Jul. 22, 2020, Accessed: Jul. 24, 2020. [Online]. Available: https://en.wikipedia.org/w/index.php?title=Adsorption&oldid=969019834.
[42] “Absorption (chemistry),” *Wikipedia*. Jul. 14, 2020, Accessed: Jul. 24, 2020. [Online]. Available: https://en.wikipedia.org/w/index.php?title=Absorption_(chemistry)&oldid=967665870.
[43] A. W. Adamson and A. P. Gast, *Physical chemistry of surfaces*, 6th ed. New York: Wiley, 1997.
[44] W. K. El-Zawawy, “Preparation of hydrogel from green polymer,” *Polym. Adv. Technol.*, vol. 16, no. 1, pp. 48–54, 2005, doi: 10.1002/pat.537.
[45] W. K. El-Zawawy and M. M. Ibrahim, “Preparation and characterization of novel polymer hydrogel from industrial waste and copolymerization of poly(vinyl alcohol) and polyacrylamide,” *J. Appl. Polym. Sci.*, vol. 124, no. 5, pp. 4362–4370, 2012, doi: 10.1002/app.35481.
[46] Q. Feng, F. Chen, and H. Wu, “Preparation and Characterization of a temperature-sensitive lignin-based hydrogel," p. 11.

[47] L. I. Grishechko, G. Amaral-Labat, A. Szczurek, V. Fierro, B. N. Kuznetsov, and A. Celzard, "Lignin–phenol–formaldehyde aerogels and cryogels," *Microporous Mesoporous Mater.*, vol. 168, pp. 19–29, Mar. 2013, doi: 10.1016/j.micromeso.2012.09.024.
[48] Z. Peng and F. Chen, "Synthesis and Properties of Lignin-Based Polyurethane Hydrogels," *Int. J. Polym. Mater. Polym. Biomater.*, vol. 60, no. 9, pp. 674–683, Aug. 2011, doi: 10.1080/00914037.2010.551353.
[49] L. Passauer *et al.*, "Dynamic Moisture Sorption Characteristics of Xerogels from Water-Swellable Oligo(oxyethylene) Lignin Derivatives," *ACS Appl. Mater. Interfaces*, vol. 4, no. 11, pp. 5852–5862, Nov. 2012, doi: 10.1021/am3015179.
[50] I. E. Raschip, E. G. Hitruc, A. M. Oprea, M.-C. Popescu, and C. Vasile, "In vitro evaluation of the mixed xanthan/lignin hydrogels as vanillin carriers," *J. Mol. Struct.*, vol. 1–3, no. 1003, pp. 67–74, 2011, doi: 10.1016/j.molstruc.2011.07.023.
[51] J. E. Peñaranda A. and M. A. Sabino, "Effect of the presence of lignin or peat in IPN hydrogels on the sorption of heavy metals," *Polym. Bull.*, vol. 65, no. 5, pp. 495–508, Sep. 2010, doi: 10.1007/s00289-010-0264-3.
[52] I. E. Raschip, G. E. Hitruc, C. Vasile, and M.-C. Popescu, "Effect of the lignin type on the morphology and thermal properties of the xanthan/lignin hydrogels," *Int. J. Biol. Macromol.*, vol. 54, pp. 230–237, Mar. 2013, doi: 10.1016/j.ijbiomac.2012.12.036.
[53] W. L. Griffith and A. L. Compere, "Separation of Alcohols from Solution by Lignin Gels," *Sep. Sci. Technol.*, vol. 43, no. 9–10, pp. 2396–2405, Jul. 2008, doi: 10.1080/01496390802148571.
[54] Y. Wang, Y. Xiong, J. Wang, and X. Zhang, "Ultrasonic-assisted fabrication of montmorillonite-lignin hybrid hydrogel: Highly efficient swelling behaviors and super-sorbent for dye removal from wastewater," *Colloids Surf. Physicochem. Eng. Asp.*, vol. 520, pp. 903–913, May 2017, doi: 10.1016/j.colsurfa.2017.02.050.
[55] Y. Ma, Y. Sun, Y. Fu, G. Fang, X. Yan, and Z. Guo, "Swelling behaviors of porous lignin based poly (acrylic acid)," *Chemosphere*, vol. 163, pp. 610–619, Nov. 2016, doi: 10.1016/j.chemosphere.2016.08.035.
[56] C. Yu, F. Wang, C. Zhang, S. Fu, and L. A. Lucia, "The synthesis and absorption dynamics of a lignin-based hydrogel for remediation of cationic dye-contaminated effluent," *React. Funct. Polym.*, vol. 106, pp. 137–142, Sep. 2016, doi: 10.1016/j.reactfunctpolym.2016.07.016.
[57] H. Zhao, Q. Feng, Y. Xie, J. Li, and X. Chen, "Preparation of Biocompatible Hydrogel from Lignin-Carbohydrate Complex (LCC) as Cell Carriers," *BioResources*, vol. 12, no. 4, Art. no. 4, Sep. 2017.
[58] L. I. Grishechko *et al.*, "New tannin–lignin aerogels," *Ind. Crops Prod.*, vol. 41, pp. 347–355, Jan. 2013, doi: 10.1016/j.indcrop.2012.04.052.
[59] L. Perez-Cantu, F. Liebner, and I. Smirnova, "Preparation of aerogels from wheat straw lignin by cross-linking with oligo(alkylene glycol)-α,ω-diglycidyl ethers," Microporous Mesoporous *Mater.*, vol. 195, pp. 303–310, 2014.
[60] D. Mahata *et al.*, "Lignin-graft-Polyoxazoline Conjugated Triazole a Novel Anti-Infective Ointment to Control Persistent Inflammation," *Sci. Rep.*, vol. 7, Apr. 2017, doi: 10.1038/srep46412.
[61] Y. S. Kim and J. F. Kadla, "Preparation of a thermoresponsive lignin-based biomaterial through atom transfer radical polymerization," *Biomacromolecules*, vol. 11, no. 4, pp. 981–988, Apr. 2010, doi: 10.1021/bm901455p.
[62] D. Kai *et al.*, "Development of Lignin Supramolecular Hydrogels with Mechanically Responsive and Self-Healing Properties," *ACS Sustain. Chem. Eng.*, vol. 3, no. 9, pp. 2160–2169, Sep. 2015, doi: 10.1021/acssuschemeng.5b00405.
[63] A. E. Ofomaja, "Kinetic study and sorption mechanism of methylene blue and methyl violet onto mansonia (Mansonia altissima) wood sawdust," *Chem. Eng. J.*, vol. 143, no. 1, pp. 85–95, Sep. 2008, doi: 10.1016/j.cej.2007.12.019.
[64] R. W. Sabnis, *Handbook of Biological Dyes and Stains: Synthsis and Industrial Applications*. John Wiley & Sons, Ltd, 2010.
[65] Y. Wang, L. Zeng, X. Ren, H. Song, and A. Wang, "Removal of Methyl Violet from aqueous solutions using poly (acrylic acid-co-acrylamide)/attapulgite composite," *J. Environ. Sci.*, vol. 22, no. 1, pp. 7–14, Jan. 2010, doi: 10.1016/S1001-0742(09)60068-1.
[66] J. Rahchamani, H. Z. Mousavi, and M. Behzad, "Adsorption of methyl violet from aqueous solution by polyacrylamide as an adsorbent: Isotherm and kinetic studies," *Desalination*, vol. 267, no. 2, pp. 256–260, Feb. 2011, doi: 10.1016/j.desal.2010.09.036.
[67] G. Al-Enezi, M. F. Hamoda, and N. Fawzi, "Ion Exchange Extraction of Heavy Metals from Wastewater Sludges," *J. Environ. Sci. Health Part A*, vol. 39, no. 2, pp. 455–464, Jan. 2004, doi: 10.1081/ESE-120027536.

[68] R. D. Lentz, F. F. Andrawes, F. W. Barvenik, and A. C. Koehn, “Acrylamide Monomer Leaching from Polyacrylamide-Treated Irrigation Furrows,” *J. Environ. Qual.*, vol. 37, no. 6, pp. 2293–2298, Nov. 2008, doi: 10.2134/jeq2007.0574.
[69] S.-Y. Huang, D. W. Lipp, and R. S. Farinato, “Acrylamide Polymers,” in *Kirk-Othmer Encyclopedia of Chemical Technology*, American Cancer Society, 2001.
[70] J. A. Entry, R. E. Sojka, M. Watwood, and C. Ross, “Polyacrylamide preparations for protection of water quality threatened by agricultural runoff contaminants,” *Environ. Pollut.*, vol. 120, no. 2, pp. 191–200, Dec. 2002, doi: 10.1016/S0269-7491(02)00160-4.
[71] H.-K. Lee and W.-L. Jong, “Synthesis and applications of polyacrylamide derivatives in the wet end of papermaking (Part II. Reactive N-chloropolyacrylamide),” *J. Polym. Res.*, vol. 4, no. 2, pp. 119–128, Apr. 1997, doi: 10.1007/s10965-006-0015-1.
[72] R. M. LoPachin, “Acrylamide Neurotoxicity: Neurological, Morhological and Molecular Endpoints in Animal Models,” in *Chemistry and Safety of Acrylamide in Food*, Boston, MA, 2005, pp. 21–37, doi: 10.1007/0-387-24980-X_2.
[73] J. Duca, “Kaolin,” in *Functional Fillers for Plastics*, John Wiley & Sons, Ltd, 2010, pp. 241–258.
[74] M. Hubbe and R. Gill, “Fillers for Papermaking: A Review of their Properties, Usage Practices, and their Mechanistic Role,” *BioResources*, vol. 11, Feb. 2016, doi: 10.15376/biores.11.1.2886-2963.
[75] T. M. Herrington, A. Q. Clarke, and J. C. Watts, “The surface charge of kaolin,” *Colloids Surf.*, vol. 68, no. 3, pp. 161–169, Nov. 1992, doi: 10.1016/0166-6622(92)80200-L.
[76] K. Kabiri and M. J. Zohuriaan-Mehr, “Superabsorbent hydrogel composites,” *Polym. Adv. Technol.*, vol. 14, no. 6, pp. 438–444, 2003, doi: 10.1002/pat.356.
[77] S. R. Shirsath, A. P. Patil, R. Patil, J. B. Naik, P. R. Gogate, and S. H. Sonawane, “Removal of Brilliant Green from wastewater using conventional and ultrasonically prepared poly(acrylic acid) hydrogel loaded with kaolin clay: A comparative study,” *Ultrason. Sonochem.*, vol. 20, no. 3, pp. 914–923, May 2013, doi: 10.1016/j.ultsonch.2012.11.010.
[78] A. Pourjavadi, M. Ayyari, and M. S. Amini-Fazl, “Taguchi optimized synthesis of collagen-g-poly(acrylic acid)/kaolin composite superabsorbent hydrogel,” *Eur. Polym. J.*, vol. 44, no. 4, pp. 1209–1216, Apr. 2008, doi: 10.1016/j.eurpolymj.2008.01.032.
[79] A. Pourjavadi, H. Ghasemzadeh, and R. Soleyman, “Synthesis, characterization, and swelling behavior of alginate-g-poly(sodium acrylate)/kaolin superabsorbent hydrogel composites,” *J. Appl. Polym. Sci.*, vol. 105, no. 5, pp. 2631–2639, 2007, doi: 10.1002/app.26345.
[80] H. Ceylan, T. Şahan, R. Gürkan, and Ş. Kubilay, “Removal of Some Heavy Metal Cations from Aqueous Solution by Adsorption onto Natural Kaolin:,” *Adsorpt. Sci. Technol.*, Nov. 2016, doi: 10.1260/026361705775212475.
[81] M. Laufmann and S. Hubschmid, “Mineral Fillers in Papermaking,” in *Handbook of Paper and Board*, John Wiley & Sons, Ltd, 2013, pp. 109–143.
[82] R. Barbucci, D. Pasqui, R. Favaloro, and G. Panariello, “A thixotropic hydrogel from chemically cross-linked guar gum: synthesis, characterization and rheological behaviour,” *Carbohydr. Res.*, vol. 343, no. 18, pp. 3058–3065, Dec. 2008, doi: 10.1016/j.carres.2008.08.029.
[83] G. Tripodo *et al.*, “Hydrogels for biomedical applications from glycol chitosan and PEG diglycidyl ether exhibit pro-angiogenic and antibacterial activity,” *Carbohydr. Polym.*, vol. 198, pp. 124–130, Oct. 2018, doi: 10.1016/j.carbpol.2018.06.061.
[84] “Poly(ethylene glycol) diglycidyl ether 475696,” *PEG diglycidyl ether*. https://www.sigmaaldrich.com/catalog/product/aldrich/475696 (accessed Jul. 24, 2020).
[85] V. Nair, A. Panigrahy, and R. Vinu, “Development of novel chitosan–lignin composites for adsorption of dyes and metal ions from wastewater,” *Chem. Eng. J.*, vol. 254, pp. 491–502, Oct. 2014, doi: 10.1016/j.cej.2014.05.045.
[86] G. Crini and P.-M. Badot, “Application of chitosan, a natural aminopolysaccharide, for dye removal from aqueous solutions by adsorption processes using batch studies: A review of recent literature,” *Prog. Polym. Sci.*, vol. 33, no. 4, pp. 399–447, Apr. 2008, doi: 10.1016/j.progpolymsci.2007.11.001.
[87] V. Mechtcherine *et al.*, “Testing superabsorbent polymer (SAP) sorption properties prior to implementation in concrete: results of a RILEM Round-Robin Test,” *Mater. Struct.*, vol. 51, no. 1, p. 28, Jan. 2018, doi: 10.1617/s11527-018-1149-4.
[88] Z. M. M.j.a.d and K. K, “Superabsorbent polymer materials: A review," *Iran. Polym. J.*, vol. 17, no. 6, pp. 451–447, Jan. 2008.
[89] D. Rowe, *Chemistry and Technology of Flavours and Fragrances*. John Wiley & Sons, 2009.

[90] M. Li, Y. Pu, and A. J. Ragauskas, “Current Understanding of the Correlation of Lignin Structure with Biomass Recalcitrance,” *Front. Chem.*, vol. 4, Nov. 2016, doi: 10.3389/fchem.2016.00045.
[91] J. Domínguez-Robles, M. S. Peresin, T. Tamminen, A. Rodríguez, E. Larrañeta, and A.-S. Jääskeläinen, “Lignin-based hydrogels with ‘super-swelling’ capacities for dye removal,” *Int. J. Biol. Macromol.*, vol. 115, pp. 1249–1259, Aug. 2018, doi: 10.1016/j.ijbiomac.2018.04.044.
[92] C. Crestini, H. Lange, M. Sette, and D. S. Argyropoulos, “On the structure of softwood kraft lignin,” *Green Chem.*, vol. 19, no. 17, pp. 4104–4121, Aug. 2017, doi: 10.1039/C7GC01812F.
[93] E. Sjöström, “Chapter 4 - LIGNIN,” in *Wood Chemistry (Second Edition)*, E. Sjöström, Ed. San Diego: Academic Press, 1993, pp. 71–89.
[94] A. Lourenço and H. Pereira, “Compositional Variability of Lignin in Biomass,” *Lignin - Trends Appl.*, Dec. 2017, doi: 10.5772/intechopen.71208.
[95] G. Kowalski, K. Kijowska, M. Witczak, Ł. Kuterasiński, and M. Łukasiewicz, “Synthesis and Effect of Structure on Swelling Properties of Hydrogels Based on High Methylated Pectin and Acrylic Polymers,” *Polymers*, vol. 11, no. 1, Jan. 2019, doi: 10.3390/polym11010114.
[96] V. Guarino, F. Causa, and L. Ambrosio, “Porosity and Mechanical Properties Relationship in PCL Porous Scaffolds,” *J. Appl. Biomater. Biomech.*, vol. 5, no. 3, pp. 149–157, Sep. 2007, doi: 10.1177/228080000700500303.
[97] C. Lian, Y. Zhuge, and S. Beecham, “The relationship between porosity and strength for porous concrete,” *Constr. Build. Mater.*, vol. 25, no. 11, pp. 4294–4298, Nov. 2011, doi: 10.1016/j.conbuildmat.2011.05.005.
[98] D. Ciolacu, A. M. Oprea, N. Anghel, G. Cazacu, and M. Cazacu, “New cellulose–lignin hydrogels and their application in controlled release of polyphenols,” *Mater. Sci. Eng. C*, vol. 32, no. 3, pp. 452–463, Apr. 2012, doi: 10.1016/j.msec.2011.11.018.

Chapter IV

Extraction of Bioactive Compounds from Chaga and Synthesis of Chaga-Silver Nanoparticles

---

1. Introduction:

Chaga mushroom is the common name for the sterile conk of basidiomycete fungus *Inonotus obliquus* (Family: *Hymenochaetaceae*). It is generally found in boreal forests in extremely cold climates, such as Russia, China and North America [1], [2]. It mainly grows as a wood-destroying parasite on tree trunks rich in betulinic acid (Figure 1), which is a pentacyclic triterpenoid and the main component of trees in the *Betulaceae* family, such as white birch (*Betula papyrifera*), yellow birch (*Betula alleghaniensis*), black birch (*Betula nigra*) and ironwood (*Carpinus caroliniana*) [3].

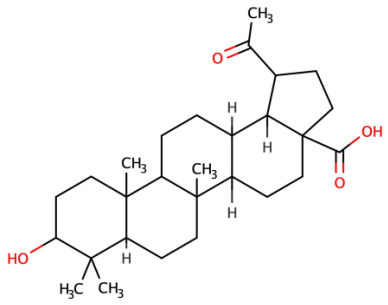

Figure 1: Betulinic acid

In a typical lifecycle of chaga, the airborne basidiospores of the fungus fall into damaged sites on the tree trunk, where they form a mycelium into the wood. The wood is gradually destroyed as the hyphae consume the nutrients from the tree. New spores are formed just under the surface of the trunk, while the fruitless (sterile) tissue emerges on the surface (Figure 2).

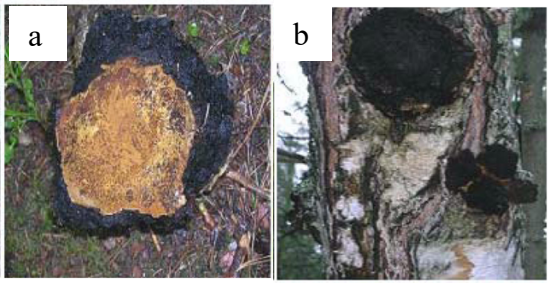

Figure 2: Sterile conk of chaga mushroom; (a) Outside surface (b) Inside surface. Reprinted with permission from [2]

After 10-15 years of parasitism, this growth generally measures 0.5-1.5 m long and 10-15 cm thick, weighing upwards of 5 kg [3]. This eventually leads to the loss of the tree and the spores are released into the air where a fresh lifecycle begins.

Approximately 700 different species of higher basidiomycetes have been documented to possess bioactive components, and over 130 different pharmaceutical activities have been contributed to these, including anti-tumor, antimicrobial, anti-diabetic, cardiovascular, and anti-mutagenic properties [1], [4]. In general, medicinal mushrooms including chaga are currently used as [4]:

1) Dietary foods

2) Dietary supplement products

3) 'Mushroom pharmaceuticals' which is a recent new class of drugs

4) Insecticides, fungicides, bactericides and herbicides

5) Cosmeceuticals - mushroom polysaccharides like β-glucans, enzymes, e.g. tyrosinase, are used in cosmetics for their anti-oxidant, anti-allergic and anti-inflammatory activity.

Although some of these uses are modern, medicinal mushrooms have been a part of traditional folk medicine in Russia and China for centuries and are commonly employed in home remedies. Examples of chaga being used in such preparations are the 'Infusum fungus betulinus' and

‘Befunginum’, mushroom extract preparations enriched with trace amounts of cobalt chloride and cobalt sulfate [1].

1.1. Extraction of bioactive compounds from chaga: Antioxidizing, hepatoprotectant, immunomodulatory and antimicrobial activities are the most common biological activities attributed to chaga, while polysaccharides, alkaloids, phenolic compounds, sterols and triterpenoids are the most commonly recognized active ingredients in the extracts (Figure 3) [4]–[6]. However, the chemical composition and biological activity vary depending on the extraction method, age of harvested chaga, and the part of chaga used [3]. Lanosterol (a tetracyclic triterpene derivative), inotodiol (triterpene alcohol), and ergosterol have been reported to show antiblastoma activity [4]. Lectins (agglutinins) have also been detected in chaga. These are complex glycoproteins, which reversibly bind to carbohydrates and are involved in their transportation and deposition, thus producing a hypoglycemic effect in serum. They also play a role in glycoprotein regulation and immune system function, by stimulating the growth and multiplication of lymphocytes [4]. Mushroom polysaccharides have shown direct antitumor activity against various tumors and have been found to prevent oncogenesis and tumor metastasis, especially in synergism with chemotherapy, both in vitro and in vivo [1], [4], [7]–[9]. Polar extracts of chaga (aqueous and alcoholic) have been found to contain polyphenolic compounds which have shown good antioxidant activity [5]. A catechol containing polyphenol (3,4-dihydroxybenzolactone) has been reported to have antioxidant properties and has been shown to be effective in Parkinson’s disease by decreasing cellular oxidative stress [10]. Apart from these, chaga has also been found to contain polyphenolic pigments classified under the class melanins. These are high-molecular weight brown/black polymeric pigments formed by oxidative polymerization of phenols. Melanins are involved in radioprotection of animal cells by

deactivating the harmful free radicals produced on exposure to UV or other ionizing radiation. They are also involved in DNA repair, respiratory chain functioning and modulate cell metabolism [4]. Additionally, chaga contains several enzymes such as laccase, superoxide dismutase, glucose oxidase and peroxidase [6].

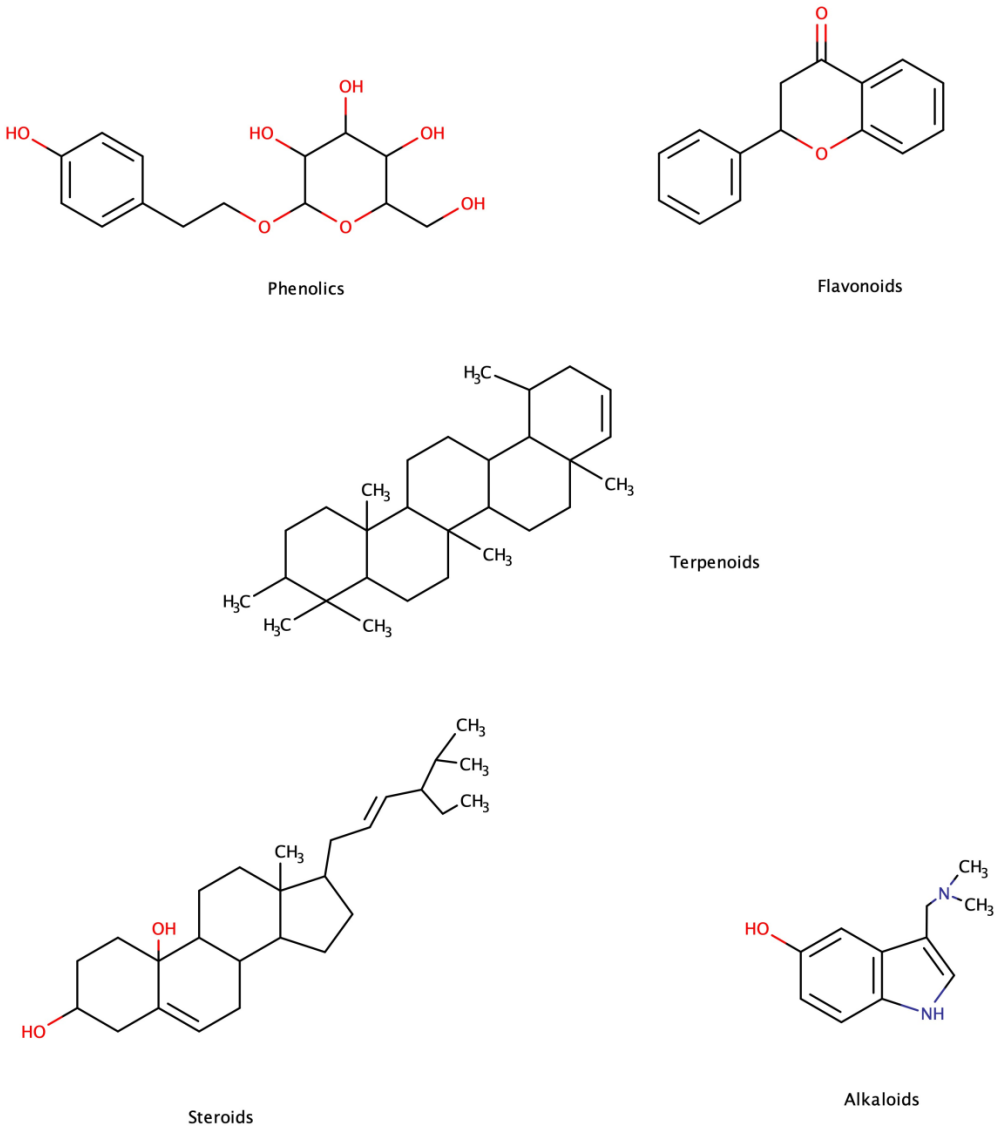

Figure 3: General categories of compounds present in chaga. Redrawn from [11]

Most of the biological activity of these compounds comes from their radical quenching ability (antioxidant activity) and their ability to diminish oxidative stress in cells. Reactive oxygen

species, such as superoxide anion and hydroxyl radicals cause severe pathological damage to the cell and are responsible for development of a number of chronic diseases. Superoxide anion combines with nitric oxide producing highly cytotoxic peroxynitrite anion. Hydroxyl radical can directly interact with unsaturated fatty acids of the cell membrane resulting in lipid peroxidation and cellular damage. Therefore, these radicals are involved in pathology of a number of diseases. Accordingly, naturally-occurring antioxidant compounds, including those present in various medicinal mushrooms should explored in treating stress-induced diseases, such as cancer and autoimmune and Parkinson's disease [4].

A look at the chaga-based products available in local farmers' markets and on various websites suggests that a lot of interest has recently been focused on commercialization of chaga as a dietary health supplement for the management of several chronic diseases. The scientific support to such claims is inconsistent, and currently used extraction procedures lack organization and uniformity across the literature. Current procedures vary in extraction solvents (aqueous and organic solvents of different polarity), temperature (from room temperature to 100 ºC), and the duration of extraction (from 30 minutes to two days) (Table 1).

Table 1: A brief summary of solvents used for extraction of chaga and corresponding extractive composition and activity

Abbreviations: EtOH: Ethanol, EtOAc: Ethyl acetate, MeOH: Methanol, PBS: Phosphate buffer saline, RT: Room temperature

Extraction Solvent	Product	Activity	Reference
Hot water (80 ºC, 2 hours) 70 % EtOH (70 ºC, overnight)	Oxalic acid, Phenolic acids (gallic acid, protocatechuic, *p*-hydroxybenzoic acid)	Antioxidant, antimicrobial and anti-quorum sensing	[12]
Chloroform (50 ºC, 7 days, percolation)	Lanostane-type triterpenoids (spiroinonotsuoxodiol, inonotsudiol, and inonotsuoxodiol)	Cytotoxic (antitumor)	[13]
Hot water (60 ºC, 4 hours, 3x)	Polysaccharides	Antioxidant	[14]
Hot water (100 ºC, 1 hour) MeOH (20%, 50%, 80%, RT, overnight)	Polyphenols	Antioxidant	[15]
Chloroform, EtOAc, acetone, EtOH, and distilled water (reflux,1.5 hours)	Phenolics, triterpenoids, polysaccharides	Antioxidant	[5]
Sequential: 95% EtOH (70 ºC, 3 hours), distilled water (80 ºC, 3 hours), precipitated with EtOH	Polysaccharides	Antioxidant	[16]
80-95% EtOH (80 ºC-RT, 2-24 hours, 2x)	Polysaccharides	Antioxidant	[17], [18]
80% MeOH (RT, two days, 2x)	Triterpenoids	Cytotoxic (antitumor)	[19]
Cyclohexane (RT, 90 minutes, 2x), EtOAc, (RT, 4 days), water (90 minutes), water (100 ºC, 15 minutes)	Betulin, betulinic acid, inotodiol	Cytotoxic (antitumor)	[20]
PBS (100 ºC), 80% and 95% EtOH, and 80% and 95% MeOH (RT)	Polyphenolics	Cytotoxic (antitumor) Antioxidant	[21]

1.2. Use of mushroom / plant extracts in green synthesis of nanoparticles: Nanoparticles are a wide class of materials which have at least one dimension that measures less than 100 nm [22]. Of all the different types of nanomaterials, silver and gold nanoparticles (AgNPs and AuNPs, respectively) have been prominently used in the biomedical field, for drug delivery in cancer therapy and in biosensensing applications [23]. The utility of nanoparticles stems from their nano-scale size, comparable to that of the cell receptors and other biomolecules such as DNA, enzymes and proteins (2-20 nm), facilitating binding and transportation of nanoparticles to these molecules and their transportation within the cell [24], [25]. AgNP-based products are an especially popular choice in antiseptic sprays and catheters due to the inherent broad-spectrum antimicrobial activity of silver. Apart from the biomedical field, AgNPs are also being explored in textiles and food storage containers [26].

The methods of synthesis of AgNPs can be divided into three categories: chemical methods (e.g. electrochemical precipitation, irradiation), physical methods (e.g. ball milling, vapor condensation) and biological methods (e.g. use of microbes, such as algae and bacteria to produce silver nanotubes). The chemical methods lead to the production of toxic waste, while physical methods have a very high energy demand [26]. In contrast, biological methods are environmentally friendly, and the generated byproducts are non-toxic. The use of mushroom / plant extracts for production of AgNPs also belongs into this category. This approach is additionally advantageous because it is cost-effective, easily scalable, and can produce large quantities of NPs in a relatively shorter time [27]. This is a 'bottom up' approach, where AgNPs are synthesized as the result of a redox reaction between reductive components in mushroom / plant extracts (secondary metabolites such as phenols, polysaccharides, alkaloids, terpenoids, and proteins; Figure 3) and silver ions (Ag^{+1}) in an aqueous solution (Figure 4) [11], [27], [28].

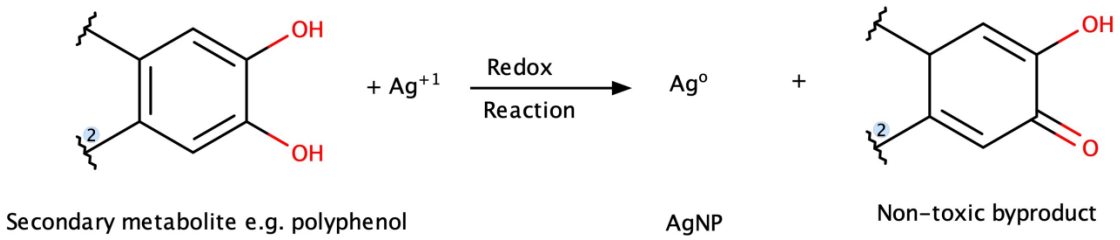

Figure 4: Schematic reaction during silver nanoparticle synthesis (AgNP). Redrawn from [11]

Initially, Ag^{+1} ions react with the reductants in the extract to form a silver atom. Colloidal AgNPs are yielded from the growth and agglomeration of silver atoms into oligomeric clusters. In the termination phase, the growth stops as specific shape and size are reached. This is generally accompanied by changes in the visible color of the solution [24]. Besides bringing about the reduction of Ag^{+1} ions, the mushroom / plant components may also remain associated with AgNPs as 'capping agents'. They surround the AgNPs as they are formed, and are responsible for stabilizing AgNPs in aqueous solutions, and for controlling their size and shape (Figure 5) [24], [27], [29]. Further, these compounds often possess bioactive properties themselves, and can exert a synergistic effect along with the AgNPs in health management [24].

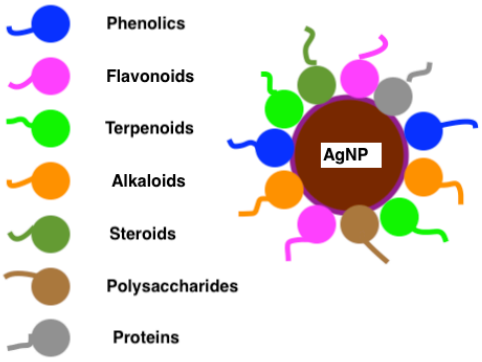

Figure 5: Conceptual drawing showing capping of silver nanoparticle by compounds in mushroom / plant extract. Redrawn from [11], [24].

AgNPs synthesized in this fashion have been extensively reviewed in the literature [11], [24], [27], [28], [30]. While a few mushrooms such as *Agaricus bisporus* [31]–[34], *Ganoderma lucidum* [31], [33], [35], *Pleurotus ostreatus* [33], [36], and *Lactarius piperatus* [37] are popular choices for synthesis of AgNPs, use of *Inonotus obliquus* (chaga) for this purpose has been largely unexplored [38].

Considering the wide variation in the methods employed for extraction of chaga, and the lack of studies on synthesis of chaga-AgNPs, our aim was to develop a systematic protocol for preparation of chaga extracts for their potential future commercialization. Towards this aim, different extraction solvents and methods were screened and the yields, antioxidant capacities, and free phenolic hydroxyl group contents of the resultant extracts were compared. Further, chaga extract was used to synthesize chaga-AgNPs which were further explored for their suitability for delivery through lignin-based hydrogel carriers (as synthesized in Chapter 3), with potential uses as an antioxidant and antimicrobial in food packaging, agriculture, and wood preservation. The production of high-value chemicals from non-lignocellulosic forest biomass can help forest-based biorefineries develop secondary streams of revenue and stay viable while increasing local employment and aiding in rural development.

2. Experimental Materials and Methods:

2.1. Chemicals and materials: Irregular chunks of 5-6 year old chaga harvested from birch trees (*Betula alleghaniensis*, Family: *Betulaceae*) in New York state forests were donated by Allegany Trails, Inc. The chunks were ground to #18 mesh particle size, and were vacuum dried (~40 ºC). This ground, moisture-free chaga was used in subsequent experiments. All chemicals were used as received without further purification (Table 2). Deionized (DI) water was used in all experiments.

Table 2: Chemicals used in this study

Chemical	Vendor
Citric acid	Fisher Scientific
Diethyl ether	PHARMCO-AAPER
2,2-diphenyl-1-picrylhydrazyl (DPPH)	Sigma-Aldrich
Dioxane	TCI
Ethanol	PHARMCO-AAPER
Ethyl acetate	PHARMCO-AAPER
Methanol	PHARMCO-AAPER
n-Pentane	PHARMCO-AAPER
Silver nitrate solution	Fisher Scientific
Sodium hydroxide	Macron Fine Chemicals
Trisodium citrate	Fisher Scientific

2.2. Extraction solvent screening: Solvents with different polarities were compared for their extraction efficiency on the extract yield, antioxidant activity (AOA; described below) and free phenolic hydroxyl group (PhOH; described below) content (Table 3). A common extraction method was used for uniformity and simplicity (ultrasound assisted bath sonicator extraction; described below). Yields from triplicate extractions were averaged.

Table 3: Solvents used for extraction of chaga

Solvent	Boiling Point (ºC)	Relative Polarity [46]
n-Pentane (C_5H_{12})	36.1	0.009
Ethyl acetate ($C_4H_6O_2$)	77	0.228
Methanol (CH_3OH)	64.6	0.762
Water (H_2O)	100	1.00

2.3. Extraction method screening: Common extraction techniques were compared for their extraction efficiency. Each is described in detail below. Water was used as a common extraction solvent for uniformity and simplicity. Yields from triplicate extractions were averaged.

Ultrasound-assisted extraction in a bath sonicator (UAE Bath): 2 g of chaga was mixed with 40 ml of solvent in a tightly stoppered Erlenmyer flask. The flask was suspended in a bath sonicator (40 kHz, Branson 3510 Ultrasonic Cleaner, Branson Ultrasonics Corp, CT, USA), completely immersed in the bath maintained at room temperature. The extraction was continued for a total of two hours. At midpoint of the extraction period, the solvent was replaced by equal volume of fresh solvent. The two solvent portions were combined, the solvent was evaporated, and the residue was vacuum dried. Yields from triplicate extractions were averaged.

Ultrasound-assisted extraction in a probe sonicator (UAE Probe): 2 g of chaga was mixed with 40 ml of DI water in an Erlenmyer flask. The sonicator probe was inserted into the flask (Q700, 6Al4V Titanium alloy probe, ¾" diameter, pulse duration: 30 seconds, duty cycle: 50%, QSonica, Newton, CT, USA). The temperature was maintained under 50 ºC by immersing the flask in an ice bath. At midpoint during the desired extraction period, the solvent was replaced by equal volume of fresh solvent. The two solvent portions were combined at the end, the solvent was evaporated, and the residue was vacuum dried. Yields from triplicate extractions were averaged.

To compare the effect of extraction intensity (total energy input during UAE) on the extraction yield, AOA, and PhOH, two separate extractions were carried out: one for 1 hour duration (total energy input: 152 kJ) and another for 2 hours (total energy input: 314 kJ).

Soxhlet extraction (T204 cm-07): 8 g of chaga was loosely packed in Whatman extraction thimbles placed in a Soxhlet apparatus, attached to an extraction flask containing 150 ml water and boiling chips. The solvent was allowed to percolate through chaga for a total of 8 hours. Yields from triplicate extractions were averaged.

Boiling under reflux: 8 g of chaga was added to a tightly stoppered round-bottom flask containing 150 ml DI water and boiling chips, fitted with a condenser. The solvent was refluxed for a total of two hours. Yields from triplicate extractions were averaged.

Hot-water extraction in a Parr reactor (HWE): 4 g of chaga was mixed with 200 ml water in the Parr reactor (300 ml 4560 Mini bench top reactor, Parr Instrument Company, Moline, IL, USA). To compare the effect of intensity of HWE on the yield and antioxidant activity, extractions were carried out at various temperatures and durations, expressed collectively as an integral referred to as 'P-factor' (Eqn. 1) [39]. The pressure reached during the extraction was approximately 6 atm. Yields from triplicate extractions were averaged.

$$\text{P-factor} = \int_0^t e^{\left(40.48 - \frac{15106}{T}\right)} dt \qquad (1)$$

where, T is the extraction temperature in Kelvin, and t is the extraction time in hours. Although this equation is defined for acid catalyzed hydrolysis of xylan, it provides a good measure of the combined effect of temperature and pressure, and hence has been used here for convenience and for the lack of a better alternative.

2.4. Free Phenolic Hydroxyl Group (PhOH) Content: Free phenolic hydroxyl group content of all samples was determined by the UV differentiation method [40]. About 10 mg of each sample were separately dissolved in 5 mL of dioxane and 5 mL 0.2 M NaOH. From each sample solution, 2 mL was further diluted to 25 mL using either a pH 6 citrate buffer solution, or a 0.2 M NaOH solution. The PhOH content was calculated from the differential UV-spectra of the 0.2 M sodium hydroxide solution recorded on a Genesis 10s UV-Vis spectrophotometer (Thermo Scientific, MA, USA) at 300 nm and 350 nm, against the pH 6 lignin solution as reference. Two measurements were taken for each sample, and the average value was calculated.

2.5. Estimation of antioxidant activity (AOA): Antioxidant activity was measured by determining the amount of sample needed to quench 50% of the DPPH free radicals present in the solution (DPPH•) [41]. 4 mL of 6 x 10^{-5} mol/L DPPH• in methanol was added to 4 ml of sample lignin solution made in methanol, at various lignin concentrations. The absorbance was immediately measured at 515 nm using a Genesys 10 Series Spectrophotometer at room temperature as the zero-time reading. The solutions were allowed to reach steady-state for 30 minutes in dark room. The decrease in the percentage of DPPH• in solution over various lignin concentrations was measured as the decrease in the absorbance at 515 nm, and was plotted as the function of lignin concentration. The resulting equation was utilized to determine the concentration of the antioxidant that would be required to quench 50% of the free radicals from DPPH•. This value was recorded as the 50% inhibitory concentration (IC_{50}) for each antioxidant. Lower IC_{50} indicates higher antioxidant activity. Five observations each were made for every sample to compute the IC_{50} value.

2.6. Synthesis of chaga-AgNPs: 1 ml of chaga hot-water extract (as extracted at 160 ºC, 2 hours) was mixed with 19 ml of 0.01 N aqueous solution of silver nitrate [38]. The solution was stirred continuously at room temperature for 80 minutes. The development of red / brown color was measured at 439 nm in a Genesys 10 Series Spectrophotometer. The absorbance was measured every 20 minutes, up to 80 minutes. Triplicate observations were made to confirm chaga-AgNPs formation.

2.7. Absorption and release of chaga-AgNPs using lignin-PEGDGE hydrogels: Approximately 50 mg of lignin-PEGDGE hydrogels along with commercial reference hydrogels (SM-PEGDGE, W-PEGDGE, WAH-PEGDGE, MS-PEGDGE, WS-PEGDGE, and KL-PEGDGE as synthesized in Chapter 3, along with TW and CG) were allowed to soak into 2 ml of chaga-AgNPs solution (~100 mg / ml) for 1 hour. The increase in the weight as the result of absorption of chaga-AgNPs solution by the hydrogels was noted. The chaga-AgNP enriched hydrogels were then dried in a vacuum oven (~40 ºC) for 24 hours. They were then resuspended in 6 ml deionized water for 1 hour with intermittent shaking and the release of chaga-AgNPs from the hydrogel matrix was observed by reading the solutions at 439 nm in the spectrometer. The percent amount of chaga-AgNPs released was calculated based on the initial absorbed amount. Duplicate measurements were made, and the average was calculated.

A schematic summary of all experiments is shown below (Figure 6).

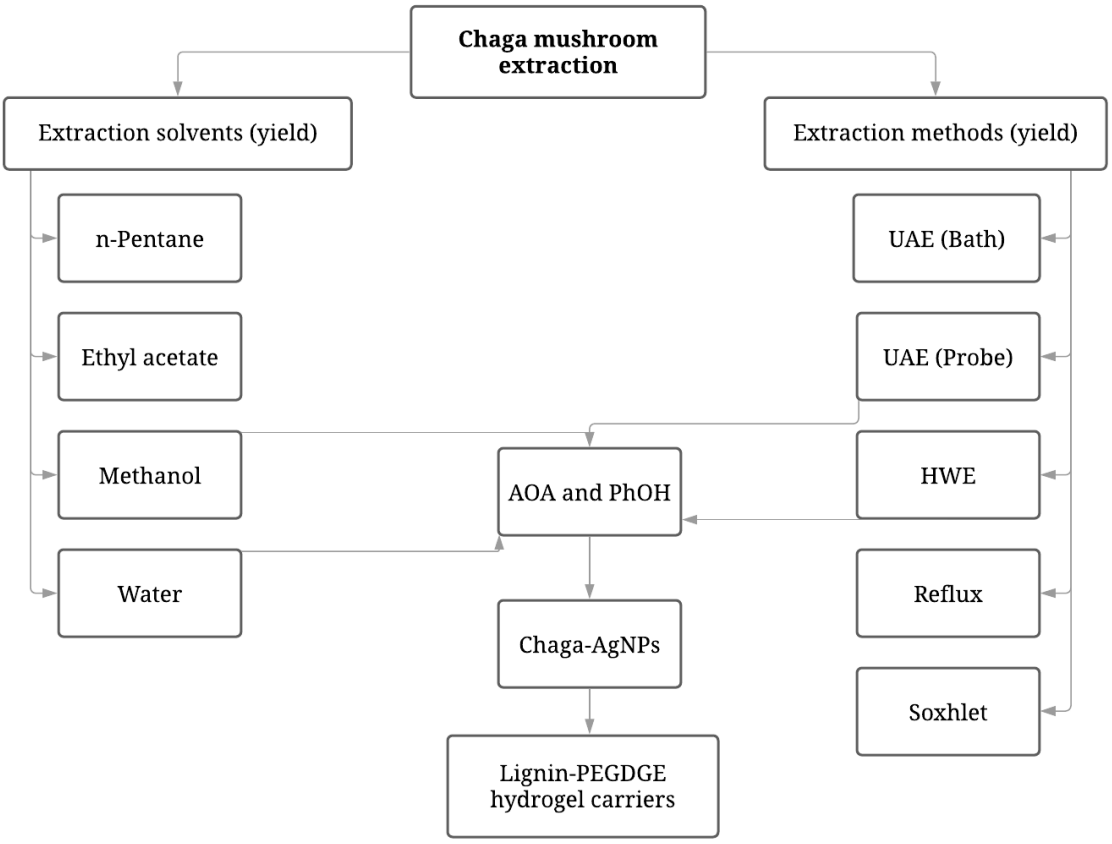

Figure 6: Scheme of experiments

AOA: antioxidant activity, chaga-AgNPs: chaga-silver nanoparticles, HWE: hot-water extraction, PEGDGE: poly(ethylene)glycol diglycidyl ether, UAE: ultrasound-assisted extraction

3. Results and Discussion:

3.1. Extraction solvent screening:

3.1.1. Effect of solvent on yield: The relatively non-polar solvents (n-pentane and ethyl acetate) were inefficient for extraction of chaga (yields $\leq$ 0.01% OD chaga). Between methanol and water, the yield increased with relative polarity (Figure 7). As expected, polar solvents such as methanol, ethanol and water have been documented to be more efficient for extraction of polar compounds such as polyphenols and flavonoids - which are thought to be the main contributors

to the antioxidant and antitumor effects of chaga, as well as some relatively less polar compounds such as inotodiol [5], [20], [21].

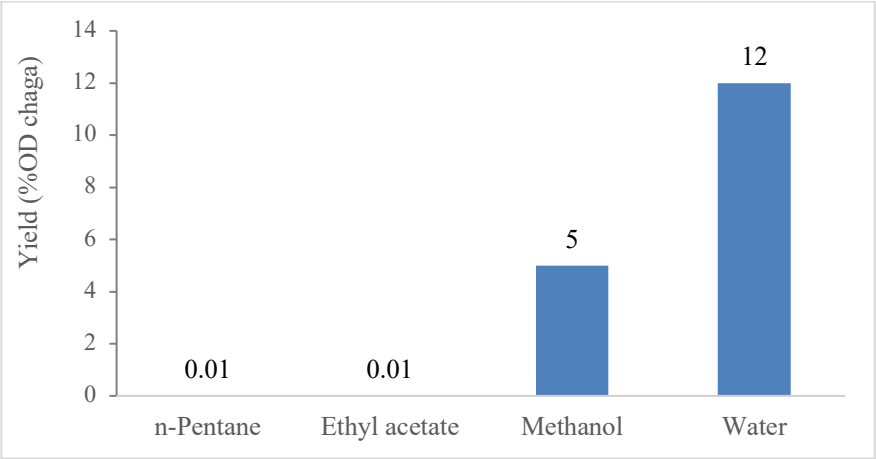

Figure 7: Extraction efficiency of solvents. Polarity increases from left to right

To further differentiate between the methanolic and aqueous extracts, the AOA and PhOH content of both the extracts were determined.

3.1.2. Effect of solvent on extract AOA and PHOH content: The AOAs of both the extracts was found to be comparable, with the aqueous extract showing very slightly superior AOA (IC_{50} 88 µg/ml), as compared to the methanolic extract (IC_{50} 106 µg/ml). This finding is in line with the reports where aqueous extracts of chaga were found to possess higher AOA as compared to the alcoholic extracts [20]. The aqueous extract also showed a higher PhOH content (0.42 mmol/g), as compared to the methanolic extract (0.19 mmol/g), even though the AOAs for the two extracts didn't show a large difference (Table 4). This finding seems to suggest that PhOH groups are not the only contributors to the AOA of chaga. Both extracts showed lower than, but good AOA when compared to that of ascorbic acid (vitamin C), which is a natural antioxidant.

Table 4: Comparison of AOA and PhOH content between aqueous and methanolic extracts of chaga

Extraction solvent	IC_{50} (µg/ml)	PhOH (mmol/g)
Water	88	0.42
Methanol	106	0.19
Ascorbic acid[a]	33	22
[a]: Vitamin C		
[b]: Theoretical value		

3.2. Extraction method screening:

3.2.1. Effect of extraction method on yield: Hot-water extraction (conditions: 160 ºC, 2 hours) was found to be significantly more efficient for extraction of chaga out of all techniques (Figure 8). This result underlines the efficacy of high temperature and pressure to penetrate the fungal cell walls and give relatively higher yields, as reported in the literature [42], [43]. Interestingly, the yield from boiling under reflux (operating at ~100 ºC) was slightly lower than that of UAE (probe, 2 hours, operating under 50 ºC), indicating that temperature was not the only factor that controlled the yield. The presence of high-energy ultrasound waves (total energy input 314 kJ) and replacement of the saturated solvent by the fresh solvent during UAE might have contributed to the higher yield. Additionally, during sonication, although the bulk temperature is controlled by the use of an ice bath, local microregions of intense temperature and pressure are created within the solution due to the cavitation phenomenon [44], [45]. This might also have contributed to the higher extraction yields. As expected, the yield from UAE (probe, 2 hours) was higher than that obtained from UAE (probe, 1 hour) and UAE (bath), due to the relatively lower intensities of the latter two.

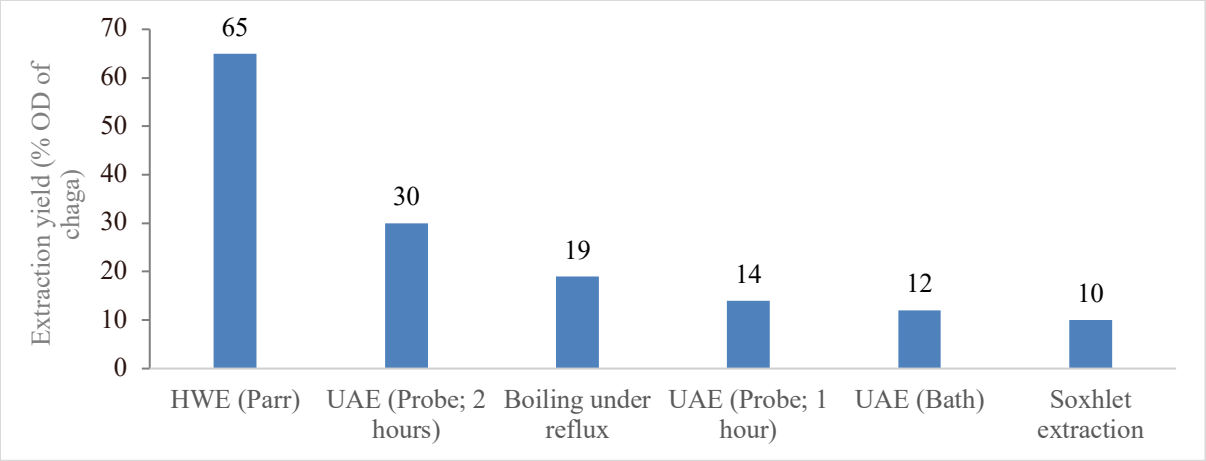

Figure 8: Extraction efficiency of different methods, with water as the common solvent

Similar to UAE (probe), to compare the effects of different intensities of HWE on yield, HWE was also carried out at different temperatures and duration, expressed as P-factor. The log plot of P-factor and chaga extract yield was found show a good correlation between the two (R^2 0.98, Figure 9), and can thus serve as a prediction tool for determining the expected yield based on the extraction conditions. At the same P-factor, chaga showed a much higher mass loss during HWE, as compared to the other lignocellulosic biomass, indicating that chaga biomass is less recalcitrant to HWE as compared to the lignocellulosic biomass (Figure 10). This difference in recalcitrance most likely arises from the differing chemical compositions of the fungal biomass and lignocellulosic biomass.

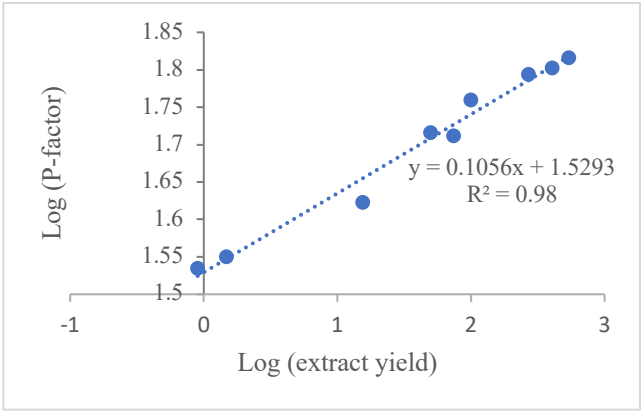

Figure 9: Correlation between P-factor during hot-water extraction and extraction yield

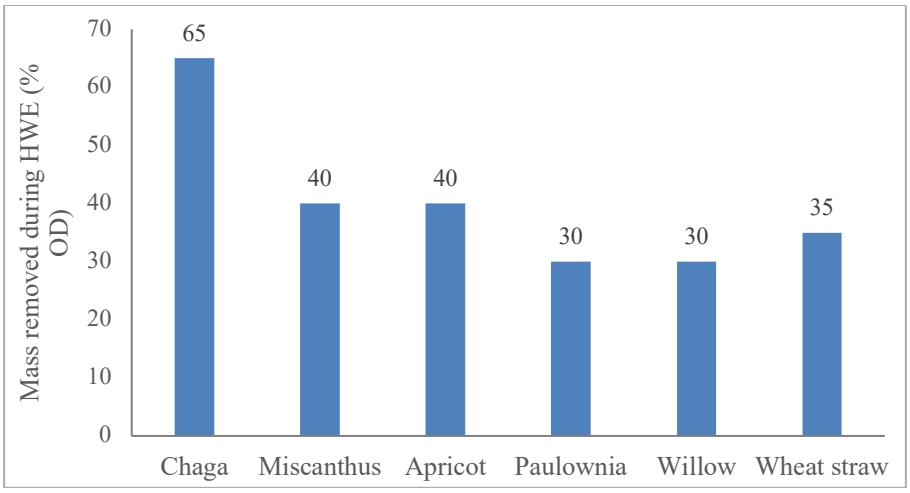

Figure 10: Mass loss from chaga versus lignocellulosic plants during hot-water extraction [48]-[50]

3.2.2. Effect of extraction method and intensity on AOA and PhOH content: A closer look was taken at the possible correlation between the extraction intensities, and the AOA and PhOH content of the resultant extracts for the top two extraction methods with the highest yields - HWE, and UAE (probe).

In the case of UAE (probe), the PhOH contents were found to remain almost unaffected (Table 5). For UAE (probe, 2 hours), the AOA slightly decreased (IC_{50} 104 µg/ml), as compared to UAE (probe 1 hour, IC_{50} 88 µg/ml).

Table 5: Effect of ultrasound extraction intensity on AOA and PhOH of aqueous extracts of chaga

UAE (probe) Duration	Total energy input	IC_{50} (µg/ml)	PhOH (mmol/g)
2 hours	314 kJ	104	0.49
1 hour	152 kJ	88	0.46

In the case of hot-water extraction, no correlation was found between the p-factor, AOA and PhOH content. The IC_{50} ranged between 9.5 µg/ml (P-factor 537) and 177 µg/ml (P-factor 0.9), while the PhOH content ranged between 1 mmol/g (p-factor 99) and 0.53 mmol/g (P-factor 1.5). The corresponding values for each P-factor are available in the Appendix (Table 6) for more

information. This further suggests that components other than PhOH are probably involved in mediation of AOA in chaga extracts.

3.3. Synthesis of chaga-AgNPs: A visual color change from colorless to an intense red / brown was observed almost immediately after the addition of silver nitrate solution into the chaga extract prepared by hot-water extraction at 160 ºC, for 2 hours. The UV absorbance at 439 nm increased for the first 40 minutes after the mixing, and then stabilized. This color change is attributed to a phenomenon called 'surface plasmon resonance', characteristic of metal nanoparticles. It arises due to the oscillation of their conduction electrons called 'localized surface plasmons' on excitation by electromagnetic radiation such as UV or visible light. The resultant color and absorption maxima depend on the size, shape and dielectric properties of the nanoparticle [46]. The development of red / brown color (with absorption maxima around 439 nm) is a typical feature of AgNPs [47]. This indicates that the antioxidant compounds present in chaga were able to reduce Ag^{+1} ions in the silver nitrate solution to produce chaga-AgNPs.

3.4. Absorption and release of chaga-AgNPs using lignin-PEGDGE hydrogels: The extent of absorption varied widely between the different hydrogels (Figure 11). The trend observed for the extent of absorption of chaga-AgNPs by the hydrogels (WS-PEGDGE > MS-PEGDGE > W-PEGDGE ≥ WAH-PEGDGE > SM-PEGDGE = KL-PEGDGE) showed some similarities and some differences in comparison to the trend seen in the free absorbency capacity measurements seen for the hydrogels as measured by the filtration method (WS-PEGDGE > MS-PEGDGE > SM-PEGDGE > WAH-PEGDGE ≥ W-PEGDGE = KL-PEGDGE; Chapter 3, Figure 26, red). The main similarities were the consistently higher free absorbency capacities and chaga-AgNPs absorption capacities of WS-PEGDGE and MS-PEGDGE among all lignin-based hydrogels, and

the commercial hydrogels TW and CG. The main difference was the incongruence between the free absorbency capacity and chaga-AgNPs absorption capacity of SM-PEGDGE. The different protocols used for these two measurements might be the contributing factors for these discrepancies.

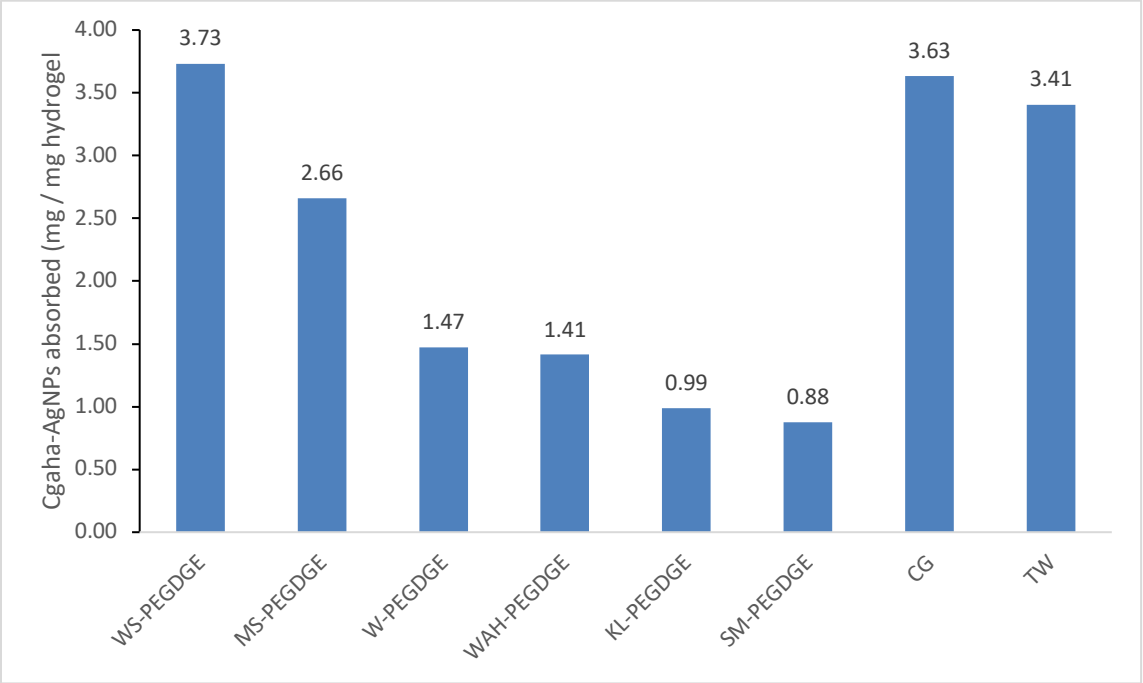

Figure 11: Amount of chaga-AgNPs absorbed by the hydrogels

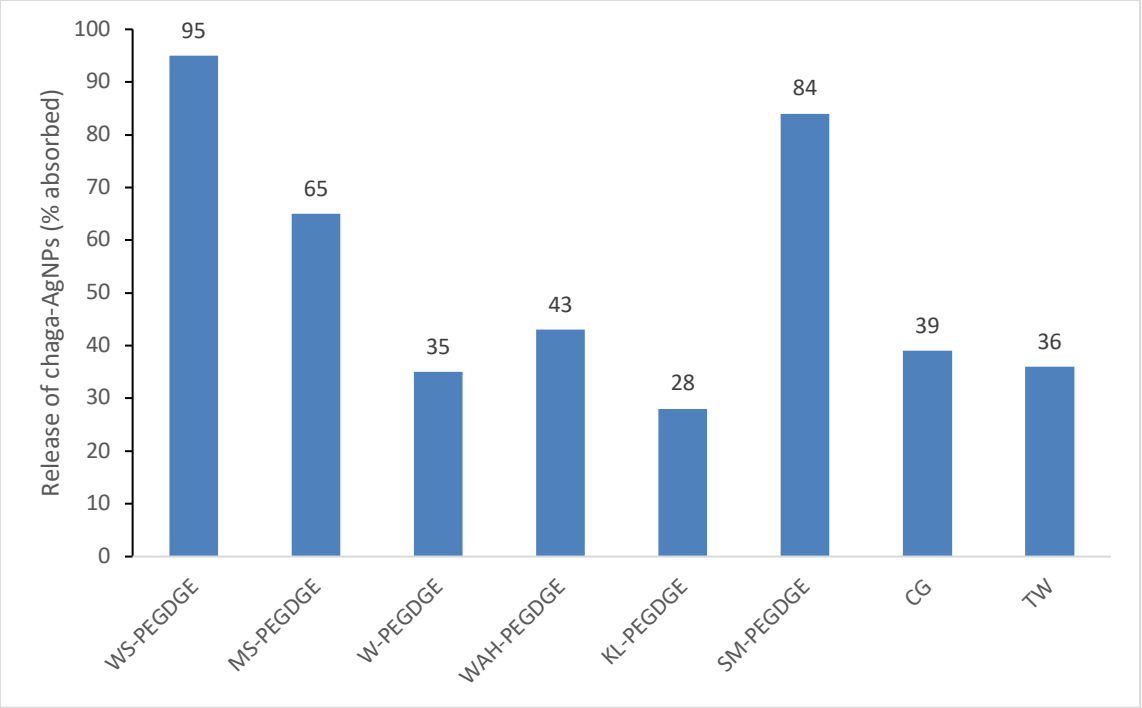

Figure 12: Release of chaga-AgNPs from hydrogels

Similar to the absorption, the release of chaga-AgNPs also varied widely between the hydrogels Figure 12). Generally, higher absorption of chaga-AgNPs was found to result in higher release, with the exception of SM-PEGDGE and the commercial hydrogels. Although SM-PEGDGE had absorbed the lowest amount of chaga-AgNPs (Figure 11), it was found to release a high amount (Figure 12). The opposite was true for the commercial hydrogels, CG and TW, which released only a small amount of chaga-AgNPs, despite absorbing high amounts. The differential interactions between the hydrogel matrix and chaga-AgNPs might have led to these discrepancies. Thus, WS-PEGDGE and MS-PEGDGE were found to be especially suitable carriers for chaga-AgNPs, due to their favorable absorption and release behaviors. KL-PEGDGE, W-PEGDGE, TW and CG were found to be unsuitable as carriers, due to their unfavorable interactions with chaga-AgNPs resulting in low release.

4. Conclusions: Common extraction solvents and methods were screened for their efficiency on chaga mushroom, in terms of extract yield, its antioxidant activity and free phenolic hydroxyl group content. Relatively polar solvents (water and methanol) were found to be good solvents, while hot-water extraction and ultrasound-assisted extraction using a probe sonicator were found to be good extraction methods. All extracts of chaga showed good antioxidant activity. The extraction yield increased with the extraction intensity, but did not correlate with higher antioxidant activity or free phenolic hydroxyl group content. These results suggested that the antioxidant activity of chaga extracts is probably mediated by a combination of phenolics and non-phenolics. Further, hot-water extracts of chaga (160 ºC, 2 hours) were found to be capable of reducing Ag^{+1} ions and participate in green synthesis of chaga-silver nanoparticles. Lignin-based hydrogels (specifically, wheat straw and miscanthus) were found to be good carriers for these nanoparticles. These results are a promising step toward commercial utilization of non-woody forest biomass for additional revenue.

Appendix:

Table 6: Observed AOA and PhOH content for hot-water extracts of chaga at different P-factors

HWE conditions	P-factor	IC_{50} (µg/ml)	PhOH (mmol/g)
100 ºC, 60 min	0.9	177	0.68
120 ºC, 120 min	15.417	25	0.57
140 ºC, 90 min	74.36	115.5	0.94
160 ºC, 60 min	268.6	18	0.77
100 ºC, 90 min	1.47	200	0.53
140 ºC, 60 min	49.58	16.6	0.65
140 ºC, 120 min	99.17	14	1
160 ºC, 120 min	537.17	9.5	0.75
160 ºC, 90 min	402.87	15	0.76

References:

[1] M. E. Balandaykin and I. V. Zmitrovich, "Review on Chaga Medicinal Mushroom, Inonotus obliquus (Higher Basidiomycetes): Realm of Medicinal Applications and Approaches on Estimating its Resource Potential," *Int. J. Med. Mushrooms*, vol. 17, no. 2, pp. 95–104, 2015, doi: 10.1615/intjmedmushrooms.v17.i2.10.

[2] M.-W. Lee, H. Hur, K.-C. Chang, T.-S. Lee, K.-H. Ka, and L. Jankovsky, "Introduction to Distribution and Ecology of Sterile Conks of Inonotus obliquus," *Mycobiology*, vol. 36, no. 4, pp. 199–202, Dec. 2008, doi: 10.4489/MYCO.2008.36.4.199.

[3] M. Ya. Shashkina, P. N. Shashkin, and A. V. Sergeev, "Chemical and medicobiological properties of chaga (review)," *Pharm. Chem. J.*, vol. 40, no. 10, pp. 560–568, Oct. 2006, doi: 10.1007/s11094-006-0194-4.

[4] S. Wasser, "Medicinal mushroom science: Current perspectives, advances, evidences, and challenges," *Biomed. J.*, vol. 37, no. 6, p. 345, 2014, doi: 10.4103/2319-4170.138318.

[5] W. Zheng *et al.*, "Analysis of antioxidant metabolites by solvent extraction from sclerotia of Inonotus obliquus (Chaga)," *Phytochem. Anal. PCA*, vol. 22, no. 2, pp. 95–102, Apr. 2011, doi: 10.1002/pca.1225.

[6] J. Staniszewska, M. Szymański, and E. Ignatowicz, "Antitumor and immunomodulatory activity of Inonotus obliquus," *Herba Pol.*, vol. 63, no. 2, pp. 48–58, Jun. 2017, doi: 10.1515/hepo-2017-0013.

[7] Y. Song *et al.*, "Identification of Inonotus obliquus and Analysis of Antioxidation and Antitumor Activities of Polysaccharides," *Curr. Microbiol.*, vol. 57, no. 5, pp. 454–462, Nov. 2008, doi: 10.1007/s00284-008-9233-6.

[8] M. Jayachandran, J. Xiao, and B. Xu, "A Critical Review on Health Promoting Benefits of Edible Mushrooms through Gut Microbiota," *Int. J. Mol. Sci.*, vol. 18, no. 9, Sep. 2017, doi: 10.3390/ijms18091934.

[9] T. Mizuno *et al.*, "Antitumor and Hypoglycemic Activities of Polysaccharides from the Sclerotia and Mycelia of *Inonotus obliquus* (Pers.: Fr.) Pil. (Aphyllophoromycetideae)," *Int. J. Med. Mushrooms*, vol. 1, no. 4, 1999, doi: 10.1615/IntJMedMushr.v1.i4.20.

[10] K. Gunjima *et al.*, "3,4-dihydroxybenzalacetone protects against Parkinson's disease-related neurotoxin 6-OHDA through Akt/Nrf2/glutathione pathway," *J. Cell. Biochem.*, vol. 115, no. 1, pp. 151–160, Jan. 2014, doi: 10.1002/jcb.24643.

[11] M. Nasrollahzadeh, S. M.-G. Yek, N. Motahharifar, and M. G. Gorab, "Recent Developments in the Plant-Mediated Green Synthesis of Ag-Based Nanoparticles for Environmental and Catalytic Applications," *Chem. Rec.*, vol. 19, no. 12, pp. 2436–2479, 2019, doi: 10.1002/tcr.201800202.

[12] J. Glamočlija *et al.*, "Chemical characterization and biological activity of Chaga (Inonotus obliquus), a medicinal 'mushroom,'" *J. Ethnopharmacol.*, vol. 162, pp. 323–332, Mar. 2015, doi: 10.1016/j.jep.2014.12.069.

[13] N. Handa, T. Yamada, and R. Tanaka, "An unusual lanostane-type triterpenoid, spiroinonotsuoxodiol, and other triterpenoids from Inonotus obliquus," *Phytochemistry*, vol. 71, no. 14, pp. 1774–1779, Oct. 2010, doi: 10.1016/j.phytochem.2010.07.005.

[14] H. Mu, A. Zhang, W. Zhang, G. Cui, S. Wang, and J. Duan, "Antioxidative Properties of Crude Polysaccharides from Inonotus obliquus," *Int. J. Mol. Sci.*, vol. 13, no. 7, Art. no. 7, Jul. 2012, doi: 10.3390/ijms13079194.

[15] Y. Nakajima, Y. Sato, and T. Konishi, "Antioxidant Small Phenolic Ingredients in *Inonotus obliquus* (persoon) Pilat (Chaga)," *Chem. Pharm. Bull. (Tokyo)*, vol. 55, no. 8, pp. 1222–1226, 2007, doi: 10.1248/cpb.55.1222.

[16] S. Huang, S. Ding, and L. Fan, "Antioxidant activities of five polysaccharides from Inonotus obliquus," *Int. J. Biol. Macromol.*, vol. 50, no. 5, pp. 1183–1187, Jun. 2012, doi: 10.1016/j.ijbiomac.2012.03.019.

[17] X. Du, H. Mu, S. Zhou, Y. Zhang, and X. Zhu, "Chemical analysis and antioxidant activity of polysaccharides extracted from Inonotus obliquus sclerotia," *Int. J. Biol. Macromol.*, vol. 62, pp. 691–696, Nov. 2013, doi: 10.1016/j.ijbiomac.2013.10.016.

[18] L. Ma, H. Chen, Y. Zhang, N. Zhang, and L. Fu, "Chemical modification and antioxidant activities of polysaccharide from mushroom Inonotus obliquus," *Carbohydr. Polym.*, vol. 89, no. 2, pp. 371–378, Jun. 2012, doi: 10.1016/j.carbpol.2012.03.016.

[19] J. Baek *et al.*, "Bioactivity-based analysis and chemical characterization of cytotoxic constituents from Chaga mushroom (Inonotus obliquus) that induce apoptosis in human lung adenocarcinoma cells," *J. Ethnopharmacol.*, vol. 224, pp. 63–75, Oct. 2018, doi: 10.1016/j.jep.2018.05.025.

[20] A. Géry *et al.*, "Chaga (Inonotus obliquus), a Future Potential Medicinal Fungus in Oncology? A Chemical Study and a Comparison of the Cytotoxicity Against Human Lung Adenocarcinoma Cells (A549) and Human Bronchial Epithelial Cells (BEAS-2B)," *Integr. Cancer Ther.*, vol. 17, no. 3, pp. 832–843, 2018, doi: 10.1177/1534735418757912.

[21] K. A. Szychowski, K. Rybczyńska-Tkaczyk, J. Tobiasz, V. Yelnytska-Stawasz, T. Pomianek, and J. Gmiński, "Biological and anticancer properties of Inonotus obliquus extracts," *Process Biochem.*, vol. 73, pp. 180–187, Oct. 2018, doi: 10.1016/j.procbio.2018.07.015.
[22] I. Khan, K. Saeed, and I. Khan, "Nanoparticles: Properties, applications and toxicities," *Arab. J. Chem.*, vol. 12, no. 7, pp. 908–931, Nov. 2019, doi: 10.1016/j.arabjc.2017.05.011.
[23] A. P. Nikalje, "Nanotechnology and its Applications in Medicine," *Med. Chem.*, vol. 5, no. 2, 2015, doi: 10.4172/2161-0444.1000247.
[24] M. Bordoloi, R. K. Sahoo, K. J. Tamuli, S. Saikia, and P. P. Dutta, "Plant Extracts Promoted Preparation of Silver and Gold Nanoparticles: A Systematic Review," *Nano*, vol. 15, no. 02, p. 2030001, Dec. 2019, doi: 10.1142/S1793292020300017.
[25] E. Katz and I. Willner, "Integrated Nanoparticle–Biomolecule Hybrid Systems: Synthesis, Properties, and Applications," *Angew. Chem. Int. Ed.*, vol. 43, no. 45, pp. 6042–6108, 2004, doi: 10.1002/anie.200400651.
[26] L. Wei, J. Lu, H. Xu, A. Patel, Z.-S. Chen, and G. Chen, "Silver nanoparticles: synthesis, properties, and therapeutic applications," *Drug Discov. Today*, vol. 20, no. 5, pp. 595–601, May 2015, doi: 10.1016/j.drudis.2014.11.014.
[27] S. Ahmed, M. Ahmad, B. L. Swami, and S. Ikram, "A review on plants extract mediated synthesis of silver nanoparticles for antimicrobial applications: A green expertise," *J. Adv. Res.*, vol. 7, no. 1, pp. 17–28, Jan. 2016, doi: 10.1016/j.jare.2015.02.007.
[28] P. Kuppusamy, M. M. Yusoff, G. P. Maniam, and N. Govindan, "Biosynthesis of metallic nanoparticles using plant derivatives and their new avenues in pharmacological applications – An updated report," *Saudi Pharm. J.*, vol. 24, no. 4, pp. 473–484, Jul. 2016, doi: 10.1016/j.jsps.2014.11.013.
[29] S. P. Chandran, M. Chaudhary, R. Pasricha, A. Ahmad, and M. Sastry, "Synthesis of gold nanotriangles and silver nanoparticles using Aloe vera plant extract," *Biotechnol. Prog.*, vol. 22, no. 2, pp. 577–583, Apr. 2006, doi: 10.1021/bp0501423.
[30] N. Prabhu, S. Karunakaran, S. Karthika Devi, R. Ravya, P. Subhashree, and S. M. Vadivu, "Biogenic synthesis of myconanoparticles from mushroom extracts and its medical applications: A review," *Int. J. Pharm. Sci. Res.*, May 2019, Accessed: Jul. 20, 2020. [Online]. Available: https://ijpsr.com/bft-article/biogenic-synthesis-of-myconanoparticles-from-mushroom-extracts-and-its-medical-applications-a-review/?view=fulltext.
[31] M. Sriramulu and S. Sumathi, "Photocatalytic, antioxidant, antibacterial and anti-inflammatory activity of silver nanoparticles synthesised using forest and edible mushroom," *Adv. Nat. Sci. Nanosci. Nanotechnol.*, vol. 8, no. 4, p. 045012, Oct. 2017, doi: 10.1088/2043-6254/aa92b5.
[32] T. Sudhakar, A. Nanda, S. G. Babu, S. Janani, M. D. Evans, and T. K. Markose, "Synthesis of Silver Nanoparticles from Edible Mushroom and Its Antimicrobial Activity against Human Pathogens," p. 6.
[33] S. Mirunalini, V. Arulmozhi, K. Deepalakshmi, and M. Krishnaveni, "Intracellular Biosynthesis and Antibacterial Activity of Silver Nanoparticles Using Edible Mushrooms," *Not. Sci. Biol.*, vol. 4, no. 4, Art. no. 4, Nov. 2012, doi: 10.15835/nsb448051.
[34] D. Dhanasekaran, S. Latha, S. Saha, N. Thajuddin, and A. Panneerselvam, "Extracellular biosynthesis, characterisation and in-vitro antibacterial potential of silver nanoparticles using Agaricus bisporus," *J. Exp. Nanosci.*, vol. 8, no. 4, pp. 579–588, May 2013, doi: 10.1080/17458080.2011.577099.
[35] M. Poudel, R. Pokharel, S. K.c, S. C. Awal, and R. Pradhananga, "Biosynthesis of Silver Nanoparticles Using Ganoderma Lucidum and Assessment of Antioxidant and Antibacterial Activity," *Int. J. Appl. Sci. Biotechnol.*, vol. 5, no. 4, Art. no. 4, Dec. 2017, doi: 10.3126/ijasbt.v5i4.18776.
[36] R. Al-Bahrani, J. Raman, H. Lakshmanan, A. A. Hassan, and V. Sabaratnam, "Green synthesis of silver nanoparticles using tree oyster mushroom Pleurotus ostreatus and its inhibitory activity against pathogenic bacteria," *Mater. Lett.*, vol. 186, pp. 21–25, Jan. 2017, doi: 10.1016/j.matlet.2016.09.069.
[37] E. Vamanu, M. Ene, B. Biță, C. Ionescu, L. Crăciun, and I. Sârbu, "In Vitro Human Microbiota Response to Exposure to Silver Nanoparticles Biosynthesized with Mushroom Extract," *Nutrients*, vol. 10, no. 5, Art. no. 5, May 2018, doi: 10.3390/nu10050607.
[38] P. C. Nagajyothi, T. V. M. Sreekanth, J. Lee, and K. D. Lee, "Mycosynthesis: Antibacterial, antioxidant and antiproliferative activities of silver nanoparticles synthesized from Inonotus obliquus (Chaga mushroom) extract," *J. Photochem. Photobiol. B*, vol. 130, pp. 299–304, Jan. 2014, doi: 10.1016/j.jphotobiol.2013.11.022.
[39] M. Leschinsky, H. Sixta, and R. Patt, "DETAILED MASS BALANCES OF THE AUTOHYDROLYSIS OF EUCALYPTUS GLOBULUS AT 170°C," *BioResources*, vol. 4, no. 2, Art. no. 2, Apr. 2009.

[40] A. Gärtner, G. Gellerstedt, and T. Tamminen, “Determination of phenolic hydroxyl groups in residual lignin using a modified UV-method,” *Nord. Pulp Pap. Res. J.*, vol. 14, no. 2, pp. 163–170, May 1999, doi: 10.3183/npprj-1999-14-02-p163-170.

[41] J. M. Berger, R. J. Rana, H. Javeed, I. Javeed, and S. L. Schulien, “Radical Quenching of 1,1-Diphenyl-2-picrylhydrazyl: A Spectrometric Determination of Antioxidant Behavior,” *J. Chem. Educ.*, vol. 85, no. 3, p. 408, Mar. 2008, doi: 10.1021/ed085p408.

[42] H. K. Ju, H. W. Chung, S.-S. Hong, J. H. Park, J. Lee, and S. W. Kwon, “Effect of steam treatment on soluble phenolic content and antioxidant activity of the Chaga mushroom (Inonotus obliquus),” *Food Chem.*, vol. 119, no. 2, pp. 619–625, Mar. 2010, doi: 10.1016/j.foodchem.2009.07.006.

[43] A. Y. Hwang, S. C. Yang, J. Kim, T. Lim, H. Cho, and K. T. Hwang, “Effects of non-traditional extraction methods on extracting bioactive compounds from chaga mushroom (Inonotus obliquus) compared with hot water extraction,” *LWT*, vol. 110, pp. 80–84, Aug. 2019, doi: 10.1016/j.lwt.2019.04.073.

[44] R. J. Wood, J. Lee, and M. J. Bussemaker, “A parametric review of sonochemistry: Control and augmentation of sonochemical activity in aqueous solutions,” *Ultrason. Sonochem.*, vol. 38, pp. 351–370, Sep. 2017, doi: 10.1016/j.ultsonch.2017.03.030.

[45] S. V. Sancheti and P. R. Gogate, “A review of engineering aspects of intensification of chemical synthesis using ultrasound,” *Ultrason. Sonochem.*, vol. 36, pp. 527–543, May 2017, doi: 10.1016/j.ultsonch.2016.08.009.

[46] T. R. Jensen, M. D. Malinsky, C. L. Haynes, and R. P. Van Duyne, “Nanosphere Lithography: Tunable Localized Surface Plasmon Resonance Spectra of Silver Nanoparticles,” *J. Phys. Chem. B*, vol. 104, no. 45, pp. 10549–10556, Nov. 2000, doi: 10.1021/jp002435e.

[47] T. Premkumar, Y. Lee, and K. E. Geckeler, “Macrocycles as a Tool: A Facile and One-Pot Synthesis of Silver Nanoparticles Using Cucurbituril Designed for Cancer Therapeutics,” *Chem. – Eur. J.*, vol. 16, no. 38, pp. 11563–11566, Oct. 2010, doi: 10.1002/chem.201001325.

[48] C. Gong, and B. Bujanovic, “Impact of Hot-Water Extraction on Acetone-Water Oxygen Delignification of Paulownia Spp. and Lignin Recovery,” *Energies*, vol. 7, pp. 857-873, 2014, doi: 10.3390/en7020857.

[49] K. Wang, C. Jing, C. Wood, A. Nagardeolekar, N. Kohan, P. Dongre, T. Amidon, and B. Bujanovic, “Toward Complete Utilization of Miscanthus in a Hot-Water Extraction-Based Biorefinery,” *Energies*, vol 11, no. 39, pp.1-39, 2018, doi: 10.3390/en11010039.

[50]. D. Corbett, N. Kohan, G. Machado, C. Jing, A. Nagardeolekar, and B. Bujanovic, “Chemical Composition of Apricot Pit Shells and Effect of Hot-Water Extraction,” *Energies*, vol 8, pp. 9640-9654, 2015, doi: 10.3390/en8099640.

Chapter V

Conclusions and Future Work

This work attempted to assess the suitability of the lignocellulosic (angiosperms: sugar maple (SM), willow (W), miscanthus (MS), wheat straw (WS), and a mixture of northern and southern hardwoods and grass (MA)) and non-lignocellulosic (chaga mushroom) forest products for the production of high-value materials, as a means of creating secondary revenue streams for a modern biorefinery. The lignins recovered from hot-water extracts of the angiosperms (RecLs – SM, W, MS, WS, and MA, respectively) were characterized. In order to generate two separate fractions with distinct composition and physicochemical properties from the RecLs, they were further treated by alkali-purification and organic solvent-fractionation to generate AHs (SMAH, WAH, MSAH, WSAH, MAAH) and FRs (SMFR, WFR, MSFR, WSFR, and MAFR), respectively. The recovered lignins were used in synthesis of lignin-acrylamide-kaolin and lignin-poly(ethyleneglycol) diglycidyl ether (lignin-PEGDGE) gels, with intended applications as sorbents in wastewater, agriculture and air-freshener fields. These experiments contribute to the growing research on lignin-based gels, showing the applicability of biorefinery lignins for this use. The effect of alkali-purification and solvent-fractionation on the formation and sorption behavior of the lignin-based gels was studied. Additionally, the lignin-PEGDGE gels were explored as carriers for commercial fragrances and for bioactive chaga-silver nanoparticles. The chaga-silver nanoparticles (chaga-AgNPs) were prepared by the bottom up green synthesis approach where chaga extracts were used as bioreductants of silver ions. Suitable extraction solvent and extraction method for chaga were selected through systematic screening based on the extract yield, and the antioxidant activity of the extracts.

Specific conclusions and observations are summarized below, along with the recommended future work.

Conclusions:

1. The lignins recovered from hot-water extracts of angiosperms showed variable lignin contents (SM and W being slightly higher than MS, WS and MA), PhOH content, thermal characteristics, acetyl bromide extinction coefficients. They also showed variable antioxidant activities, but were all found to be superior to the commercial standard. All lignins showed a low ash content, and significant contamination with carbohydrates (xylans). Treatment of recovered lignins using alkali-purification and solvent-fractionation produced two distinct fractions with different physicochemical properties, for utilization in polymeric applications of lignin.
2. Alkali-purification most likely resulted in cleavage of some LCC linkages to generate a lignin-rich fraction. In comparison to RecLs, the alkali-purified lignins had a lower carbohydrate content, slightly higher free phenolic hydroxyl (PhOH) group content, similar extent of condensation (S/G ratio), and similar thermostability.
3. Solvent-fractionation resulted in differential partitioning of lignin fragments into organic solvents, leaving behind a carbohydrate-rich fraction containing a few very large, insoluble fragments of lignin predominantly associated with carbohydrates (xylans). In comparison to RecLs, the solvent-insoluble fractions had lower lignin content, higher PhOH group content, more condensed character as observed by FT-IR analysis, and partially higher thermostability.
4. SM and W were found suitable for the production of lignin-acrylamide-kaolin gels, where lignin was used as a partial replacement of acrylamide in the formulation (maximum

possible lignin content in formulation: 10.7% w/w). On the other hand, MS, WS, and MA were unable to form this type of gel. This was attributed to the hindrance in gelation by the radical quenching abilities of atypical small molecular weight aromatic residues (*p*-hydroxycinnamates, such as ferulates and coumarates) possibly present in these lignins.

5. All lignins were found suitable for the production of lignin-PEGDGE gels (maximum possible lignin content in formulation: 66.7% w/w).
6. Lignin-acrylamide-kaolin gels were found suitable for adsorption-based applications. The adsorption of methyl violet dye from an aqueous solution followed second order kinetics. Inclusion of lignin in the formulation was found to enhance the adsorption characteristics of the gels as compared to the blank formulation, with biorefinery lignins (SM and W) being more beneficial than technical lignin (Kraft, K). The opposite behavior was seen with the mechanical properties, where the formulations containing SM and W had lower compression moduli than the formulation containing K and the blank formulation. It was concluded that the probable increase in the porosity of the lignin-containing gels was the reason behind both of these observations.
7. In addition to the dye, the W-acrylamide-kaolin gel was also observed to be capable of accumulating silver cations from an aqueous solution.
8. The gels were found to be effective even during repeat use, although the adsorption behavior differed from first use.
9. The lignin-PEGDGE gels were found suitable for absorption-based applications. The free absorbency capacities of formulations containing biorefinery lignins (SM, W, MS, WS, and MA) were found to be statistically equivalent to that of technical lignin (K), but significantly lower than those of commercial formulations made from completely synthetic

materials. The mechanical properties of the gels showed significant variation, and no association was observed between the free absorbency capacity and the compression moduli.

10. W-PEGDGE gel was found to be a good matrix for absorption and sustained release of commonly used industrial fragrances (non-aqueous solutions), with release profile similar to the industrially accepted materials for fragrance emanation. The commercial gels were not able to adapt themselves for this purpose.
11. Higher lignin content of alkali-purified lignin, WAH, was found to be detrimental for the lignin-acrylamide-kaolin type of gel, resulting in failure to undergo acceptable gelation, possibly because of the higher hydrophobicity and hindered dispersion of WAH in the aqueous reaction medium. On the other hand, it was found to be beneficial for the lignin-PEGDGE type of gel, resulting in a higher compression modulus of the WAH-PEGDGE gel.
12. Higher carbohydrate content of solvent-insoluble fraction, WFR, was found to be beneficial for the lignin-acrylamide-kaolin type of gel, resulting in enhanced adsorption kinetics and mechanical properties of the WFR-acrylamide-kaolin gel, probably due to the higher PhOH content and hydrophilicity of WFR, leading to its better dispersion in the solution during synthesis. It was found to slightly decrease the free absorbency capacity of the WFR-PEGDGE gel to a statistically insignificant extent.
13. Water and methanol were found to be good solvents for extraction of chaga in terms of yield and antioxidant activity, while hot-water extraction for 2 hours, and at 160 ºC was found to be a good extraction method, followed by ultrasound-assisted extraction in a probe sonicator for 2 hours, at 50% duty cycle.

14. The antioxidant activity of chaga extracts is an indicator of their bioactive properties, and the presence of PhOH groups is an indicator of their polyphenolic composition. However, no correlation was apparent between the antioxidant activity and the PhOH group content of the extracts. This indicates that the antioxidant activity of the extracts is mediated not only by the compounds possessing phenolic hydroxyl groups, but also by other compounds (e.g. oxalic acid or polysaccharides). All chaga extracts tested showed good antioxidant activities, on the same order as ascorbic acid (vitamin C), a natural antioxidant.
15. Hot-water extract of chaga (160 ºC, 2 hours, P-factor 537, highest antioxidant activity of all extracts tested), was able to participate in bioreduction of silver ions to produce chaga-AgNPs.
16. Out of all the lignin-PEGDGE gels tested, WS-PEGDGE and MS-PEGDGE gels were found to be good carriers for chaga-AgNPs, with satisfactory absorption and release behavior. W-PEGDGE, KL-PEGDGE and the commercial gels were found to be poor carriers.

Future work:

1. Recovery and compositional analysis of soluble fractions of RecLs during alkali-purification and solvent-fractionation by further solvent extraction, GC/MS and HSQC, and further characterization such as determination of S/G ratio, PhOH and aliphatic OH group content, antioxidant activities is essential to fine tune these methods for selective fractionation of lignins, depending on the intended application.
2. Measurement of effective surface area of both types of gels (lignin-acrylamide-kaolin and lignin-PEGDGE) using mercury porosimetry or the BET adsorption method would be helpful in understanding the variation between the sorption behavior of formulations

containing different lignins, and the association between porosity and sorption characteristics in more detail.

3. The reusability behavior of lignin-acrylamide-kaolin gels could be understood better by studying the desorption kinetics, and the regenerative capacity of the gels. Further, a comparative FT-IR analysis of the gels before and after adsorption, and after regeneration could shed more light on the adsorption mechanism.
4. A study of the effect of temperature on the adsorption behavior of lignin-acrylamide-kaolin gels and development of an adsorption isotherm is recommended.
5. It would be beneficial to study the sorption behavior of both types of gels in alcoholic and other common non-aqueous media.
6. It would also be helpful to explore applicability of the gels in biomedical field, as tissue scaffolds, and topical drug release matrices where the higher carbohydrate content of the solvent-insoluble fractions might be beneficial for biocompatibility.
7. Investigation of the release kinetics of chaga-AgNPs from the lignin-PEGDGE gels is recommended to better understand the differential suitability of these gels as carriers.
8. Compositional analysis of the methanolic and aqueous extracts of chaga using techniques such as further solvent partitioning, GC/MS and HPLC would provide a clearer picture of the nature of the extracts.
9. Quantitative assays to measure the bioactive and therapeutic effects of chaga extracts, and chaga-AgNPs by methods such as the MTT assay for cytotoxicity and calculation of minimum inhibitory concentration (MIC) for antimicrobial activity are recommended.

10. The capping ability of chaga extracts can be elucidated by TEM characterization or dynamic light scattering, to determine the shape and the size of the chaga-AgNPs formed at various dilutions of chaga extract.

Aditi Nagardeolekar, PhD

Researcher in Bioprocess Engineering, Syracuse, NY.

Email: anagarde@syr.edu, Phone: (267) 538-8448, Campus Address: 418 Walters Hall, SUNY-ESF.

Professional Preparation

SUNY-ESF, Syracuse, NY	Bioprocess Engineering	PhD, August 2020
Institute of Chemical Technology, India	Bioprocess Technology	MS, June 2012
Mumbai University, India	Pharmacy	BS, June 2010

Research interests:

- Valorization of lignocellulosic biomass and lignin through synthesis of novel lignin-based products, such as lignin-based hydrogels, and through enzymatic hydrolysis of biomass
- Expression and purification of biomolecules / biopharmaceuticals
- Data analysis

Relevant research experience:

- Enzyme expression, isolation, purification and assay techniques: bench-scale shake flasks, DNA transformation, cell harvest, affinity column chromatography
- Enzymatic hydrolysis of lignocellulosic biomass for production of glucose and xylose
- Quantitative and qualitative analysis of lignin / biomolecules: gel electrophoresis, HPLC, GPC, NMR, UV Spectrometry, FT-IR spectrometry, titrimetry, TGA, SEM

Supplementary skills:

- R
- Six Sigma Yellow Belt
- MS Office

Relevant coursework and lab work: Lignocellulosic chemistry, microbiology, biochemistry, biotechnology, bioanalytical techniques, pharmaceutics, organic chemistry, physical chemistry, bioreactor designing, bioseparations, data analysis and experimental design.

Appointments:

Joachim Fellow in the Chemical Engineering Department; SUNY-ESF; **Summer 2017-Summer 2020.** Designed and executed the curriculum for an undergraduate/graduate level class (Professional Engineering Skills), arranged and facilitated guest seminars and company visits to the department.

Trainee at Ichor Therapeutics; **Summer 2017**. Expressed, isolated and purified enzyme using recombinant DNA technology.

Research Project Assistant for SyracuseCoE (RF grant # 77109-1137347-1, PI: Dr. Bujanovic); **Spring 2017.** Purified and characterized lignins extracted from hot-water extracts of angiosperms, conducted enzymatic hydrolysis of lignocellulosic biomass. Provided research training to undergraduate students.

Teaching Assistant in the PBE Department at SUNY-ESF; **Fall 2013-Fall 2016**. Graded home works and exams, supervised laboratory sessions and provided additional teaching support.

Graduate Assistant for ESF-Outreach for the STEM mentoring program in collaboration with Syracuse City School District; **Spring 2015 and Fall 2014**. Introduced kindergarten and fourth grade students at Van Duyn Elementary School to various science-related topics through weekly lessons and demonstrations.

Intern at Milan Laboratories, Navi Mumbai, India; **Summer 2009**. Trained in manufacturing of drug delivery dosage forms, material handling, documentation, quality control and quality assurance.

Publications / Conference presentations:

Nagardeolekar, A.; Ovadias, M.; Wang, K.-T.; Bujanovic, B. *Willow Lignin Recovered from Hot-Water Extraction for the Production of Hydrogels and Thermoplastic Blends*. Paper. ChemSusChem (accepted, in press). doi:10.1002/cssc.202001259. **2020**.

Nagardeolekar, A.; Ovadias, M.; Wang, K.-T.; Wood, C.; Amidon, T.; Bujanovic, B. *Valorization of Willow Lignin Recovered in a Pilot-scale Biorefinery Based on Hot Water Extraction.* Conference Paper and Oral Presentation. International Bioenergy and Bioproducts Conference by the Technical Association of Pulp and Paper Industry (IBBC-TAPPI Session 4), St. Louis, MO. **2019**.

Nagardeolekar, A.; Ovadias, M.; Wang, K.-T.; Wood, C.; Amidon, T.; Bujanovic, B. *Hydrogels and Thermoplastic Blends from Willow Lignin Recovered from Pilot-scale Hot-water Extraction.* Oral Presentation. Northeast Regional Meeting of the American Chemical Society (ACS-NERM Session Aerogels), Saratoga Springs, NY. **2019**.

Nagardeolekar, A. and Bujanovic, B. *Lignin recovered from hot-water extracts of angiosperms for hydrogels*. Oral Presentation. International Bioenergy and Bioproducts Conference by the Technical Association of Pulp and Paper Industry (IBBC-TAPPI Session 5), Portland, OR. **2018**.

Nagardeolekar, A. and Bujanovic, B. *Lignin recovered from hot-water extracts of angiosperms: Lignin-based hydrogels*. Poster Presentation. International Bioenergy and Bioproducts Conference by the Technical Association of Pulp and Paper Industry (IBBC-TAPPI Session 4), Portland, OR. **2018**.

Wang, K.-T.; Jing, C.; Wood, C.; **Nagardeolekar, A.;** Kohan, N.; Dongre, P.; Amidon, T.E.; Bujanovic, B. Toward Complete Utilization of Miscanthus in a Hot-Water Extraction-Based Biorefinery. Paper. Energies, 11, 39. doi: 10.3390/en11010039. **2018**.

Nagardeolekar, A.; Wang, K.-T.; Jing, C.; Dongre, P.; Wood, C.; Amidon, T.; Bujanovic, B. *Prospects of complete utilization of miscanthus in a biorefinery based on hot water extraction.* Keynote Oral Presentation. First International Forest Biorefining Conference, Thunder Bay, ON, Canada. **2017**.

Nagardeolekar, A.; Dongre, P.; Wang, K.-T.; Jing, C.; Wood, C.; Elniski, A.; Amidon, T.; Bujanovic, B. *Lignin recovered from hot water extracts of Angiosperm-based biomass produced in 65 ft^3 digester.* Oral Presentation. TAPPI International Bioenergy and Bioproducts Conference, Norfolk, VA. **2017**.

Nagardeolekar, A.; Dongre, P.; Wang, K.-T.; Jing, C.; Wood, C.; Elniski, A.; Amidon, T.; Bujanovic, B. *Lignin as a by-product of hot-water extraction: potential increase in the value of biorefineries based on angiosperms.* Oral Presentation. Syracuse CoE Symposium, Syracuse, NY. **2017**.

Nagardeolekar, A.; Dongre, P.; Jing, C.; Bujanovic, B. *Lignin recovered from hot-water extracts of xylan-rich angiosperm-biomass: Characterizations and uses*. Poster Presentation. SyracuseCoE Innovation Showcase & Summer BBQ. Syracuse, NY. **2017**.

Nagardeolekar, A.; Bujanovic, B. *Preparation of lignin hydrogels as a carrier system for bioactive extracts of Chaga mushroom*. Poster Presentation. New York State Biotechnology Symposium. Syracuse, NY. **2016**.

Nagardeolekar, A. and Bujanovic, B. *Preparation and analysis of chaga mushroom (Inonotus obliquus) extracts for antioxidant activity and free phenolic hydroxyl group content.* Poster Presentation. International Chemical Congress of Pacific Basin Societies, Honolulu, HI. **2015**.

Corbett, D.B.; Kohan, N.; Machado, G.; Jing, C.; **Nagardeolekar, A.**; Bujanovic, B. Chemical Composition of Apricot Pit Shells and Effect of Hot-Water Extraction. Paper. Energies, 8, 9640-9654. doi: 10.3390/en8099640. **2015**.